GROUNDWATER MODELING OF THE ABERJONA BASIN

by

EDWARD CHAUNCEY BRAINARD

B.S. Cornell University, Ithaca, NY
(1980)

Submitted to the Department of Civil Engineering
in Partial Fulfillment of
the Requirements for the Degree of

MASTER OF SCIENCE IN CIVIL ENGINEERING

at the

Massachusetts Institute of Technology

May 1990

Signature of Author ______________________________
Department of Civil Engineering
May 18, 1990

Certified by ______________________________
Lynn W. Gelhar
Professor, Civil Engineering
Thesis Supervisor

Accepted by ______________________________
Ole S. Madsen
Professor, Civil Engineering
Chairman, Department Committee on Graduate Studies

GROUNDWATER MODELING OF THE ABERJONA BASIN

by

Edward Chauncey Brainard

Submitted to the Department of Civil Engineering
in Partial Fulfillment of
the Requirements for the Degree of
Master of Science in Civil Engineering

ABSTRACT

An understanding of groundwater flow is necessary to describe transport of dissolved contaminants. The research provides a fundamental analysis of groundwater flow, and is part of a larger project studying the transport, transformations, and health effects of hazardous waste. The region of interest is the Aberjona watershed located ten miles north of Boston. Hydrogeological information describing the Aberjona watershed is analyzed, including the hydraulic conductivity, anisotropy, water budget, and the response time of the aquifer. High conductivity regions consisting of bedrock valleys filled with glacial outwash occur along the center of the watershed, while low conductivity regions of glacial till comprise the upland areas. The aquifer, with a short time constant, responds rapidly to seasonal variations of recharge.

A two-dimensional, finite element groundwater flow is calibrated for the Aberjona River sub-basin, which contains approximately half of the entire watershed. The calibrated steady state flow model provides the basis for determining flow paths for contaminant transport, and may also be used for prescribing boundary conditions for future modeling of areas of interest.

Finally, there is a detailed examination of vertical flow, which is neglected in two-dimensional modeling. Vertical flow is particularly important when considering contaminant transport. The analytical solution approximates the flow as radial in the vicinity of a partially penetrating river, and as essentially horizontal in the remainder of the region. The analytical solution may be used either as a screening tool to determine the importance of vertical flow for a specific field location, or as a correction to apply to flow paths predicted by vertically averaged two-dimensional analysis. For contaminant sources located near the groundwater divide or near the aquifer bottom, vertical flow may cause contaminants to travel large distances, on the order of miles, before discharging into surface water bodies.

Thesis Supervisor: Dr. Lynn W. Gelhar
Title: Professor of Civil Engineering

ACKNOWLEDGMENTS

A number of people assisted me with this research project, and I would like to thank them for their help. My advisor, Lynn Gelhar, provided direction in addition to a wealth of experience in hydrology. John Durant was very helpful in the collection of numerous reports, and was a welcome partner on many field expeditions. Harry Hemond offered his experience concerning field instrumentation. The use of the Camp Dresser & McKee Inc. flow and transport model was helpful in conducting numerical simulations.

I would also like to thank Bob Simonds of Woburn for authorizing access to town property, and the Woburn Conservation Commission for permission to install a well on their property. Barbara Newman, of the EPA, was very accommodating in allowing me to monitor groundwater levels at the Wells G & H site.

The funding for this work was provided by the National Institute of Environmental Health Sciences.

Finally I would like to thank Florence, my wife and partner. As fellow students, we experienced the mixed joys of graduate school together. She's a joy to be with, and added a sense of perspective to the total immersion of MIT work.

This work is dedicated to all the Wild Things.

CONTENTS

LIST OF TABLES

LIST OF FIGURES

1. INTRODUCTION

1.1 Motivation for work

The large extent of groundwater contamination has become an issue of public concern in the United States, with groundwater contamination having been found in most sections of the country [Pye and Kelley, 1984]. The consequences of groundwater contamination will continue to be important in the future because of the slow movement of contaminants in the subsurface. Human health is affected by groundwater contamination by exposure at a point of contact, which is often when the contaminated groundwater discharges into surface waters or the groundwater is withdrawn for use as drinking water.

The potential impact of contaminated groundwater is of significant importance in Massachusetts where approximately one third of the population obtains its water supply from groundwater [Roy, 1988]. The majority of the state's municipal groundwater withdrawals are from stratified drift aquifers, which are often overlaid by industrial and waste disposal activities. In addition to the potential contamination from activities on the surface, water from induced infiltration of surface water bodies is a source of contamination.

The research documented in this thesis is part of a larger project studying the basic principles controlling the transport, transformations, and ecological effects of hazardous waste. The initial focus of the larger project is the distribution and transport of chemical wastes in the Aberjona watershed located ten miles north of Boston. The watershed scale perspective is unique in that hazardous waste studies tend to focus on specific parcels of property while the hydrological processes controlling the transport occur on a larger regional scale.

The use of a watershed scale perspective is advantageous in a number of ways. First, insight may be developed concerning the broad question of contamination distribution, transport and human exposure, rather than the conventional analysis of focusing on isolated contaminated real estate parcels. Consequently a general understanding of the possible contaminant transport pathways and ensuing human exposure are possible. Secondly, by using the natural boundaries of the watershed to delineate the study area, analysis techniques such as mass balance analysis may be applied. In addition, reasonable boundary conditions may be used when performing modeling.

1.2 Organization of thesis

This thesis is comprised of three major sections, dealing with the physics of groundwater flow. The first section analyzes hydrogeological information describing the watershed. Hydrogeological data, including field measurements of transient groundwater piezometric heads and gradients, is presented while forming a conceptual description of groundwater flow. The second section contains two-dimensional modeling of groundwater flow for a sub-basin containing approximately half of the entire watershed. The modeling process provides a method to organize and evaluate the existing hydrogeological data, as well as to develop a conceptual description and understanding of the groundwater flow.

The third section of the thesis involves a detailed examination of vertical flow, which is neglected in two-dimensional modeling. The vertical flow is particularly important when considering contaminant transport. Vertical gradients are large near locations where groundwater discharges into bodies of surface water such as streams overlying the aquifer. Consequently, the effect of vertical flow is significant for interactions of ground and surface waters.

An analytical solution analyzing the effect of vertical flow on contaminant flow paths is presented. The analytical solution quantifies the effect of vertical flow on contaminant transport, and the influence of parameters such as anisotropy of the hydraulic conductivity and the contaminant source location are included in the analysis. Consequently the analytical solution may be used either as a screening tool to determine the importance of vertical flow for a specific field location, or as a correction to apply to flow paths predicted by vertically averaged two-dimensional analysis.

2. HYDROGEOLOGICAL BACKGROUND

2.1 Overview of the Region

The Aberjona watershed is located ten miles north of Boston, and includes the seven towns of Woburn, Reading, Wilmington, Burlington, Lexington, Winchester, and Stoneham (Figure 1). The total area is 24.3 square miles, with the town of Woburn located in the center of the watershed and occupying the majority of the area. The watershed may be defined on the basis of the surface water drainage, with the height of land constituting the surface water divide. The Aberjona watershed may be divided into two sub-basins as shown in Figure 2. The Horn Pond sub-basin is to the west and has an area of 9.9 square miles. The Aberjona sub-basin is to the east and has an area of 14.4 square miles.

The Aberjona River drains the watershed, and flows from north to south with an average slope of 0.0016 ft/ft (Figure 2). Exiting the watershed, the Aberjona River feeds into the Mystic Lakes, which are drained by the Mystic River into Boston Harbor. There are three major tributaries to the Aberjona River: Hall's Brook which drains northwestern Woburn, Sweetwater Brook which originates in Stoneham, and Horn Pond Brook which drains western Woburn and feeds Horn Pond. The flow of many of the smaller tributaries located at the higher elevations are intermittent.

The headwaters of the Aberjona River in northern Woburn, Burlington, and Reading consist of red maple swamps, which are seasonally submerged. Along the main branch of the Aberjona River there are sections of fresh water marshes with emergent herbaceous vegetation such as *typha* and *phragmites*. The marshes are flooded during periods of high precipitation when the river stage rises, and at those times constitute large expanses of surface water.

The Aberjona River originates in the swamps at an elevation of 120 feet above mean sea level and discharges into Upper Mystic Lake at an elevation of 9 feet. The main branch of the Aberjona flows through a valley and drops only forty feet while it travels the 4.8 miles from Route 128 to Upper Mystic Lake. The hillsides rise rapidly from the valley floor away from the river to a maximum elevation in the watershed of 287 feet at Horn Pond Mountain located immediately south of Horn Pond.

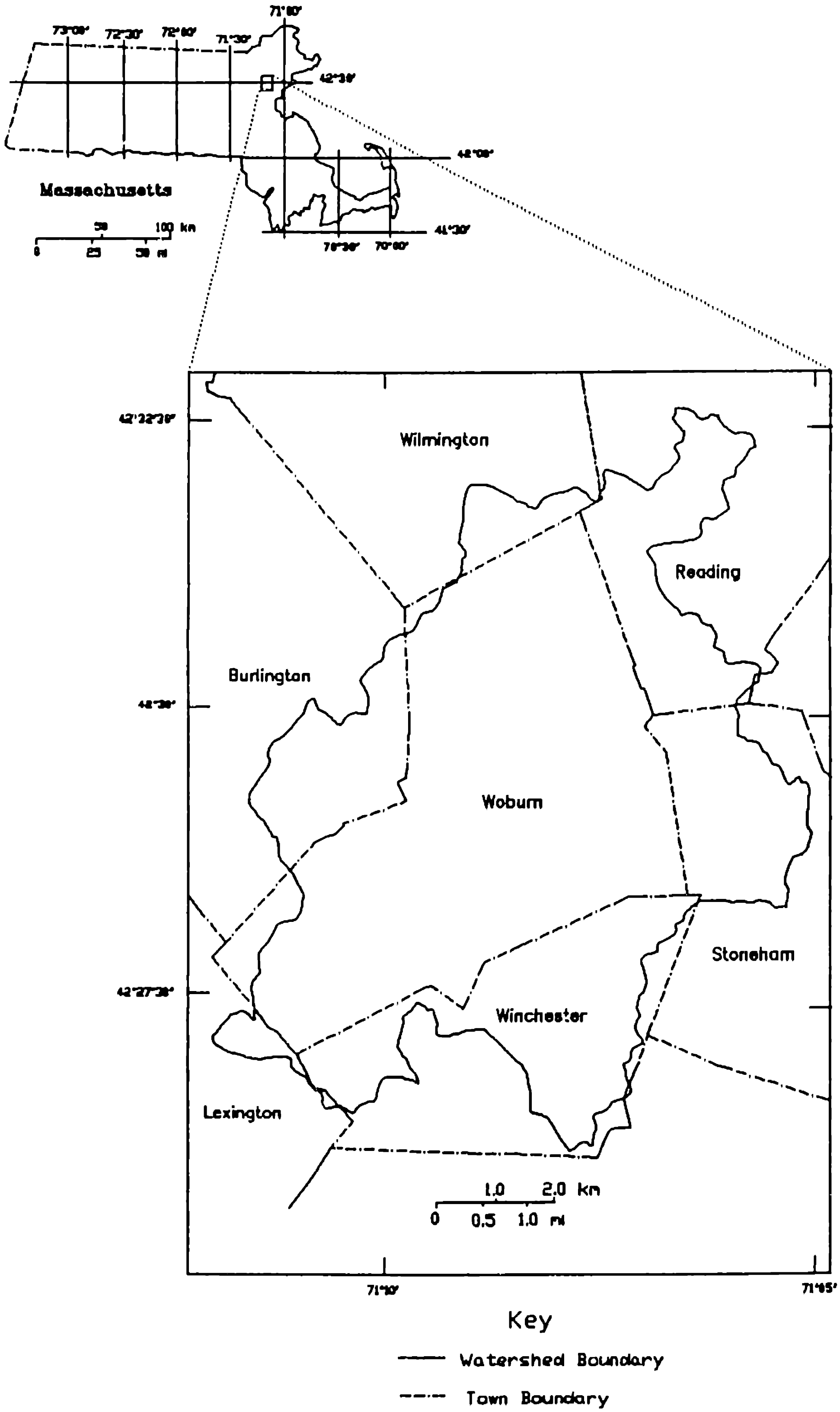

Figure 1. Site Map

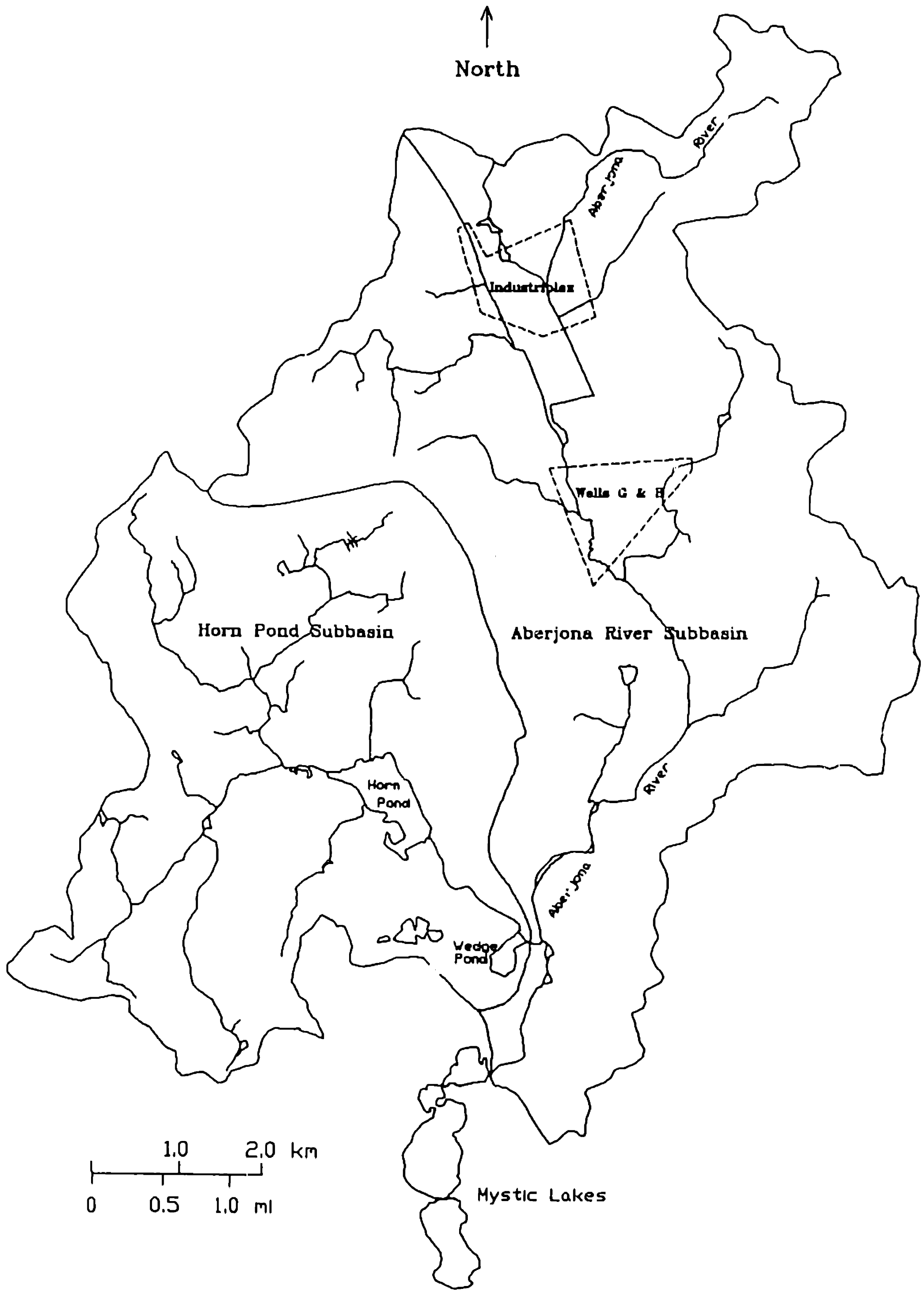

Figure 2. Map Showing Subbasins

2.2 Land Use

The town of Woburn, which includes the majority of the land area of the watershed, is a region experiencing rapid growth. From 1971 to 1985 the land area used as industrial areas more than doubled [Metropolitan Area Planning Council, 1988]. Currently, the area is quite urban with land use of: 13% industrial, 4% commercial, 40% residential, 30% agricultural and forested land, and 6% wetlands.

Woburn has a long and extensive industrial history, which is well documented by Tarr [1987]. Industrial development essentially began in 1837 with the construction of the Middlesex Canal. During the initial industrial period, the dominant industry was leather processing and related industries. The industries included machine shops and chemical companies supporting the tanning industry. The tanning and chemical industries grew over time, and most waste disposal occurred on site. Beginning in approximately 1940, Woburn experienced diversification of its industrial base into light manufacturing. In 1989 there were more than 135 manufacturing firms, with the area having experienced similar growth as did the rest of the Route 128 area.

There is considerable evidence of chemical contamination in the watersheds. There are two sites, Industriplex-128 and Wells G & H, on the EPA's Superfund list of uncontrolled hazardous waste sites. In addition, in 1989 there were 40 potential hazardous waste sites under investigation by the state [DEQE, 1989]. The documented contamination involves a wide range of chemicals including metals and organic compounds. The two Superfund sites as well as the majority of the state-identified sites are located in the Aberjona sub-basin.

2.3 Surficial Geology

The surficial geology of the watershed is characterized by glacial outwash and till deposits. Figure 3 shows the surficial geology divided into these two components [Chute, 1959; USGS, 1959; USGS, 1962]. Although there is considerable variability of the materials, this general schematic highlights the distinction between the location of the two major components, with the distribution caused by glaciation.

The valleys are filled with thick deposits, often over 100 feet, of well-sorted glacial outwash. The outwash material has a high hydraulic transmissivity, with areas greater than 4000 ft^2/day, and are used for industrial and municipal water supplies (Delaney and Gay, 1980). The water sorted outwash material contains lenses of gravel and clay.

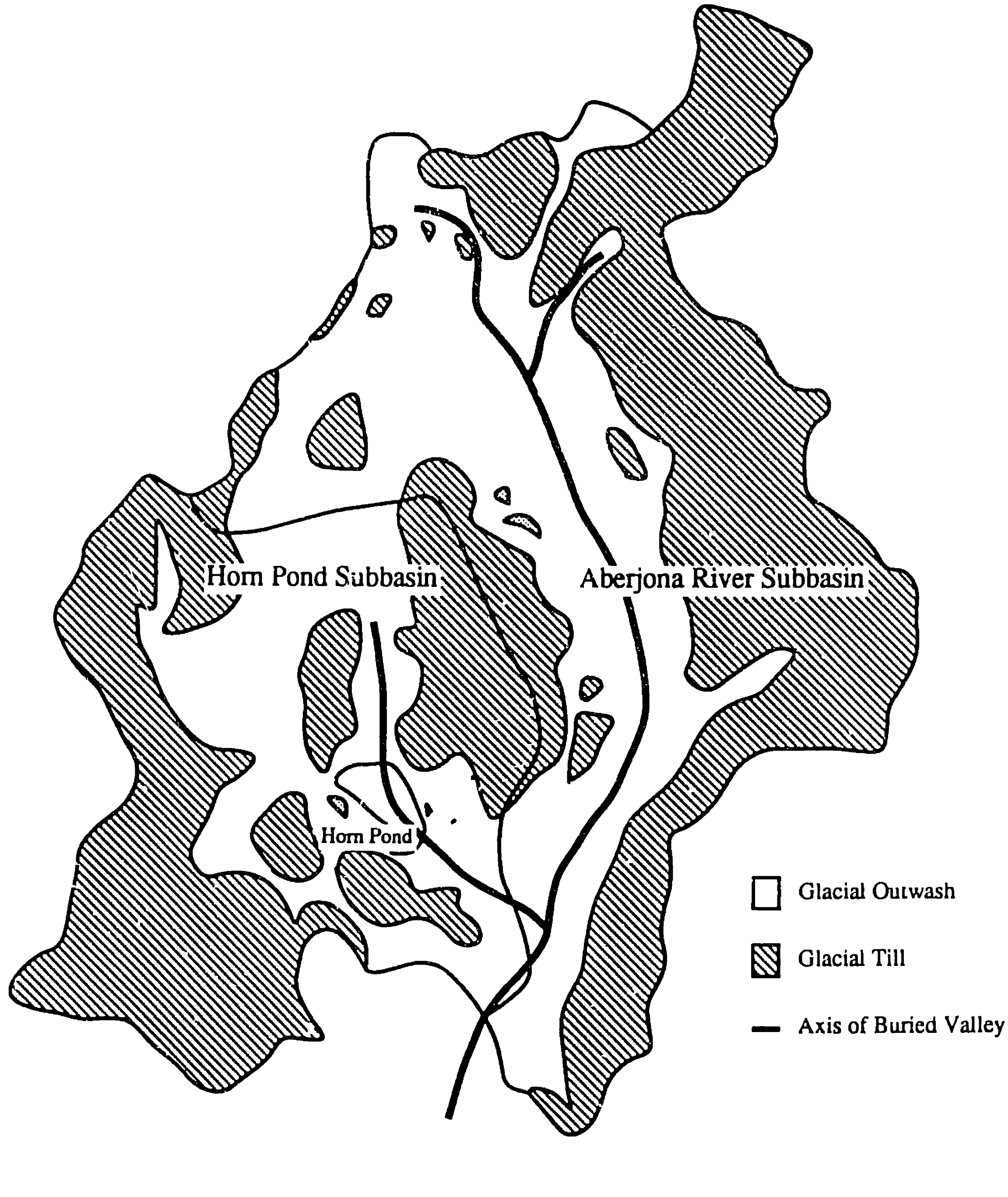

Figure 3. Surficial Geology

The hill slopes are covered with a mantle of till. Till is thickest near the valley floors and thin towards the hilltops. In areas there are numerous bedrock outcrops. Glacial tills are directly deposited by glacial ice and consequently poorly sorted. Tills generally have low hydraulic conductivities.

The marshes located in the valley floor are underlain by peat deposits. At the Wells G and H site, the thickness of the peat varies from 2 to 26 feet [Myette, et. al., 1987]. Some wetlands have been filled, most notable what was Mishuam Pond near the Industriplex site [Stauffer Chemical Company, 1983].

2.4 Bedrock Geology

The major bedrock units are Salem Gabbro-diurite, Dedham Granodiurite, and Precambrian Gneisses and Schists. Because of the high water yielding overburden, few wells have been drilled into the bedrock, and limited information is available concerning the extent of fracturing. At the Wells G & H site it has been reported that the bedrock is fairly fractured [Ecology and Environment, 1982]. At the Unifirst Property, a hydraulic conductivity of 0.86 ft/day was calculated from a three day pumping test [Cherry et. al., 1989].

The extent of fracturing of the bedrock is of interest for two reasons. First, there is the possibility of the transport of dense nonaqueous phase contaminants in fractures. Second, the bedrock could form an impermeable boundary for modeling groundwater flows, but this is dependent on the magnitude of the flux of water across the boundary.

There are two major troughs of bedrock, buried valleys, which filled with glacial outwash form the transmissive regions of the aquifer. One trough runs beneath the main branch of the Aberjona River, and the other runs to the west under Horn Pond [Chute, 1959]. The two troughs connect near Wedge Pond and the combined trough runs south beneath the Mystic Lakes.

2.5 Water Level Data

2.5.1 Well Data

Water level data is available from a number of sources, ranging from well driller records to USGS pumping tests. Figure 4 shows the location of wells with well logs and/or water level data in the Aberjona sub-basin. The units on the axis are feet, measured north and east from an origin at 4,700,000 meters north and 319,000 meters east on the Massachusetts 1000-meter Universal Transverse Mercator grid. This point is equivalent to a latitude of 42°27.41' north and longitude of 71°11.46' west. The data for the Horn Pond sub-basin is discussed separately.

The data provides reasonable spatial coverage of the basin but was collected from sources over the extremely long time period of 1900 to the present. Consequently, differences from both seasonal and long term variability of precipitation are likely. Synoptic data is available for the Wells G & H site.

The greatest density of water level data is located at the Industriplex and Wells G & H Superfund Sites. Other hazardous waste sites also provide clusters of data. In general, there is poor data in the till areas, since both the water supply wells and hazardous waste sites are mainly in the valleys. The data for each well is presented in Appendix 1.

2.5.2 Transient Water Level Data

Transient water level data are available from wells monitored by the USGS, and for wells monitored by myself. Data will be presented for four wells, with the locations displayed in Figure 5. Wells Winchester 14 and Wilmington 448 are monitored by the USGS. Wells S89 and M1 are monitored by MIT.

Long term data is available for wells Wilmington 448 and Winchester 14 beginning in 1959 and 1940 respectively and measured monthly [USGS, 1975]. Well Wilmington 448 is located in the town of Wilmington in silty organic muck near a swamp north of the watershed, and would have similar trends to the water level of the swamps at the headwaters of the Aberjona River (Figure 6). The water level varies very little, with a maximum annual amplitude of approximately 2 feet.

Well Winchester 14 is located in the town of Winchester in glacial till material. The water level varies significantly with annual variations of almost ten feet (Figure 7). The water level is related to the infiltration rate with the maximum values in the winter and the minimum values in the summer. Considering Darcy's equation

$$q=KJ \qquad (1)$$

where the flux, q, is proportional to the product of the hydraulic conductivity, K, and the gradient, J. It is apparent that the till must have a low hydraulic conductivity to cause such large variations of head. Well Winchester 14 should be representative of water levels in the glacial till at the watersheds.

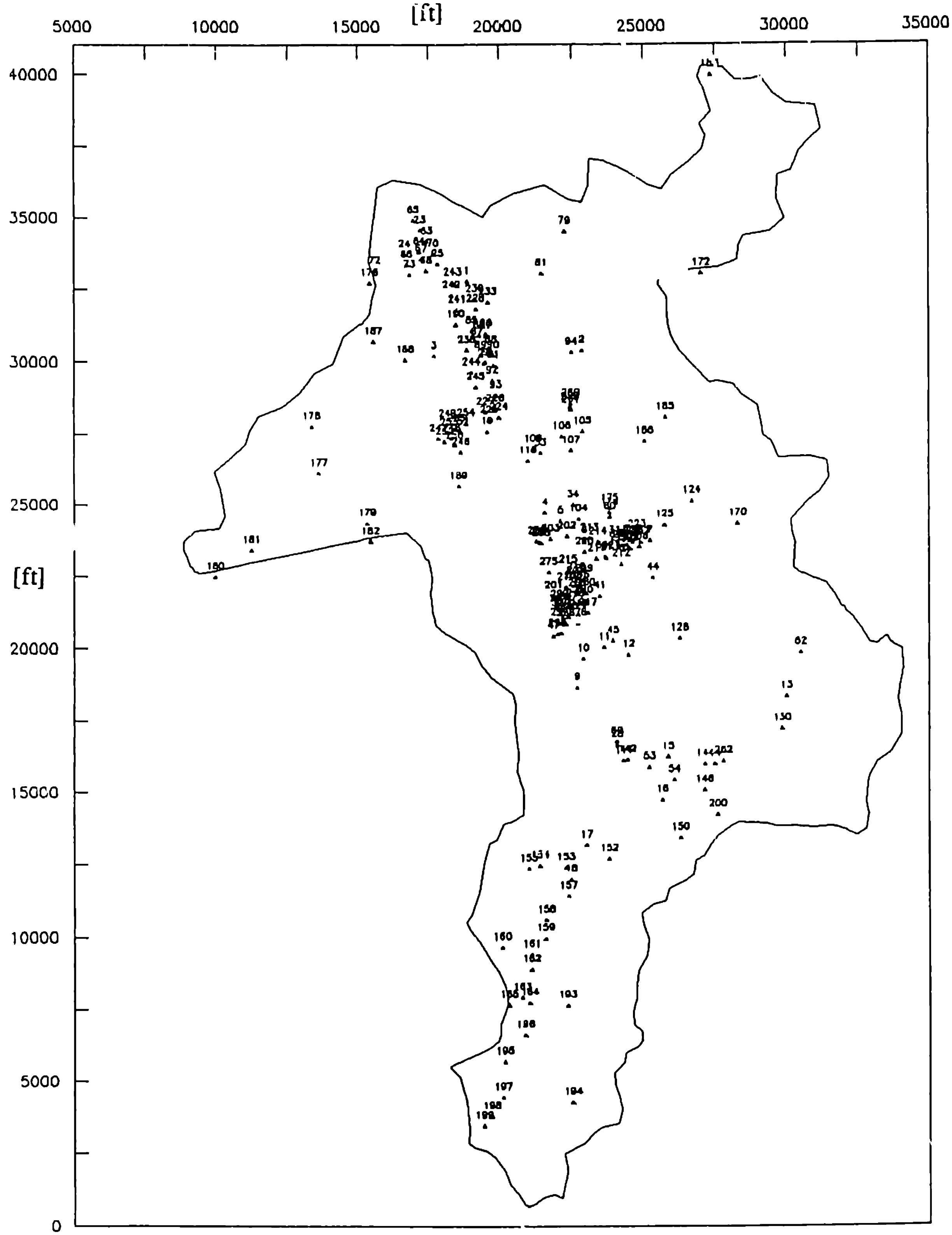

Figure 4. Well Locations

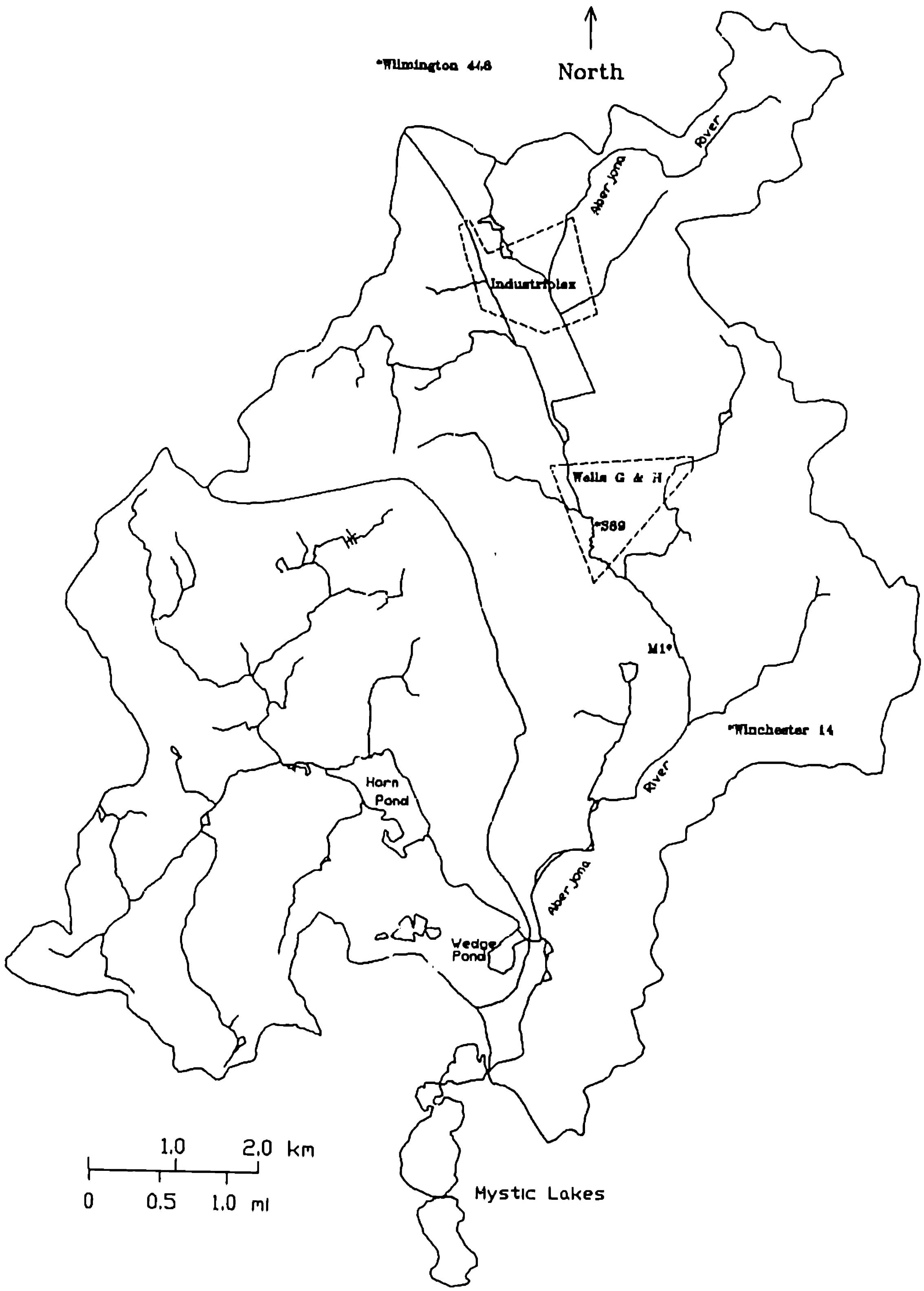

Figure 5. Recording Well Locations

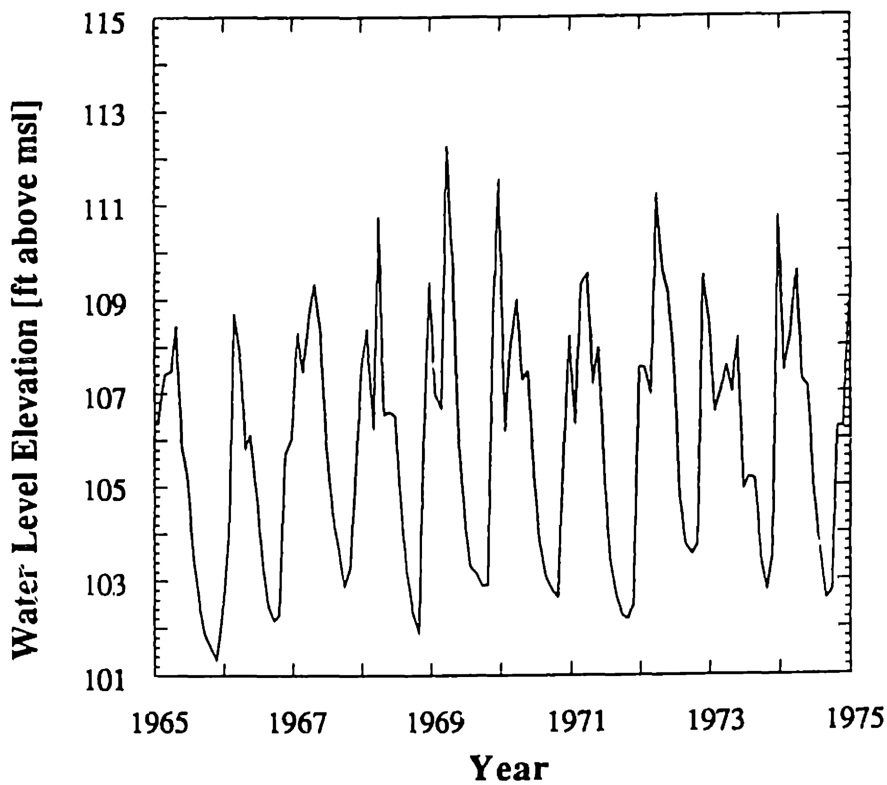

Figure 7. Well Winchester 14 - heads

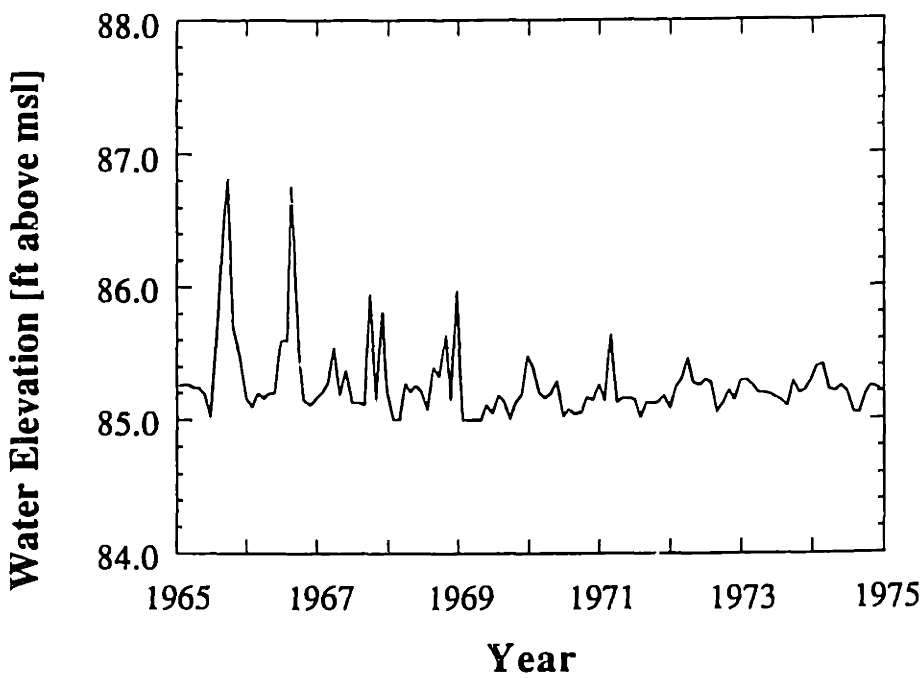

Figure 6. Well Wilmington 448 - heads

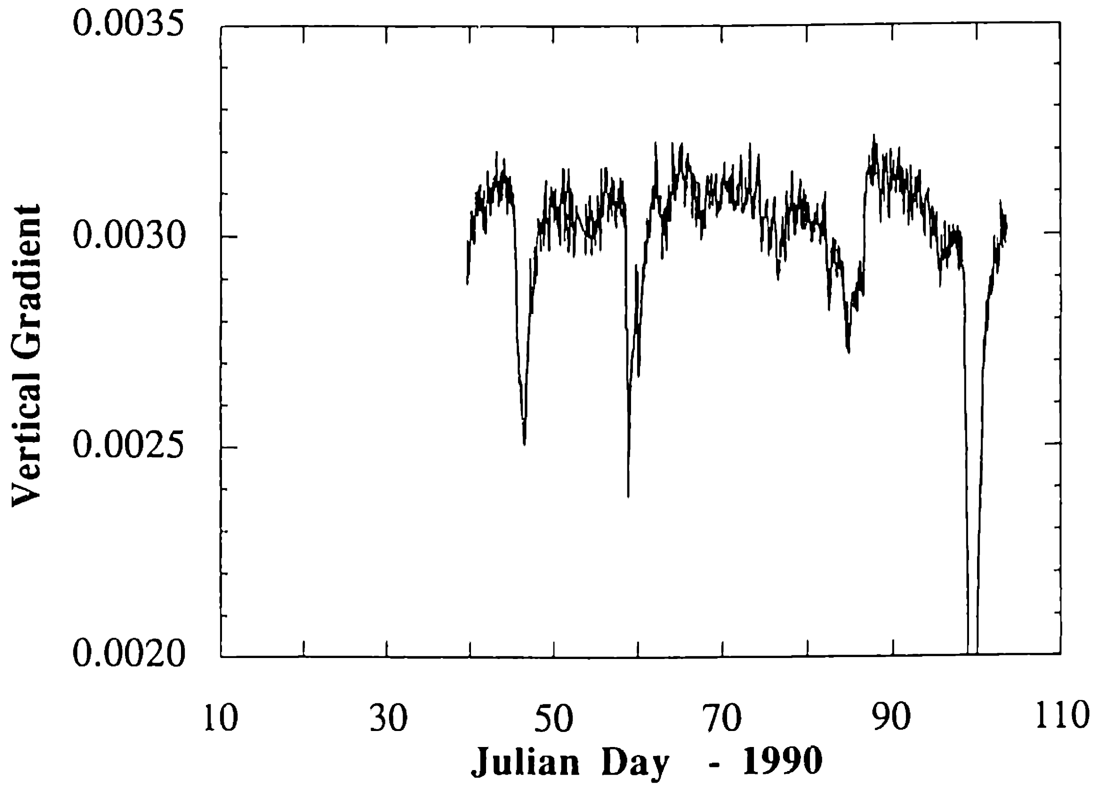

Figure 9. Well M1 - gradients

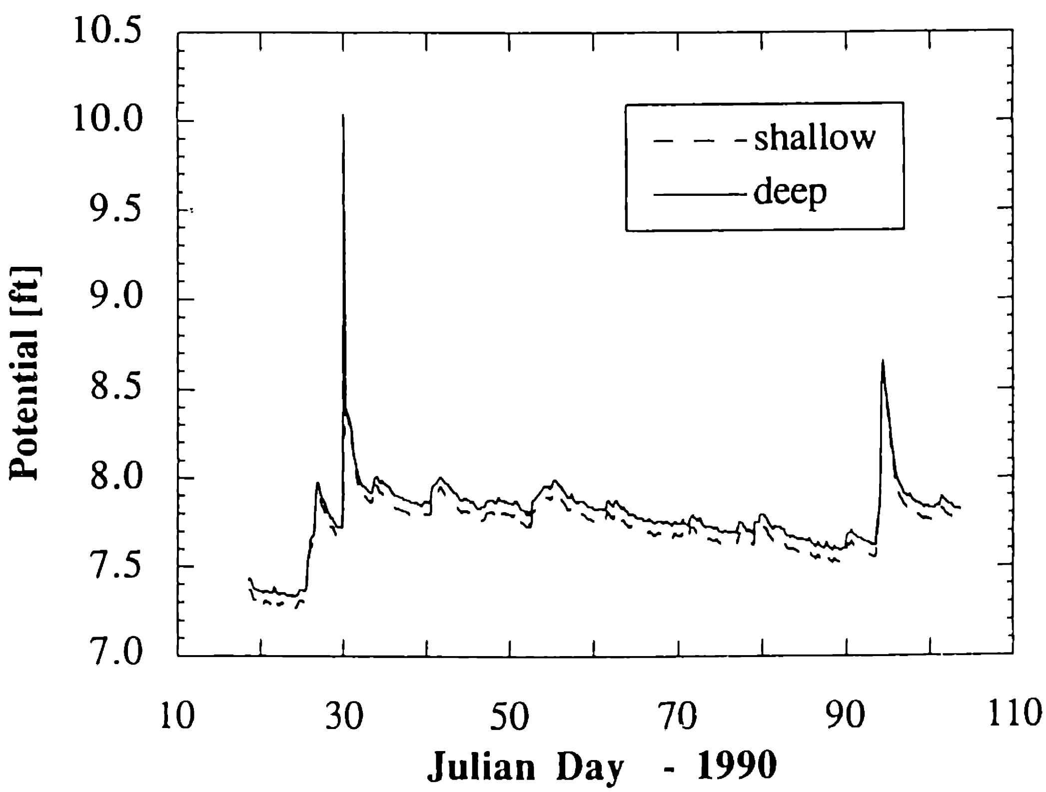

Figure 8. Well M1 - heads

Well cluster S89 consists of a group of three wells finished at different depths. The shallow, medium, and deep wells are screened at 32, 56, and 121.5 feet below the land surface respectively [NUS, 1986]. The three wells are located along a line perpendicular to the river with the deep, medium and shallow wells at distances of 10, 16 and 24 feet from the river. The wells were installed as part of the USGS thirty-day pumping test at the site [Myette et al., 1987]. The wells are screened over the bottom two feet of length. Since the deep boring did not reach bedrock, the overlaying material is over 120 feet thick.

Figure 10 displays the river stage and head in the medium level well for the period from March 16 through April 14, 1990, with the elevation in feet above mean sea level. The data is not displayed for the shallow well because of a failure of the pressure transducer. The head at depth follows the variations of the river stage, with the damped amplitude and time lag. The time lag at the peak of depth is approximately one hour, which is the sampling rate of the data logger.

The gradients at Well S89 are all in the positive vertical direction. On March 16, 1990, the vertical gradients were: deep to medium, 0.0011; medium to shallow, 0.0015; shallow to river, 0.0098. The horizontal gradient of the river in the vicinity is approximately 0.0002. The vertical gradient between the deep well and the river varied from 0.002 to 0.01 during the period of observation (Figure 11). The gradient decreases significantly when the river stage increases rapidly.

2.6 Water Budget

A mass balance may be performed on the watershed to estimate the magnitude of the various fluxes. An annual mass balance assuming steady state conditions was done. There are four components to the mass balance: the input from precipitation, groundwater withdrawal, discharge through the Aberjona River, and evapotranspiration. The precipitation data is available from the weather station at Logan Airport. The majority of the area is served by the MDC sewer system so that groundwater which is withdrawn in the area is exported from the watershed via the sewer mains. The major users of groundwater are required by the state to document their withdrawals with the Massachusetts Department of Environmental Protection. The discharge from the watershed by the Aberjona River is monitored by the USGS at their gauging station in Winchester.

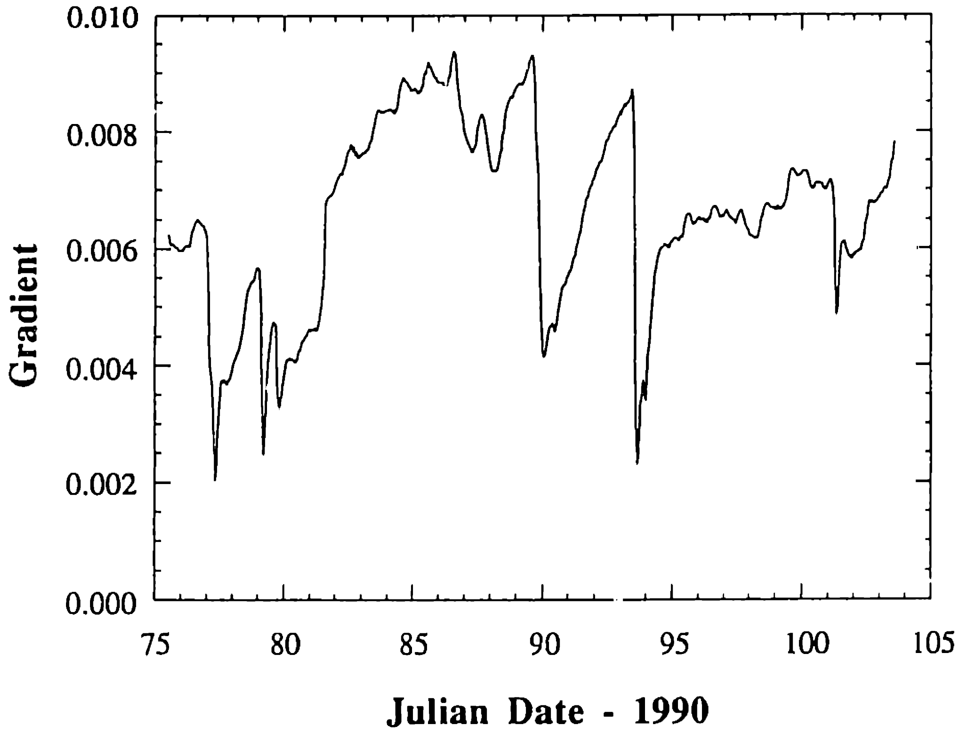

Figure 11. Well S89 - gradients

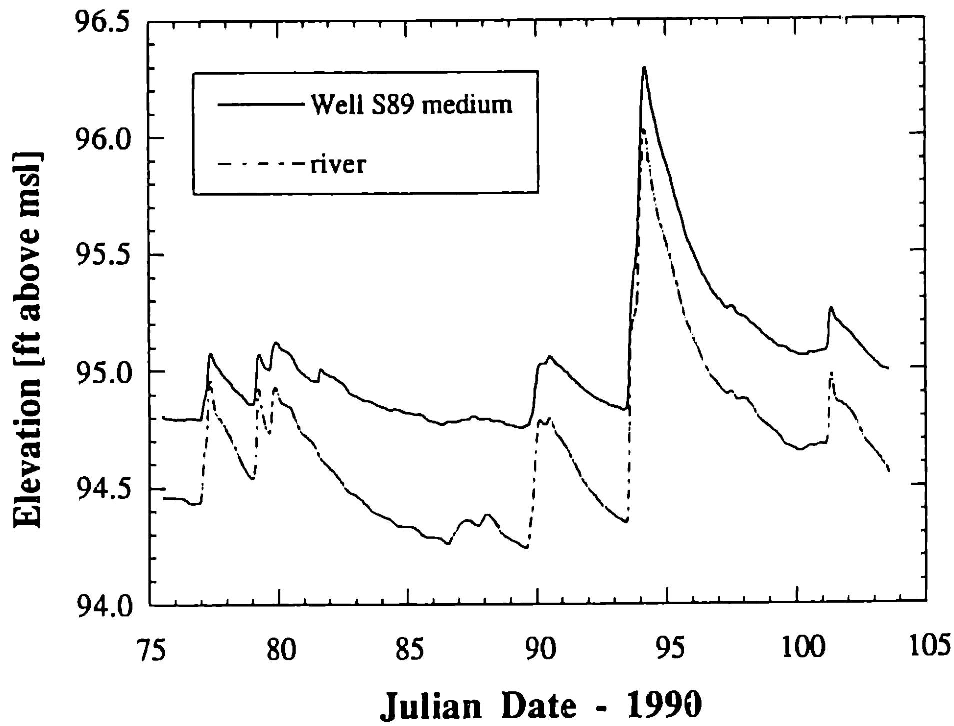

Figure 10. Well S89 - heads

The steady state mass balance is formulated as

$$Q_p = Q_w + Q_r + Q_e \tag{2}$$

Q_p the precipitation, Q_W the groundwater withdrawal, Q_r the river discharge and Q_e the losses to evapotranspiration. Assuming no flux through the bedrock beneath the aquifer and a minimal flux of groundwater out of the aquifer downgradient boundary, the losses due to evapotranspiration may be calculated. Because of the uncertainty of evapotranspiration values, it is difficult to make a justifiable estimate of the evapotranspiration directly. The water balance is calculated for 1967 and 1987 to illustrate changes over that period.

Table 1 shows groundwater withdrawals in 1967 and 1987. The total withdrawals decreased by almost fifty percent over the period, from 12.0 mgd to 6.4 mgd. During the twenty year period Stauffer Chemical and J.O. Whitten Gelatin companies went out of business. The town of Woburn shut down Wells G & H and supplemented its water supply with MDC water. Woburn currently withdraws approximately 4.4 mgd from wells near Horn Pond.

Groundwater Withdrawals [MGD]:

	1967	1987
Woburn		
Horn Pond	4.4	4.4
Wells G&H	0.9	0
Burlington	0	0.2
Atlantic Gelatin	2.9	1.8
Stauffer Chemical	1.0	0
J.O. Whitten Gelatin	2.8	0
Total	12.0	6.4

TABLE 1

Water Balance:

	1966	1987
Precipitation - Logan	42.4 in/yr 100 %	42.4 in/yr 100 %
Discharge - Winchester	26.6 cfs 37 %	36.0 cfs 49 %
Groundwater Withdrawal	12.0 mgd 27 %	6.4 mgd 14 %
Losses from totals	36 %	37 %

TABLE 2

The values used to calculate the mass balance are shown in Table 2. For precipitation, the long-term average value at Logan Airport was used, and a watershed area of 23.3 square miles. In 1987 the groundwater withdrawals account for 14% of the precipitation, down from a very sizable fraction of 27% in 1967. The discharge of the Aberjona River accounts for 49% of the total flux in 1987, leaving an evapotranspiration flux of 37%. The reduction of groundwater withdrawal over the period was compensated by a corresponding increase in the discharge of the river.

2.7 Hydraulic Conductivity

Data on hydraulic conductivity are available from both water supply investigations and studies of hazardous waste sites. The data consists of pumping tests, specific capacity data, slug tests, and grain size analysis. Using these sources of information estimates can be made concerning the hydraulic conductivity of the outwash and till regions of the watershed, and also the anisotropy of the hydraulic conductivity.

Specific capacity is the measure drawdown of a pumping well for a given yield. An estimate of the transmissivity can be made from specific capacity values. Theis's equation for transient drawdown is

$$s = \frac{Q}{4\pi T} W(u) \tag{3}$$

and for $u < 0.01$

$$s = \frac{Q}{4\pi T} \ln\left[\frac{2.25Tt}{r^2 S} \right] \tag{4}$$

with drawdown s, pumping rate Q, transmissivity T, time t, radius of well r, and storage coefficient S. Using estimates for the outwash region of the aquifer: T = 10,000 ft^2/d; t = 1 day; r = 1 ft; and S = 0.25; and estimate for the transmissivity is

$$T = \frac{Q}{4\pi s} \ln\left[\frac{2.25Tt}{r^2 S} \right] = \frac{Q}{s} 211 \tag{5}$$

with T in ft^2/day and Q/s in gpm/ft. The value of T in Equation 5 is linearly dependent on the specific capacity Q/s, and less dependent on the remainder of the terms because of the logarithm. Equation 5 is equivalent to graphical techniques presented by Walton [1970].

The data used to calculate the transmissivity is from Delaney and Gay [1980] except for Wells 419 and 420 [Myette et al., 1987]. The data is presented in Appendix 2, and the well locations are shown in Figure 12. Figure 13 displays the transmissivity estimates for the watershed. The majority of the data is from water supply wells located along the Aberjona River and Horn Pond. The geometric mean of T for all except the bedrock wells (10, 262, 424, 434) is 4614 ft^2/day, which represents a very transmissive aquifer. The geometric mean is used to reduce the influence of the extreme values and is appropriate since hydraulic conductivity is often log normally distributed. Using an average aquifer thickness of 80 ft, the hydraulic conductivity would equal 58 ft/day.

Corrections may be made to the transmissivity estimate for the effects of partial penetration of the well, and well losses. Walton [1970] suggests a correction for the effect of partial penetration

$$s = s_p \left\{ \alpha \left[1 + 7\sqrt{\frac{r_w}{2\alpha m}} \cos\left(\frac{\alpha\pi}{2} \right) \right] \right\} \tag{6}$$

where s is the corrected drawdown, s_p the uncorrected drawdown, α equals the screen length, L, divided by m, the aquifer thickness, and r_w is the well radius. For Wells G and H, which have the best documented data, with r = 1 ft, L = 10 ft, m = 80 ft, the correction increases the transmissivity by a factor of 3. This correction is not applied to the transmissivity estimates since the specific capacity data is from water supply wells located near bodies of surface water and are screened in the most permeable stratum, which creates a high transmissivity estimate.

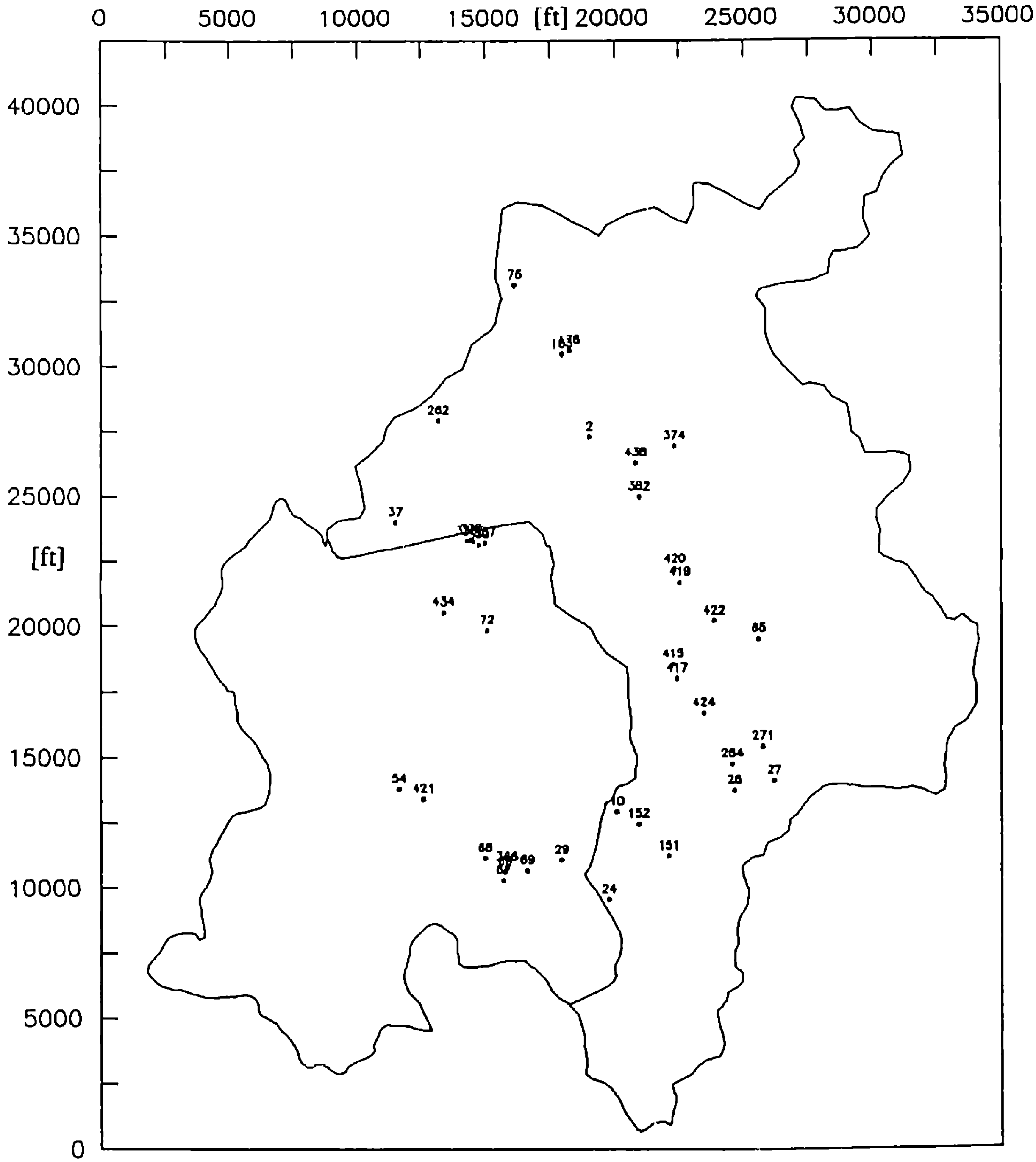

Figure 12. Specific Capacity Well Locations

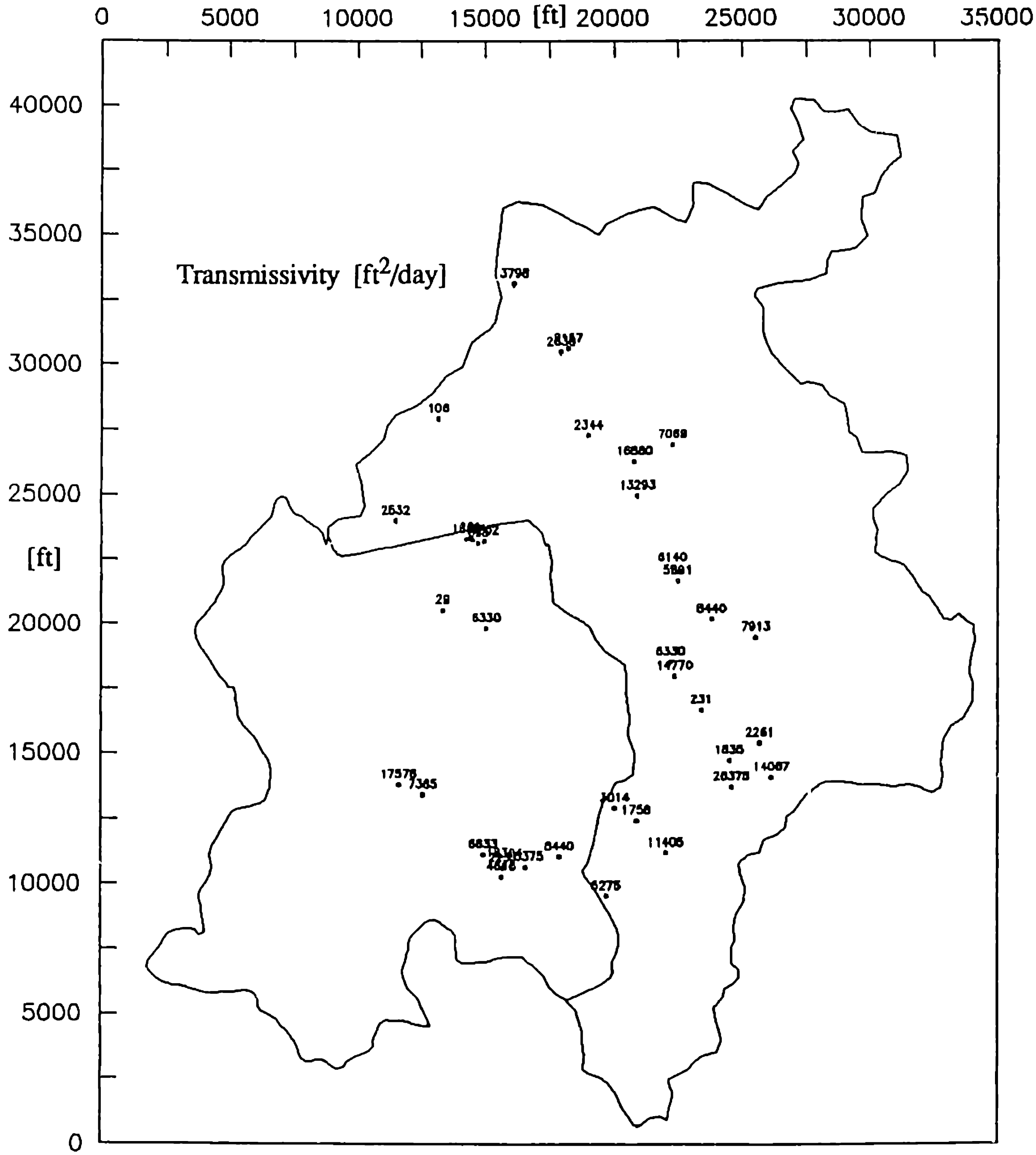

Figure 13. Transmissivity Map

Three pumping tests have been performed in the watershed with two in the overburden and one a bedrock test. In 1984 a 22-hour pumping test was performed at the Riley tannery [Woodward-Clyde, 1984]. The Riley tannery is located across the Aberjona River from Wells G & H. The data is difficult to analyze, because few water level measurements were made at early times and the influence of recharge from the Aberjona River was significant during later times. In addition, there was precipitation during the test. Transmissivity calculations vary over the large range of 2000 to 65,000 ft^2/day.

The USGS performed a thirty-day pumping test at Wells G & H to determine aquifer characteristics and the area contributing to the water supply wells [Myette et al., 1987]. Step drawdown tests were made at both wells and transmissivities were calculated from the specific capacity data and by curve matching using Boulton's method for phreatic aquifers. After correcting for partial penetration using Equation 6, the USGS calculated transmissivities from the specific capacity data of 10,000 ft^2/day and 10,700 ft^2/day for Wells G & H respectively. Using curve matching yielded 29,700 and 17,600 ft^2/day respectively. The estimated values for the hydraulic conductivity assuming an 80-ft saturated thickness range from 125 to 350 ft/day.

A three-day pumping test was undertaken at the Unifirst property located at the Wells G & H site to determine the hydraulic conductivity of the shallow fractured bedrock. The calculated hydraulic conductivity was 0.86 ft/day [Cherry et al., 1989]. Falling head slug tests at the nearby W. R. Grace property gave a hydraulic conductivity for the shallow bedrock of 1.5 ft/day [GeoEnvironmental Consultants, 1983].

Slug tests have been undertaken at three locations in the till. At the Weyerhaeuser property, located on the hill slope northwest of Wells G & H, two rising heads yielded 2.6 ft/day for the hydraulic conductivity [Weheran Engineering, 1987]. At W. R. Grace, seven falling head tests in wells screened in the overburden yielded 2.8 ft/day [GeoEnvironmental Consultants, 1983]. And at the North Woburn Industrial Park, located west of the Industriplex site, three rising head tests yielded 4.6 ft/day [Goldberg-Zoino, 1986]. The fact that all of the hydraulic conductivity estimates for till areas give close values would not be expected considering the variability of the geology, and there is probably much greater variability.

Estimates were made for hydraulic conductivity for many wells at the Wells G & H site using grain size analysis and falling head slug tests [NUS, 1986]. The data can be used to calculate the hydraulic conductivity anisotropy. Sixteen falling head tests were performed in seven wells screened at various depths. The results are plotted in Figure 14 along with the pumping test hydraulic conductivity and the arithmetic, geometric, and harmonic means of the falling head tests. The data is presented in Appendix 3. Assuming perfect horizontal layering of the porous media, the horizontal hydraulic conductivity would be the arithmetic mean and the vertical hydraulic conductivity would be the harmonic mean. The ratio is an extreme value for the anisotropy, which equals 96:1 for this data.

One would expect the arithmetic and harmonic means to bracket most measurement values. The geometric mean, appropriate for log-normally distributed data, represents an average for the horizontal hydraulic conductivity. The pumping test result lies considerably outside of this range, and is almost two orders of magnitude greater than the geometric mean. The pumping test result is a high estimate, because Wells G & H are located in the most transmissive region, and are screened in gravel layers.

The hydraulic conductivity can also be estimated from grain size analysis using the method of Hazen [Freeze and Cherry, 1979]. Using the relation that the intrinsic permeability is proportional to a length scale of the porous media squared, Hazen suggested calculating the hydraulic conductivity using d_{10}, the grain size at which 10% of the particles by weight are finer, as the length scale. The hydraulic conductivity calculated from grain size analysis data is presented in Figure 15 and Appendix 4. There is no apparent correlation between depth and hydraulic conductivity, which indicates that the aquifer should not be modeled as layers each representing different geological materials. The results from grain size analysis are similar to those from the slug tests and give an anisotropy ratio of 119:1. Consequently, an upper limit for the anisotropy ratio is approximately 100:1.

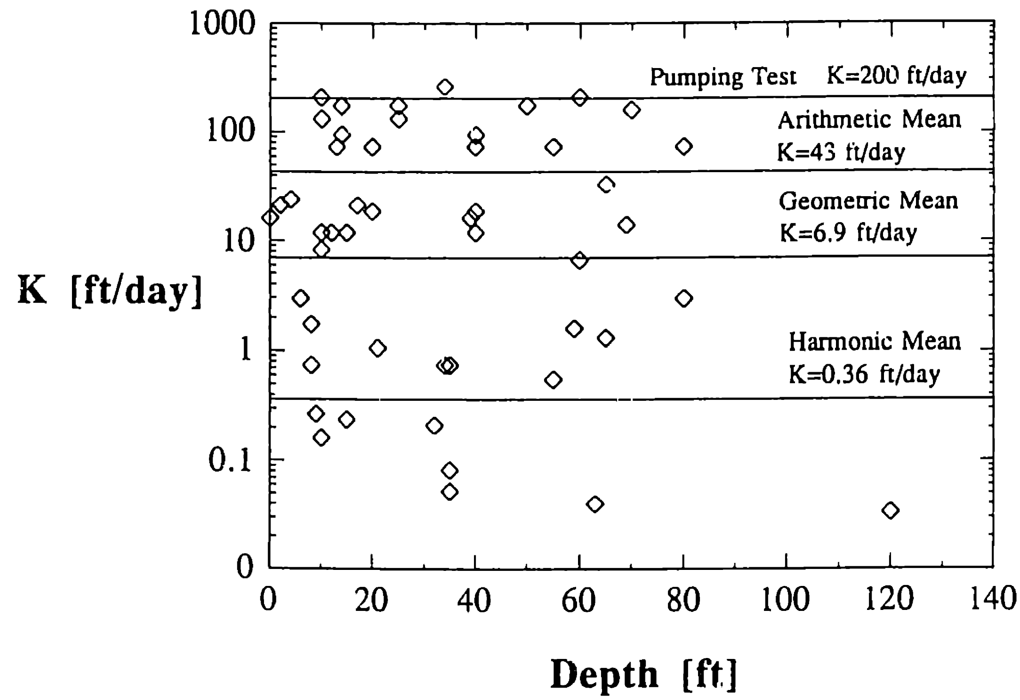

Figure 15. Conductivity from Grain Size

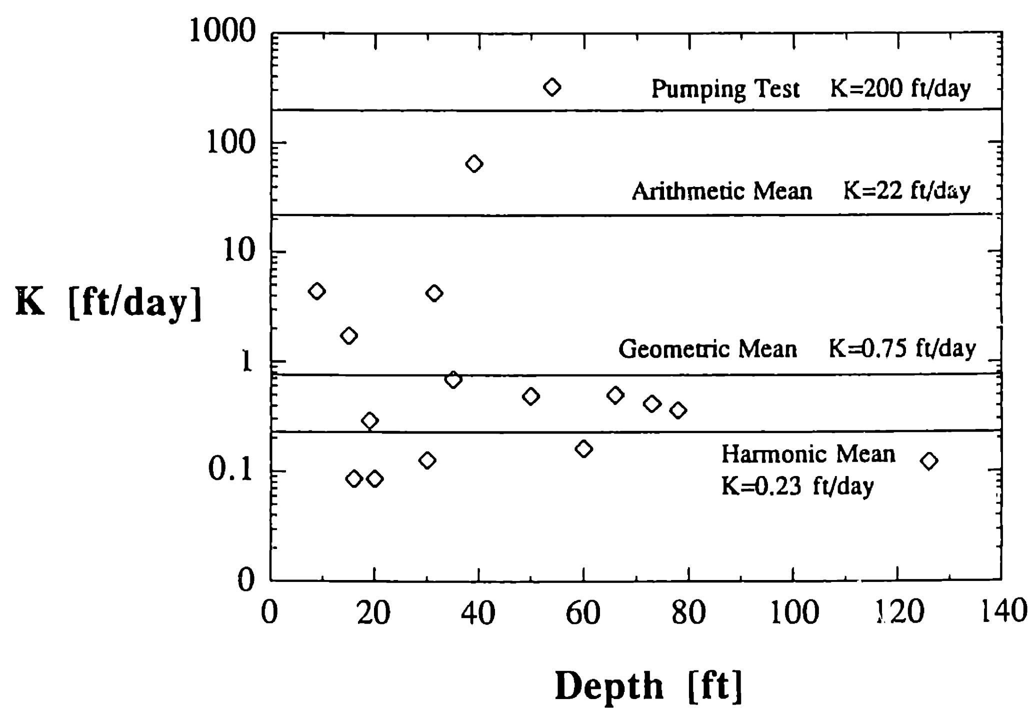

Figure 14. Conductivity from Falling Head Tests

2.8 Horn Pond Sub-basin

The Horn Pond sub-basin is analyzed separately from the Aberjona River sub-basin and not modeled, because of the limited geological data available. There is also more documentation of industrial activity and the presence of hazardous wastes in the Aberjona River sub-basin. Figure 16 shows the surface water bodies in the Horn Pond sub-basin, with Horn Pond being the major body and Wedge Pond a minor body. The majority of the surface area is drained by tributaries that feed into Horn Pond.

Figure 17 displays the location of wells with measured water elevation data [Delaney and Gay, 1980]. The tabulated values are in Appendix 5. The greatest concentration of wells is around Horn Pond, which are public water supply wells for the town of Woburn. The water table elevation data can be contoured to develop a map of the phreatic surface elevation (Figure 18). The contour map shows the general phreatic surface, which parallels the land surface.

2.9 Aquifer Time Constant

A hydraulic time constant may be calculated for the aquifer, which describes the response time of the watershed for varying precipitation inputs. Using one-dimensional analysis with a fully penetrating river and vertically averaged head, the governing equation with no recharge is

$$S\frac{\partial h}{\partial t} = T\frac{\partial^2 h}{\partial x^2} \tag{7}$$

with storage coefficient S, head h, transmissivity T, and distance from the river x. T is the average transmissivity. The solution to Equation 7 is

$$h = a\exp\left(-\frac{\pi^2 Tt}{2SL^2}\right)\sin\left(\frac{\pi}{2}\frac{x}{L}\right) \tag{8}$$

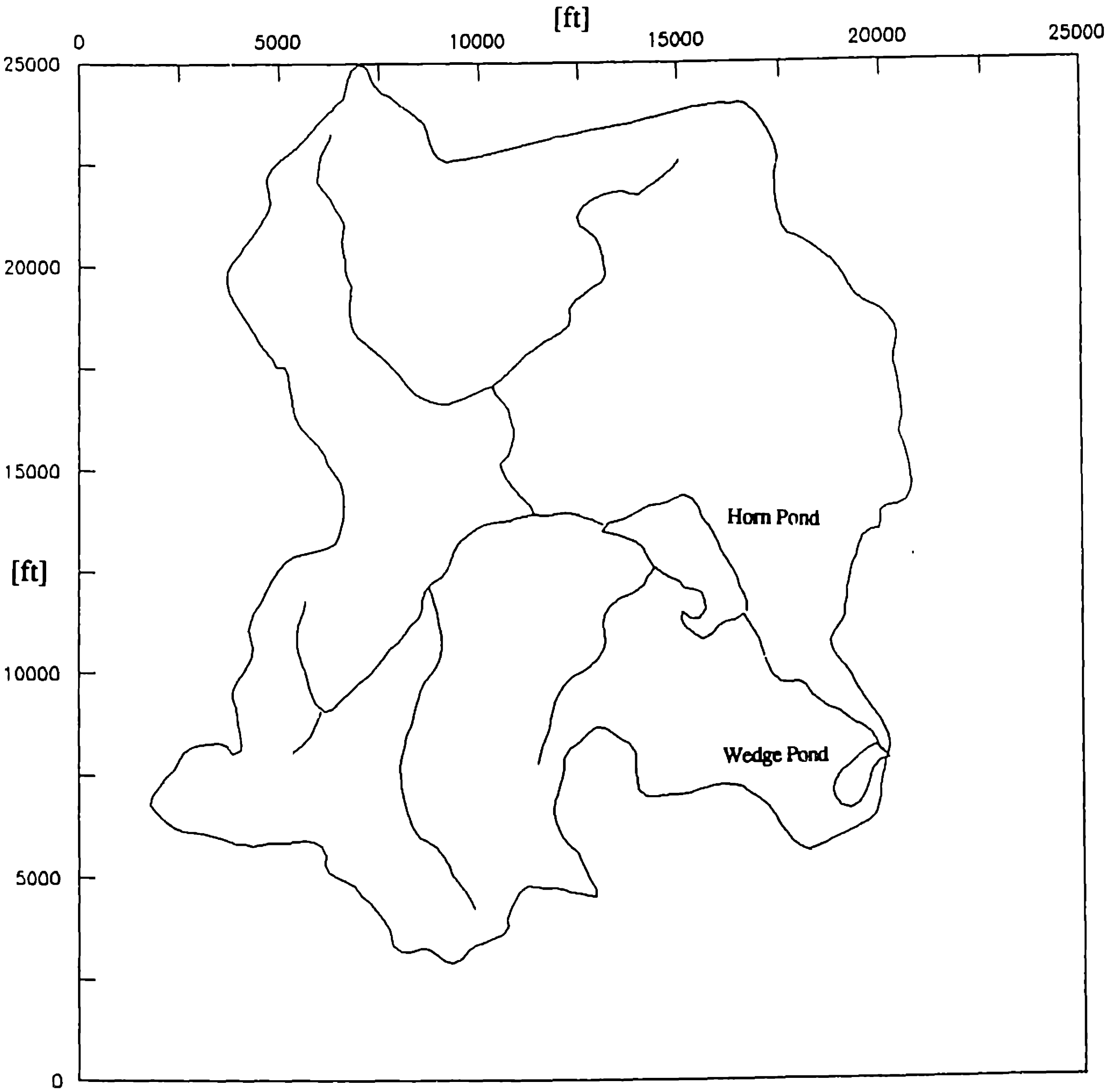

Figure 16. Horn Pond Drainage

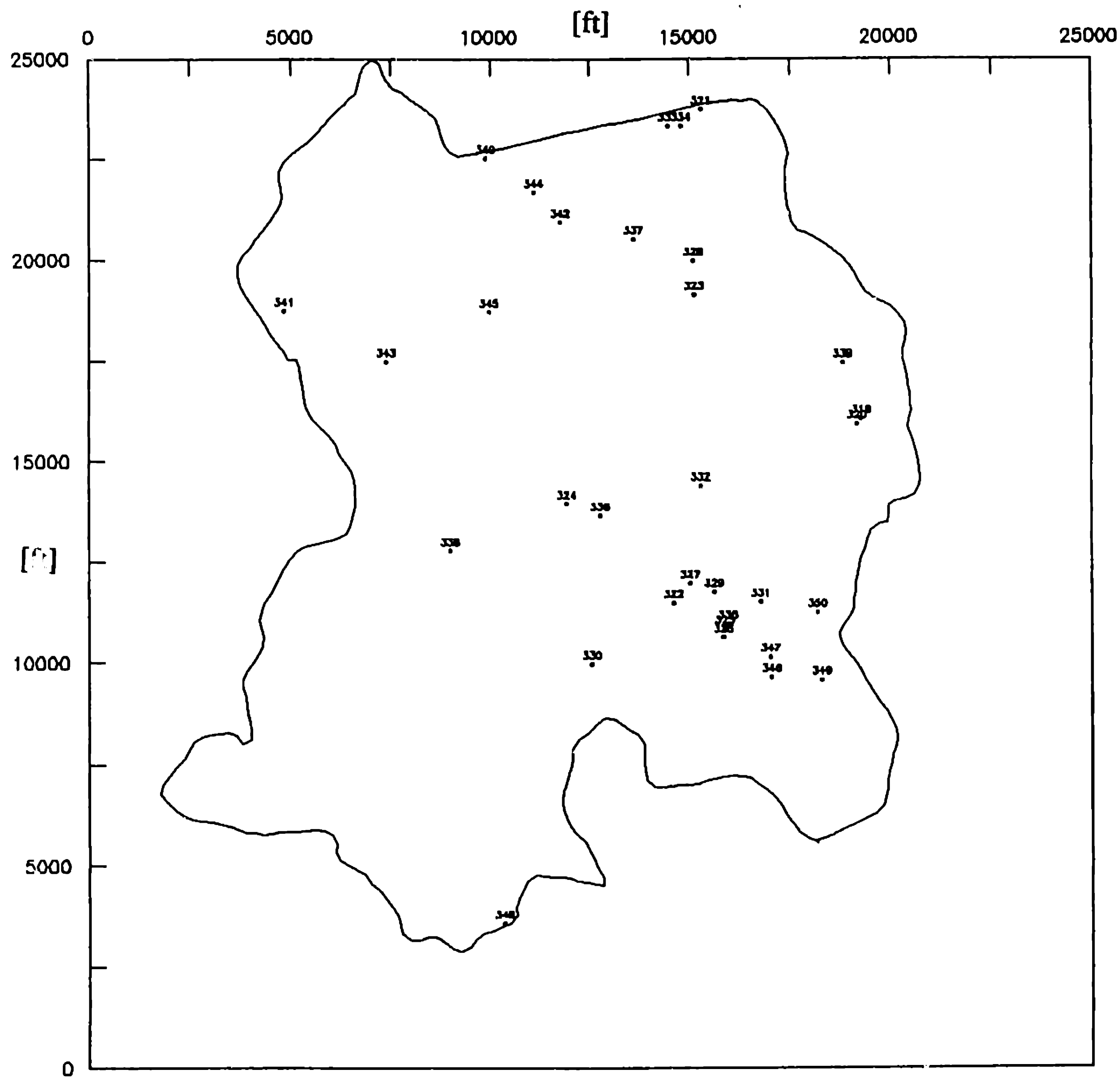

Figure 17. Horn Pond Well Locations

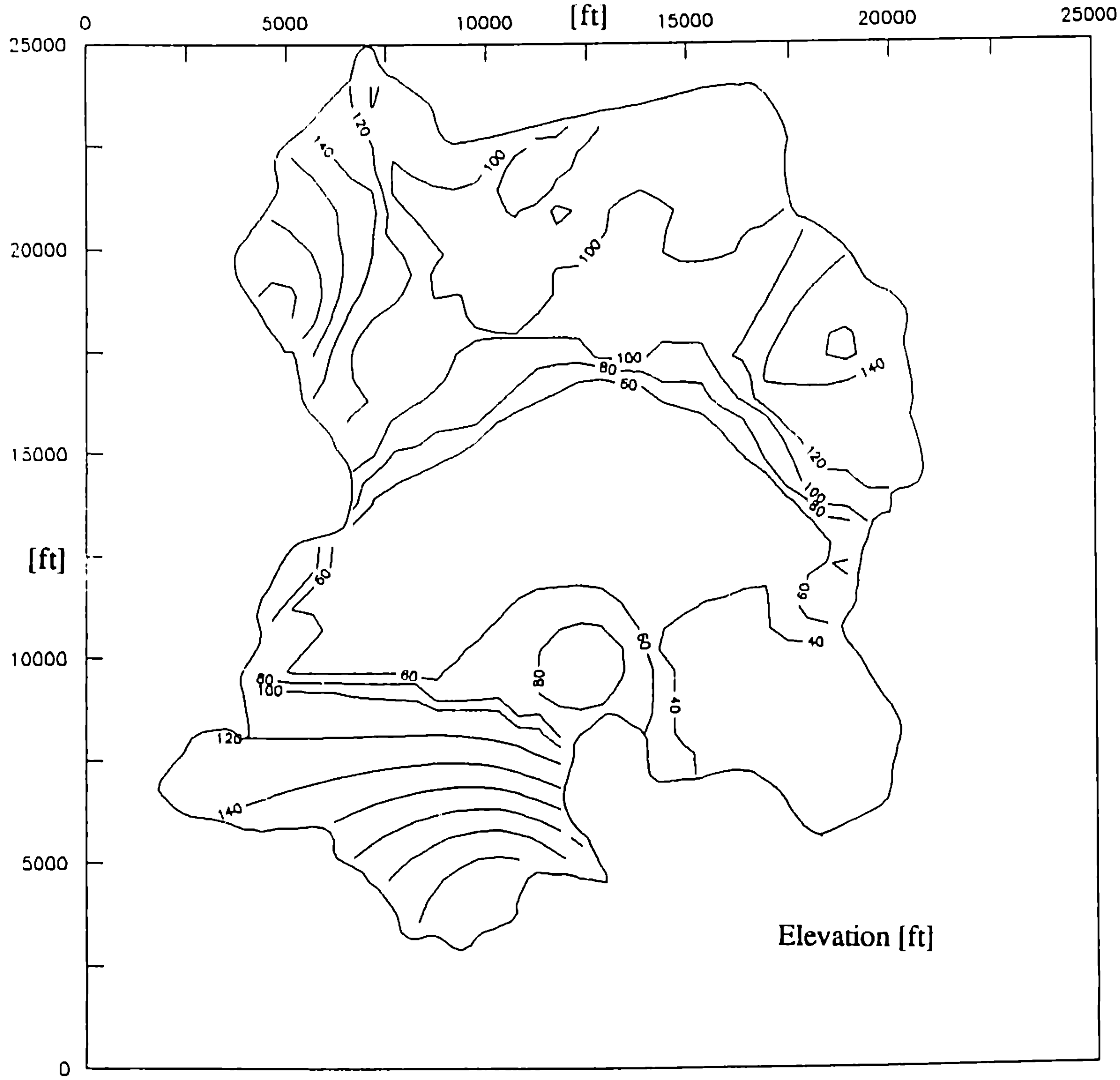

Figure 18. Horn Pond Water Table Contours

The flux into the river can be approximated as

$$Q = T\frac{\partial h}{\partial x}\Big|_{x=0} = \frac{T\pi a}{2L}\exp\left(-\frac{\pi^2 Tt}{2SL^2}\right) = Q_0 e^{-t/t_r} \quad ; \quad t_r = \frac{4SL^2}{\pi^2 T} \tag{9}$$

which indicates that the magnitude of the river discharge would decay exponentially during periods of no precipitation. Figure 19 is a semilogarithmic plot of the Aberjona River discharge at the USGS gauging station in Winchester for the 1987 water year, which ran from October 1, 1987, through September 31, 1988. Using the four recession limbs indicated on the figure, the time constant is 14.7 days.

The time constant may also be calculated with Equation 9 by using parameters appropriate for the watershed. An approximate specific yield for the unconfined aquifer of 0.20 was suggested by the USGS from the Wells G & H pumping test. Transmissivity from the specific capacity analysis is approximately 5000 ft^2/day. The solution is sensitive to the choice of the value for L, since it is squared in the equation. The width of the highly transmissive outwash regions of the aquifer located along the riser is approximately 1000 ft. The resulting time constant is 16.2 days.

The two estimates for the time constant closely agree. The low time constant calculated, approximately 15 days, indicates that the aquifer responds quickly to changes in recharge. The watershed has a small time constant because of the relatively small size of the watershed, and the high transmissivity of the glacial outwash.

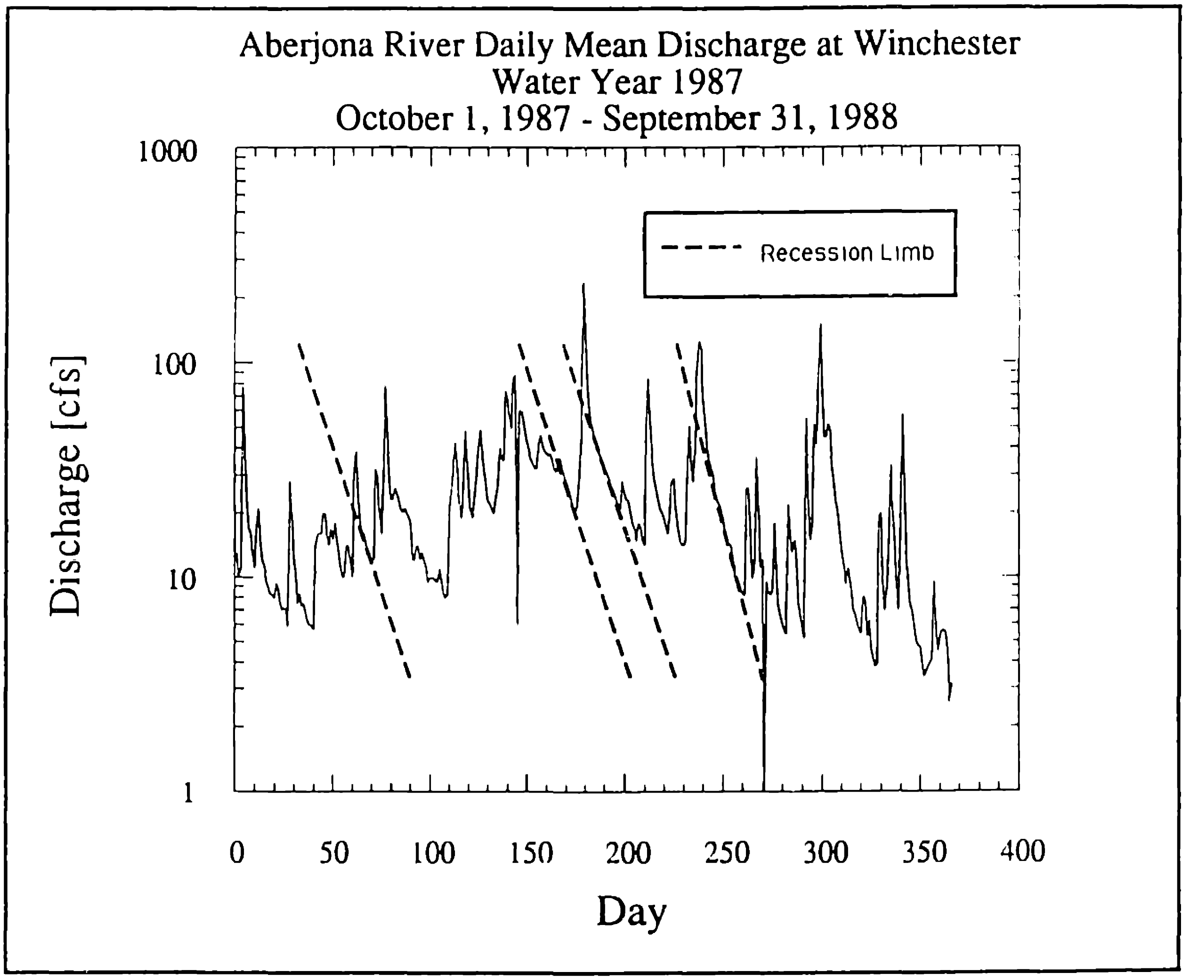

Figure 19. Aberjona River Discharge - 1987

3. REGIONAL GROUNDWATER FLOW MODELING

3.1 Goals

There are a number of motivations for developing a two-dimensional model of groundwater flow in the Aberjona basin. The process of modeling can be used to both organize and evaluate field data, as well as to develop and test a conceptual description of the important processes controlling groundwater flow. Since groundwater flow controls the advection of dissolved constituents, understanding the flow is crucial to understanding the transport of contamination. A calibrated flow model provides an estimate of piezometric potential and the distribution of hydraulic conductivity, allowing the prediction of flow paths and travel times for contaminants.

An estimate of surface-groundwater fluxes is of interest. These fluxes may be dependent on human activity such as groundwater withdrawals. A final goal of the groundwater modeling is to provide information concerning boundary conditions, which may be used for future modeling of small areas of specific interest.

3.2 Conceptual Model

A numerical groundwater flow model was calibrated for the Aberjona River sub-basin, which encompasses approximately one half of the Aberjona watershed. The model was two dimensional, vertically averaged, which is often referred to as the hydraulic approach [Bear, 1978]. The approximation assumes that the flow is essentially horizontal, which is justifiable because of the large horizontal dimensions of the aquifer relative to the vertical dimension. For the Aberjona sub-basin the thickness of the unconsolidated material is approximately 50 ft, while the horizontal distance from the river to the groundwater divide is approximately 5000 ft. Consequently the ratio of horizontal to vertical dimensions is 100:1. The hydraulic approach assumes hydrostatic conditions, with negligible vertical potential gradients, which is appropriate for the majority of the region except near boundaries such as partially penetrating rivers.

Steady state analysis was used, because of the short time constant of the aquifer of 15 days as discussed in Section 2.9. With the short time constant the system would rapidly adjust to variations of the recharge. The limited water level data available for calibration, which was measured during various seasons over many years, also did not justify transient analysis.

Recharge is from infiltration of precipitation, which was distributed uniformly over the watershed. The long-term average precipitation measured at Logan Airport in Boston of 44 inches/year was used. Assuming 50% infiltration, the recharge rate is 22 inches/year. The general flux of water is from distributed recharge to the point where the water exits the aquifer as it enters the surface waters.

The aquifer is phreatic, with the water level rising to the ground surface at discharge areas. The flow is primarily through the unconsolidated material overlying the bedrock, with the low-permeability bedrock acting as a boundary to flow.

3.3 Mathematical Basis of the Numerical Model

The groundwater flow model AQUIFEM [Wilson et al., 1979] was used, which is a two-dimensional finite-element model developed at MIT. The model uses triangular elements and linear interpolation functions. The governing equation for the system based upon a vertically averaged continuity equation and Darcy's equation is

$$S\frac{\partial h}{\partial t}=\frac{\partial}{\partial x}\left(T_{xx}\frac{\partial h}{\partial x}\right)+\frac{\partial}{\partial y}\left(T_{yy}\frac{\partial h}{\partial y}\right)+Q \tag{10}$$

where:

$S = S(x,y,t)$ = aquifer storage coefficient
$h = h(x,y,t)$ = depth-averaged piezometric head
$T_{xx} = T_{xx}(x,y)$ = transmissivity in the x direction
$T_{yy} = T_{yy}(x,y)$ = transmissivity in the y direction
$Q = Q(x,y,t)$ = net flux into the aquifer from point or distributed sources

For the case of steady flow and isotropic hydraulic conductivity Equation 10 simplifies to

$$\frac{\partial}{\partial x}\left(T\frac{\partial h}{\partial x}\right)+\frac{\partial}{\partial y}\left(T\frac{\partial h}{\partial y}\right)+Q=0 \tag{11}$$

For the phreatic aquifer, the equation is nonlinear, since the transmissivity is a function of the elevation of the phreatic surface.

$$T=K(x,y)[h(x,y)-z(x,y)] \tag{12}$$

where $z(x,y)$ is the elevation of the bottom of the aquifer

For a domain discretized into N nodes, a set of N nonlinear simultaneous equations must be solved. AQUIFEM iterates to solve the nonlinear equations, using an initial estimate for h, to calculate the transmissivity. For each iteration, the value of h is updated, until the iteration is terminated when the norm of the change of h in one iteration is less than a criteria value. The model is capable of handling rising water table conditions, which is the situation when the water table rises above the land surface. AQUIFEM has the option to set rising water table nodes to fixed head nodes at the land surface elevation.

3.4 Model Calibration

Figure 20 shows the discretization used, with a total of 282 nodes. The goal of the discretization was to have sufficient resolution in areas of interest, while minimizing the total number of nodes. The areas of interest were primarily the regions adjacent to the river, since the majority of the data available for calibration and the known hazardous waste sites are located in the high-transmissivity glacial outwash along the center of the valley. The till regions along the boundaries were included to supply the correct flux from precipitation to the areas of interest and to extend the domain to the no-flux boundary of the groundwater divide.

Boundaries must be defined in both the horizontal and vertical directions. Horizontal no-flux boundaries corresponding to a groundwater divide which was assumed to coincide with the surface water divide. A no-flux boundary was also imposed at the downgradient edge of the watershed where the river exits the watershed. The flux out of the aquifer parallel to the the river would be small compared to the flux through the river, since the gradient towards the river is much greater than the gradient parallel to the river.

The bedrock surface was used as the bottom of the aquifer. Although there is most likely flow across the bedrock upper surface, the hydraulic conductivity of the bedrock is significantly less than the hydraulic conductivity of the unconsolidated overlaying material. From Section 2.7, the ratio was approximately 0.9/80 ft/day or 1/100 for the outwash. In the till areas the ratio would be roughly 0.9/2 ft/ day or 1/2. To account for horizontal flow through the bedrock in the till regions, the thickness of the till layer was increased by lowering the elevation of the bedrock surface.

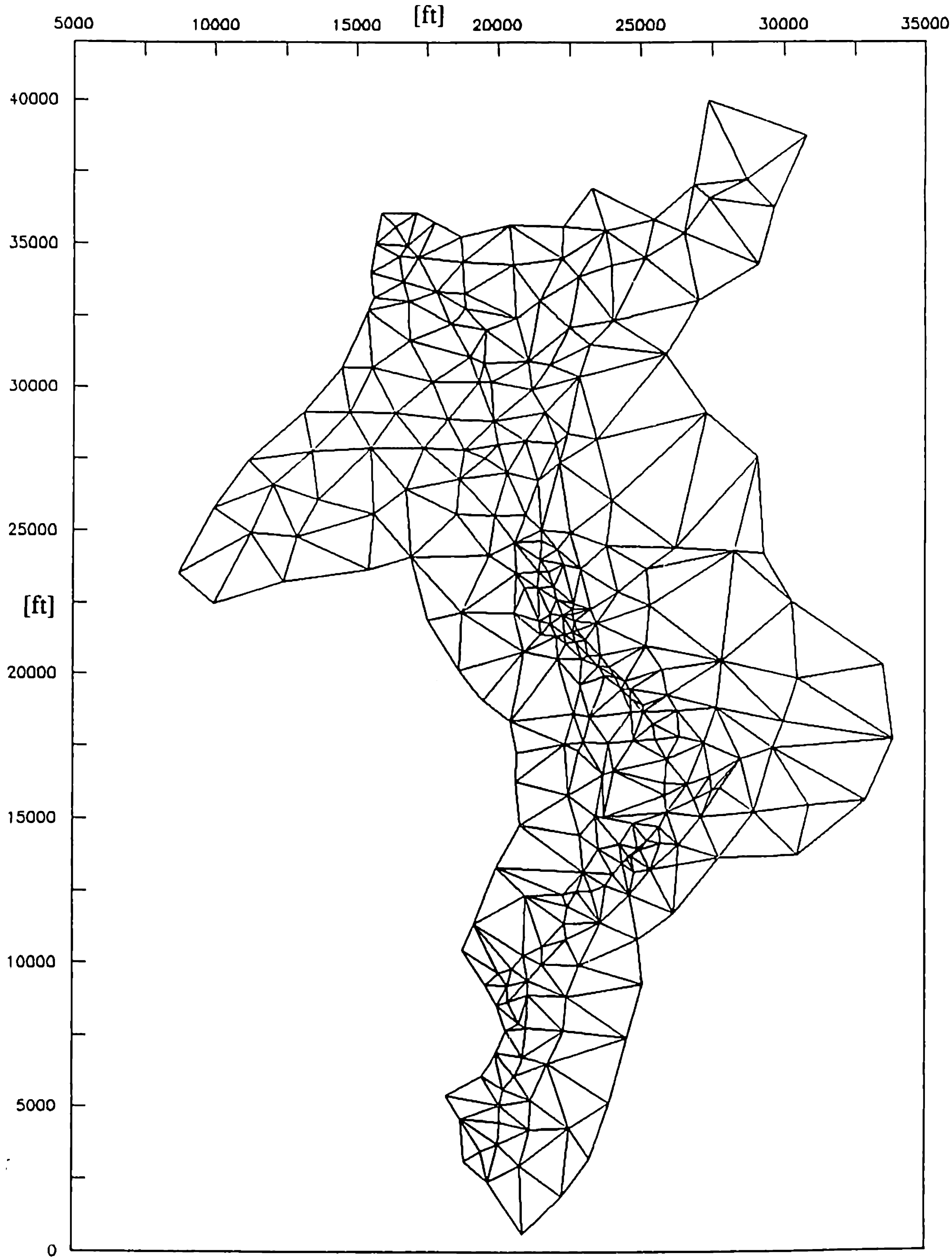

Figure 20. Two-dimensional Numerical Grid

Rivers and streams were approximated as fixed head boundary conditions. The location of the fixed head rivers is shown in Figure 21. A third type boundary condition, where the flux is dependent on the head, would be a better approximation. But this was not warranted considering the large-scale perspective and resulting averaging of a regional flow model. Third-type boundary conditions would be appropriate because the rivers are partially penetrating, and are probably lined by a layer of low-hydraulic conductivity silt. The elevation of the river for the fixed head node was interpolated from a topographical map.

Figure 22 is a contour plot of the land surface elevations used for the model. The data were taken from surveying of well data (Appendix 1) and interpolated from topographic maps. Figure 23 is a contour plot of the elevation of the bedrock surface used. The data are from well logs and maps of bedrock elevations interpolated from seismic surveys at the Well G & H site [NUS, 1986] and a region including the central area of the watershed [Ecology and Environment, 1982]. The bedrock elevation was estimated in some areas of the till regions.

Initially two hydraulic conductivity values were used: a value of 100 ft/day for the glacial outwash and 10 ft/day for the glacial till. The two regions were interpreted from the surficial geology (Figure 3) and are shown in Figure 24. The program AQUIFEM was modified to input the data values. The existing model required that data be entered as either values for each node or for each element. The data describing the bedrock elevation and the land surface are readily calculated as nodal values. The conductivity data is more appropriately treated as element values, since there are zones of different conductivities. The model was modified to allow aquifer bottom and surface elevations to be entered for nodes, and conductivities for elements.

The model was calibrated by varying the hydraulic conductivity in order to minimize the error of the calculated heads at locations where well water level data were available. Six conductivity zones were used in the final runs, with the hydraulic conductivity ranging from 0.1 to 75 ft/day. The final calculated errors at wells are shown in Figures 25 and 26. Figure 25 displays the magnitude of the error, with positive values indicating that the predicted heads were greater than the measured heads. Figure 26 represents the errors as closed and open circles, with closed circles indicating that the predicted head was too high and open circles indicating that the predicted head was too low.

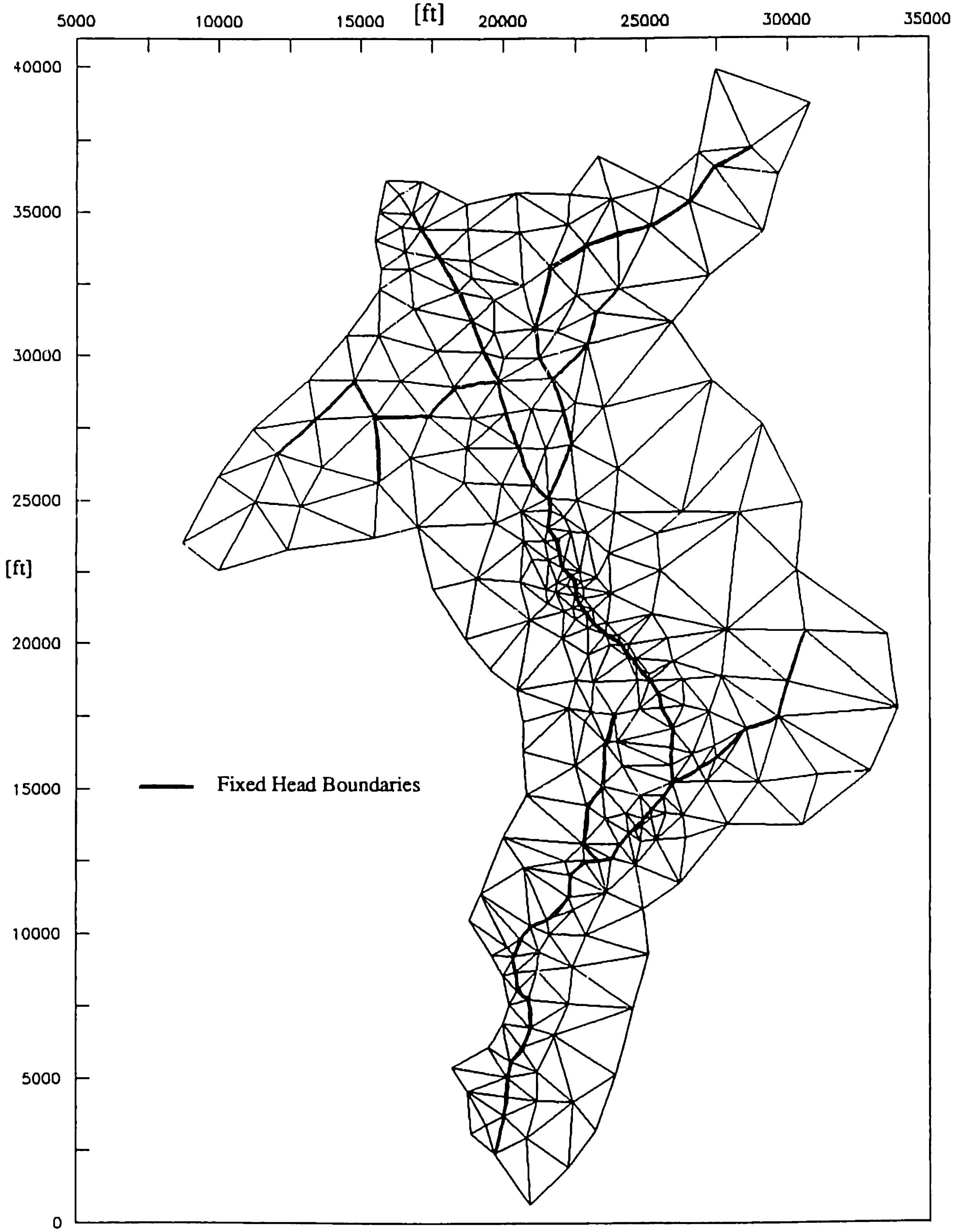

Figure 21. Fixed Head Boundaries

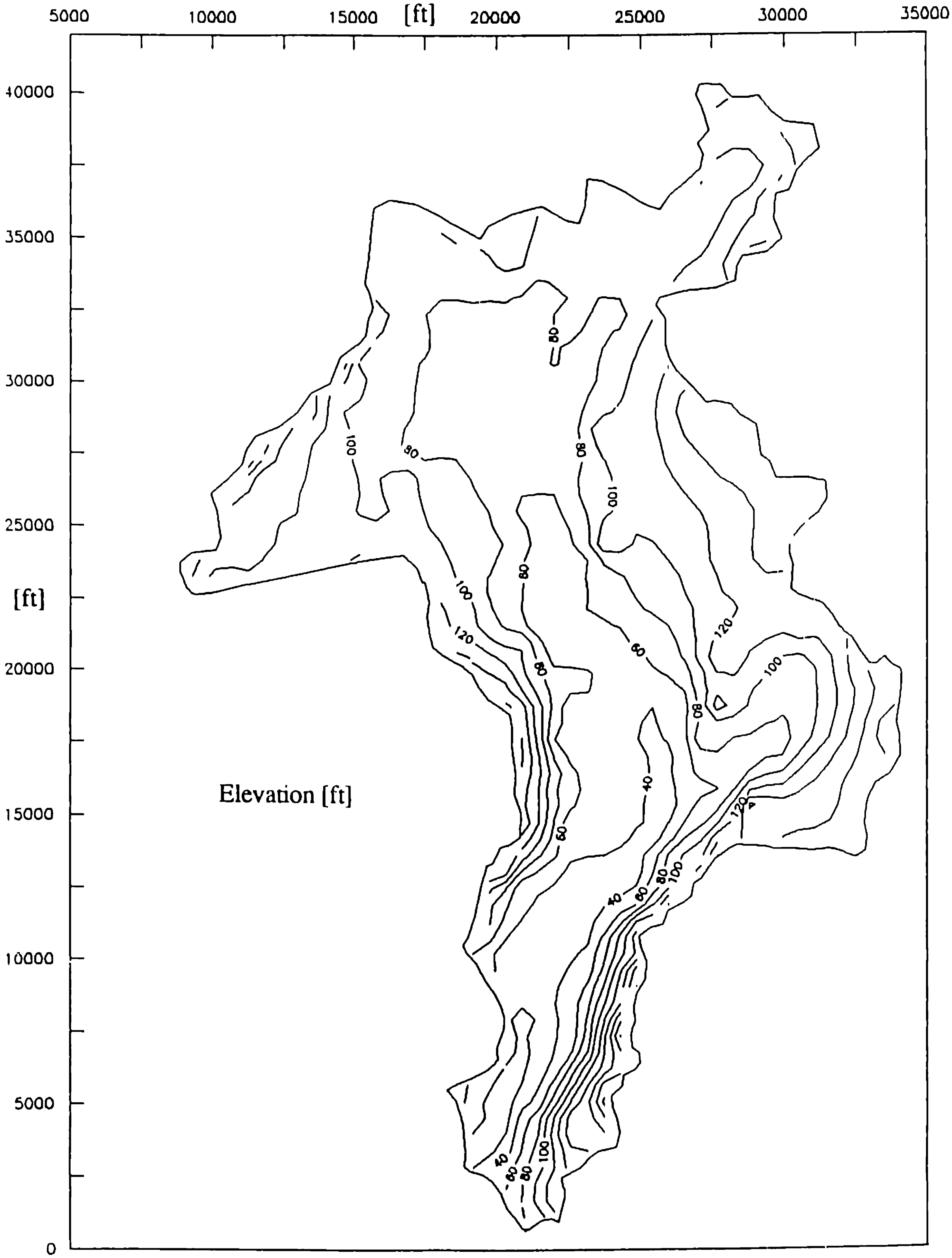

Figure 22. Land Surface Elevation

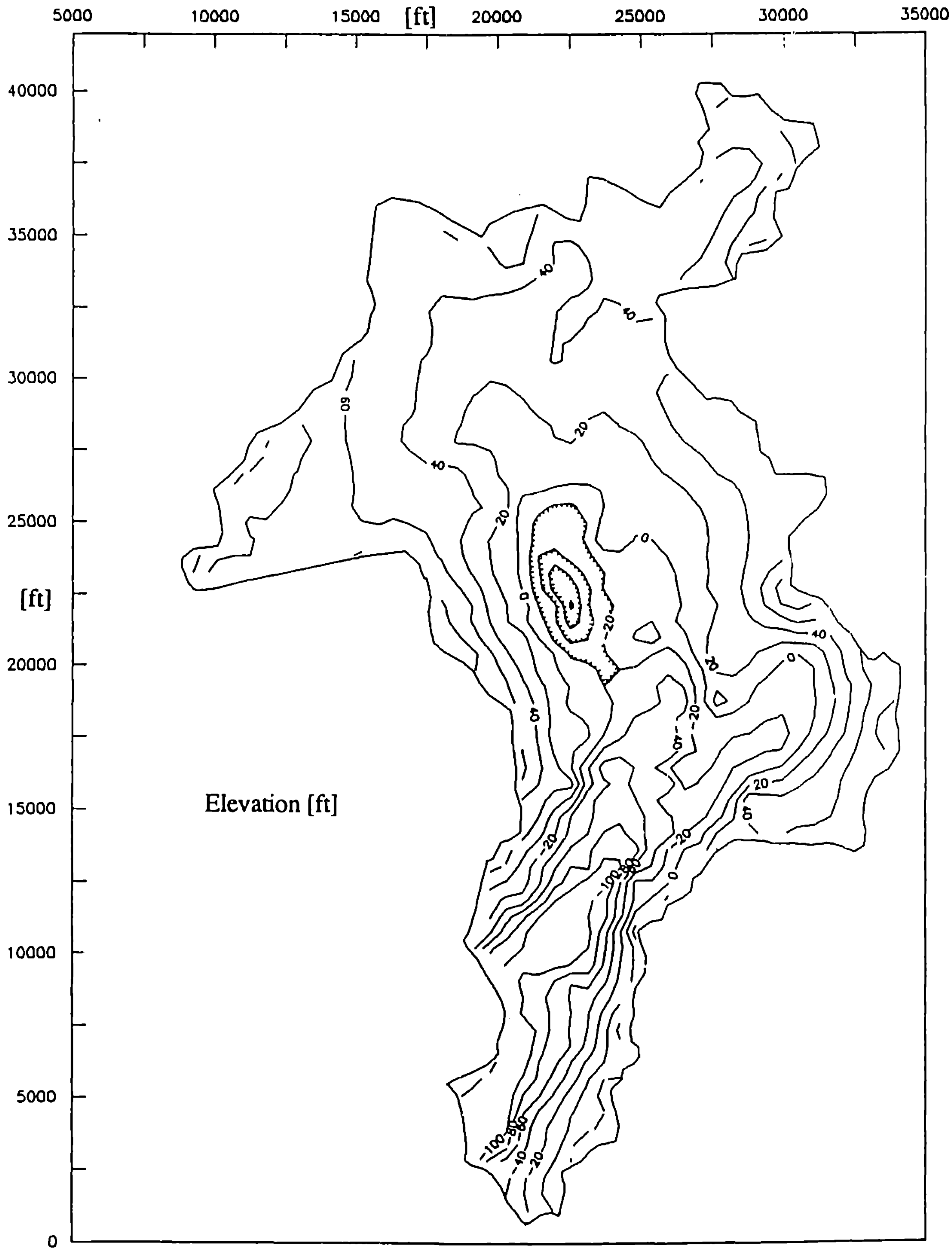

Figure 23. Bedrock Surface Elevation

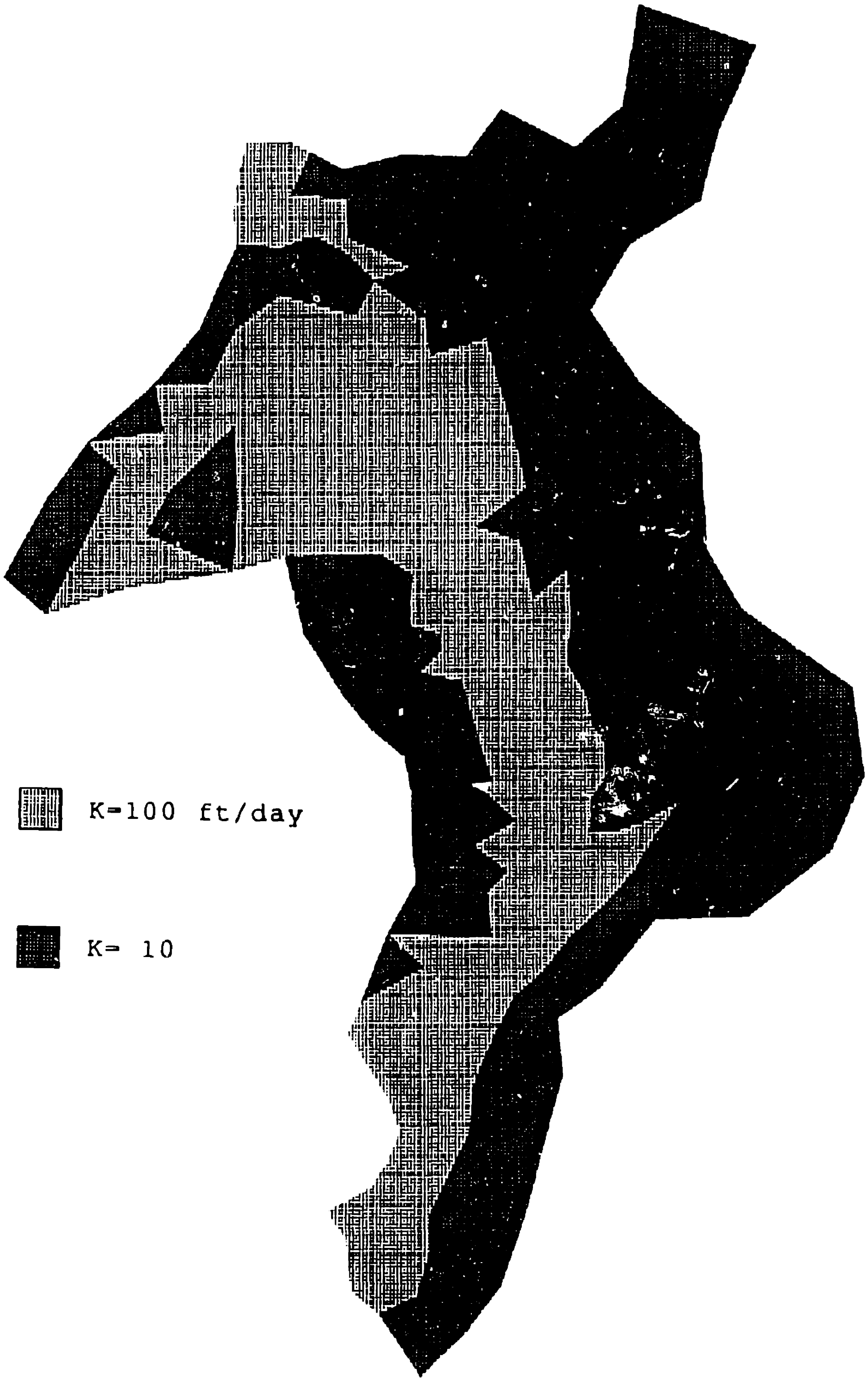

Figure 24. Initial Conductivity Zones

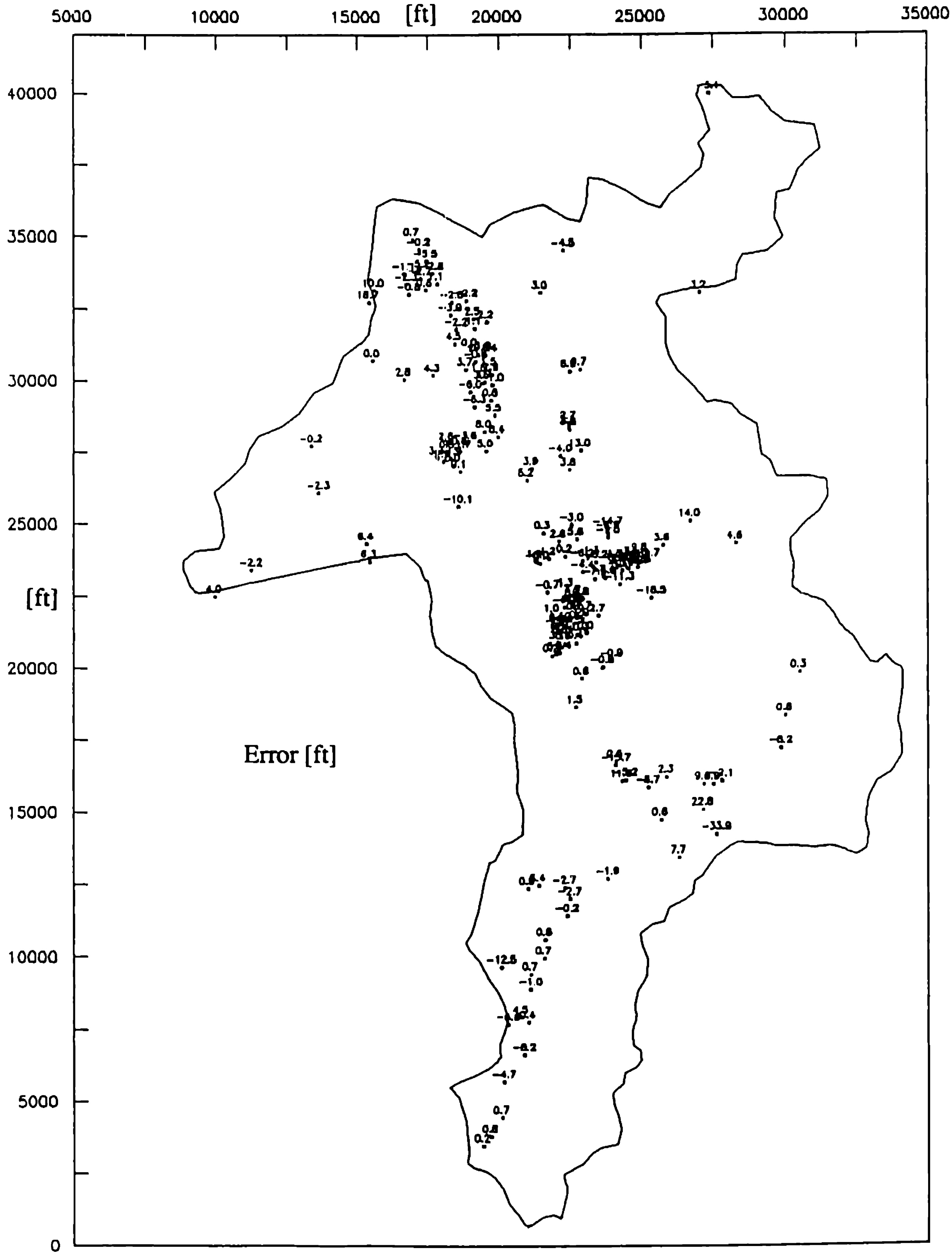

Figure 25. Final Error Map: numbers

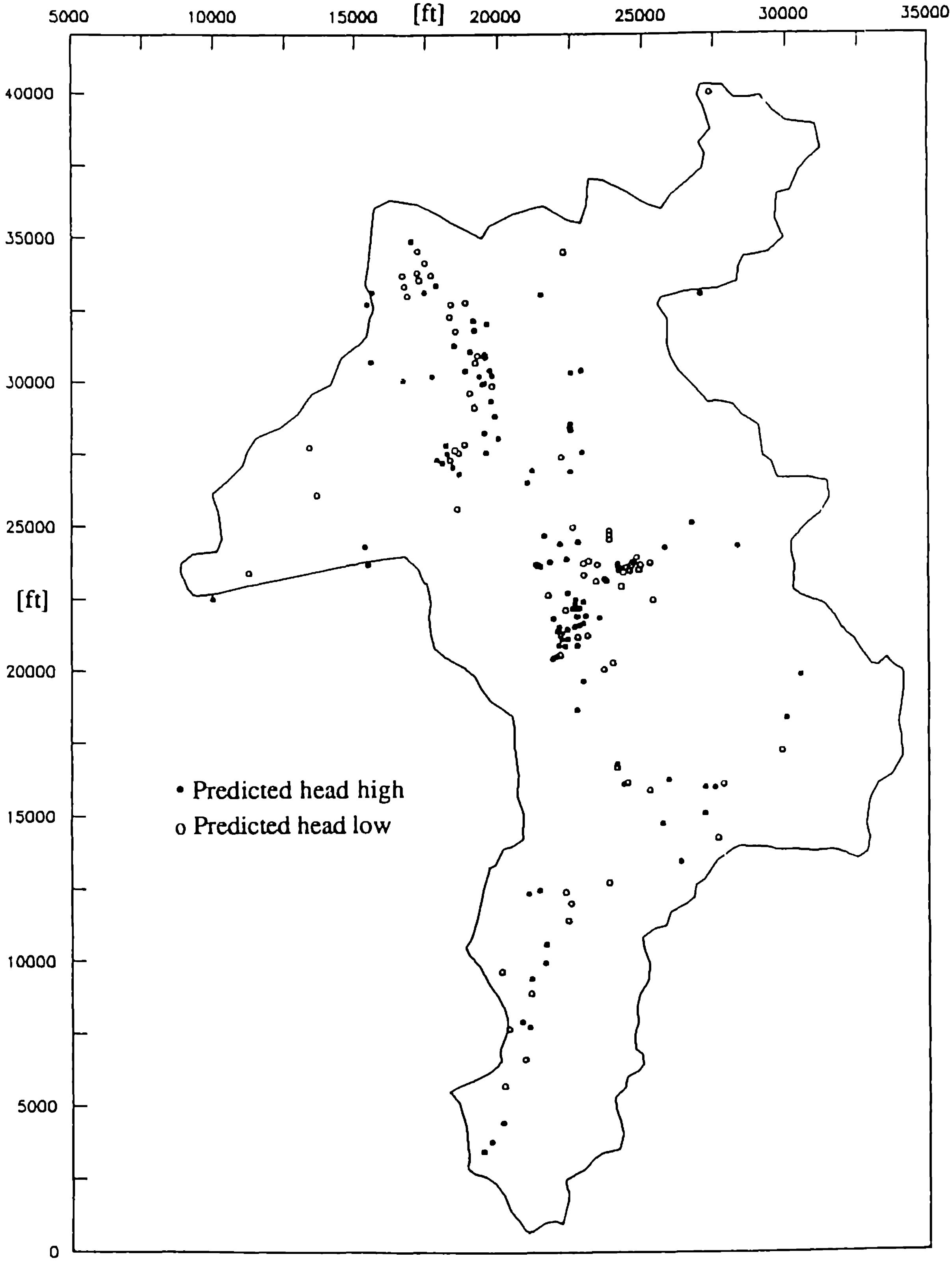

Figure 26. Final Error Map: symbols

Since there is considerable seasonal variability in the measured water elevation data, the procedure used during calibration was to remove any biases in the predicted water table elevation. Consequently in a region with many wells, approximately half of the circles should be open and half should be closed. Although the numerical values on Figure 25 are too tightly clustered to read, the general trend of the error can be interpreted from Figure 26.

3.5 Results

The final hydraulic conductivity values used in the calibration are displayed in Figure 27. The correlation to the measured water level data could have been improved by increasing the number of different conductivity zones. Considering that both the recharge and the conductivity are unknown, the solution is not unique. There is uncertainty concerning both the recharge and conductivity values. Consequently, it is not warranted to use many zones of different conductivities to exactly match the measured water level data.

Figure 28 is a contour plot of the predicted water table elevation from the final model run. In general the predicted water table is a smoothed version of the land surface. The shape of the phreatic surface follows the shape of the land surface because the surface streams and rivers are the groundwater discharge locations. These discharge locations control the groundwater potential. The smoothing of the phreatic surface is mainly a product of the resolution of the finite element grid used. The effect of the coarse grid is to smooth predicted potentials.

Streamlines may be drawn on Figure 28 perpendicular to the water table contours to estimate contaminant flow paths. The general path is perpendicular to the the river in the till regions, and turns slightly parallel to the river in the outwash region. This refraction of the flow paths is a product of the varying hydraulic conductivities. The groundwater flow is refracted as it crosses from the low transmissivity till to the high transmissivity outwash in the vicinity of the river. The refraction is apparent when viewing large scale groundwater contour maps of the Wells G & H site, where there is synoptic data.

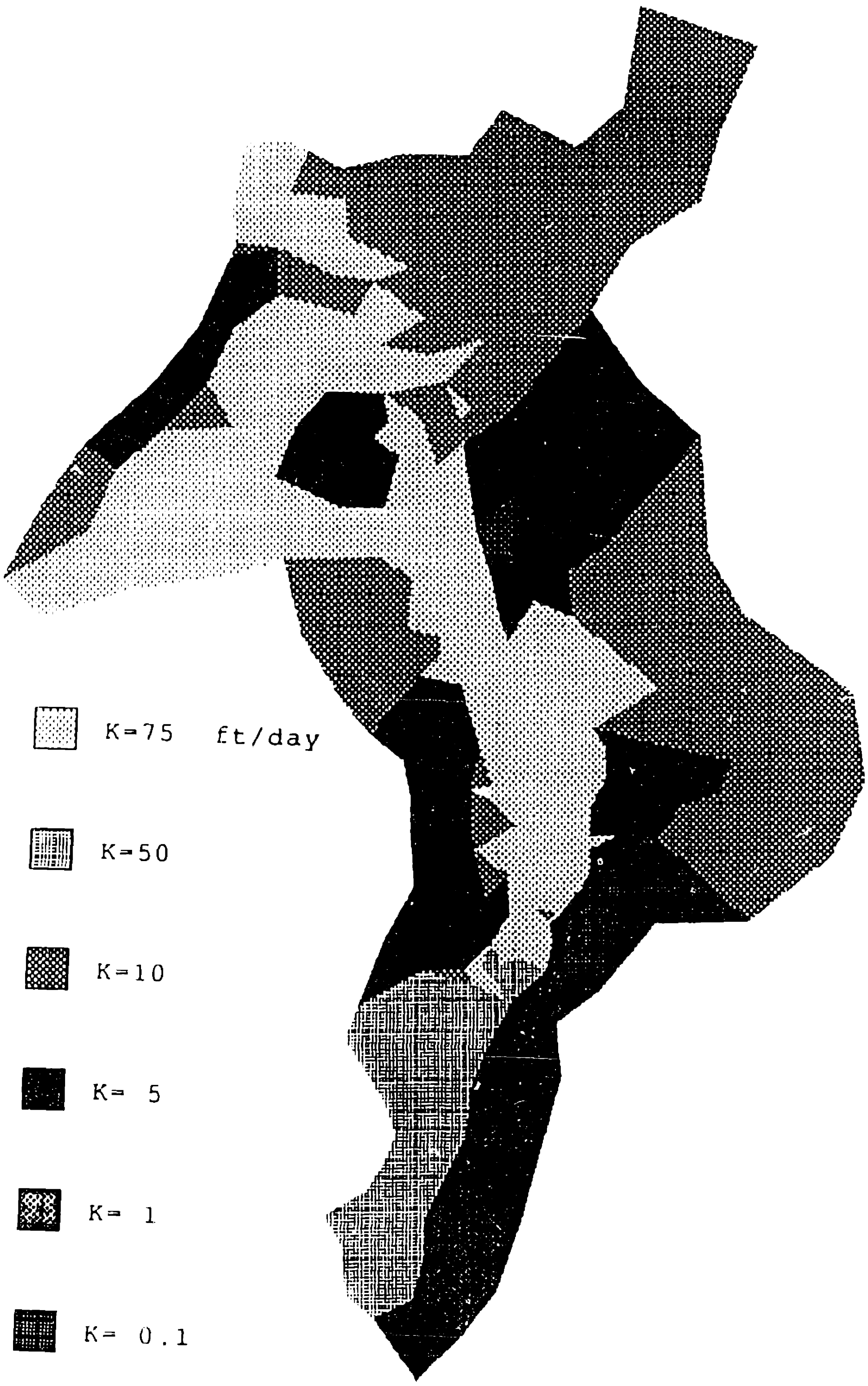

Figure 27. Final Conductivity Zones

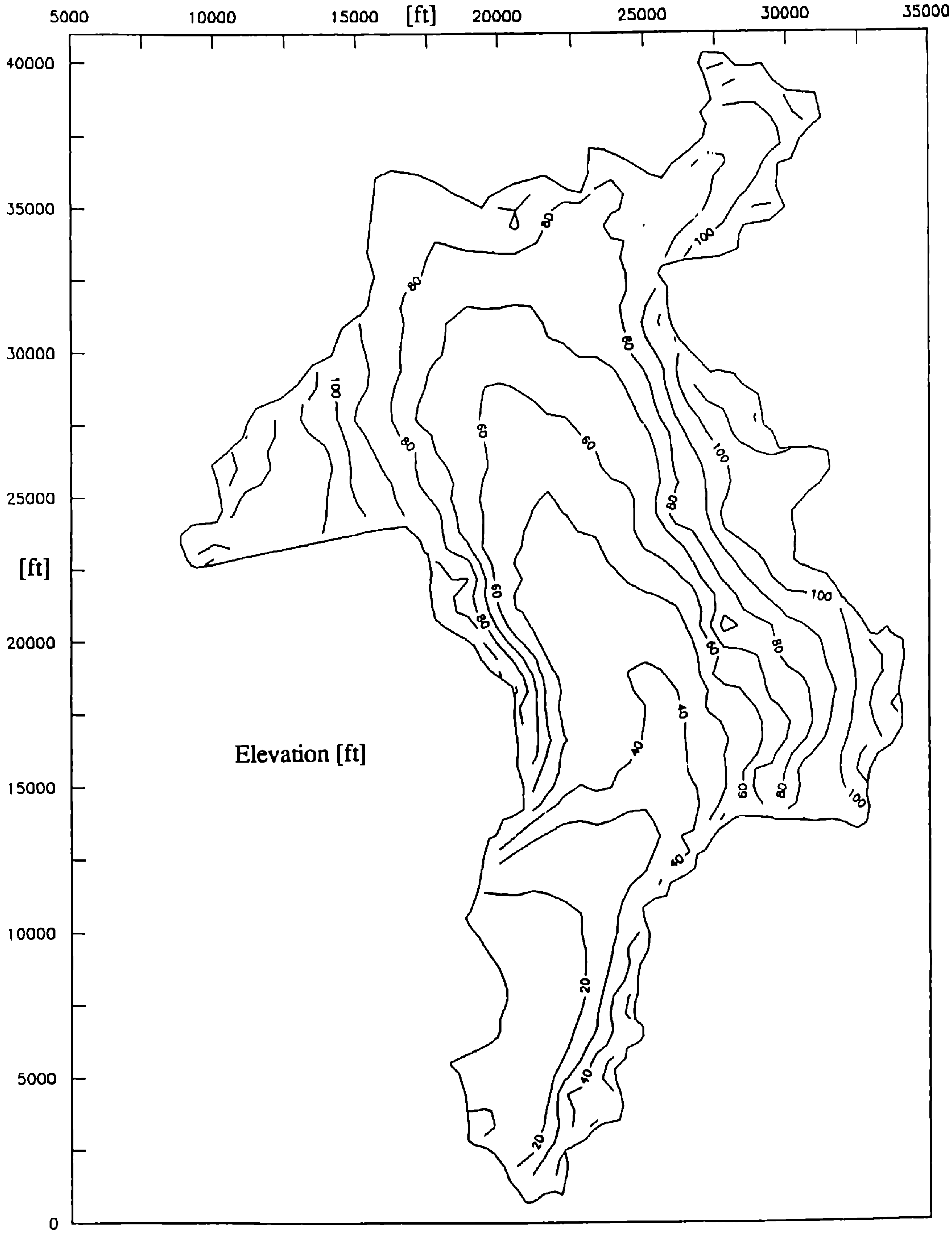

Figure 28. Simulated Water Table Contours

Using the predicted water elevation and hydraulic conductivity values, travel times for contaminants to reach points of discharge into surface water bodies may be calculated,

$$t = \int \frac{n\,ds}{q} \tag{13}$$

where t is the travel time, n the effective porosity, q is the specific discharge, and s is the distance along a streamline. The value of the time, t, would be calculated along a streamline from a contaminant source area to a discharge location. The integral may be approximated by using a flow net and summing over small segments of the streamline.

3.6 Discussion

The calibrated groundwater flow model satisfies the goal of describing the regional groundwater flow. The overall flow is from the upland areas to the surface water bodies. The largest gradients are found in the till areas, with the gentler gradients near the Aberjona River. The flow is perpendicular to the river in the till regions, and refracts to be almost parallel to the river in the outwash regions.

A relatively coarse grid was used for the modeling, because of the large area of interest. Because of the use of a coarse grid, the resulting predicted phreatic surface is a smoothed representation, and local features are not accurately described. To develop a more accurate description of the local groundwater flow, a large-scale model should be implemented. The regional model developed in this thesis could be used to provide appropriate boundary conditions for the more detailed large scale model.

As a result of the model calibration exercise, a number of suggestions for future work are possible. The goal of the model was to describe both the general groundwater flow in the till areas, and to provide a detailed description of the flow in the outwash areas. To achieve this goal, a coarse grid was used for the till regions, and a fine grid for the outwash regions. The two grid scales were necessary to limit the total number of nodes, and consequently the total number of equations to solve. The aquifer was modeled as a nonlinear phreatic aquifer where the transmissivity is dependent on the head as described in Equation 12.

Difficulties were encountered solving the nonlinear equations. The saturated thickness is relatively thin in the till regions, and changes of the estimated head have a large influence on the transmissivity. During the iterating of the nonlinear equations, the saturated thickness would become small at nodes located in the till. This would create a low transmissivity, sometimes zero, which would in turn cause greatly varying heads at upgradient nodes. To reduce the impact of widely oscillating transmissivities during iterating, the changes of head allowed during each iteration were limited. The goal was to produce a monotonic convergence of the head calculations.

Another approach would be to use linear equations with a coarse grid to solve the regional model. The results from the regional model would then be used to formulate boundary conditions for a large scale local model using a fine grid. The local model would provide high resolution results for the area of particular interest.

4. INFLUENCE OF VERTICAL FLOW ON GROUNDWATER TRANSPORT

4.1 Introduction

Considerable effort and resources are expended in the study of groundwater contamination originating from point sources such as underground storage tanks or surface and subsurface disposal sites. Growing public concern over groundwater contamination and the desire to protect water supplies have been motivating forces. Other factors include federal and state hazardous waste legislation and private liability concerns.

The initial goal of groundwater contamination studies is to analyze field data to determine the significant processes involved. Describing the groundwater flow, which represents convection, is the first step of analyzing any transport problem. The graphical technique of flow net analysis can be used to provide a preliminary interpretation of groundwater flow. Simplified analysis techniques such as flow net analysis or two-dimensional modeling are useful because of limited field data and the desire for timely analysis.

The major simplification required for the use of flow nets and two-dimensional modeling is that nearly hydrostatic conditions exist. The flow is assumed to be predominantly horizontal and the head, regarded as the vertical average, varies only in the horizontal. The effect of recharge from precipitation or discharge to partially penetrating streams can cause the heads to deviate from hydrostatic conditions. An analytical solution which may be used to understand the effect of non-hydrostatic conditions on groundwater flow in the vicinity of a partially penetrating stream is developed in this paper. The analytical solution predicts how the flow paths would deviate from the hydrostatic case, and can be used to extend the use of flow net analysis to estimate the path of contaminant transport to a stream. The analytical solution is useful as a screening tool to determine the importance of vertical flow for a specific field situation.

This section will focus on the case of groundwater flow to a partially penetrating stream which overlays an aquifer composed of unconsolidated materials. Figure 29 is a schematic representation showing the head distribution in plan and cross sectional views. This type of stream-connected aquifer system is common in humid areas and is of particular interest in New England because of the extensive development of buried valleys for industrial sites and for water supplies. Recharge from precipitation drives the groundwater flow, with the rainfall flux entering the aquifer at the phreatic surface and leaving at the stream. The stream flows from right to left in the illustration, and has a moderate hydraulic slope down the valley.

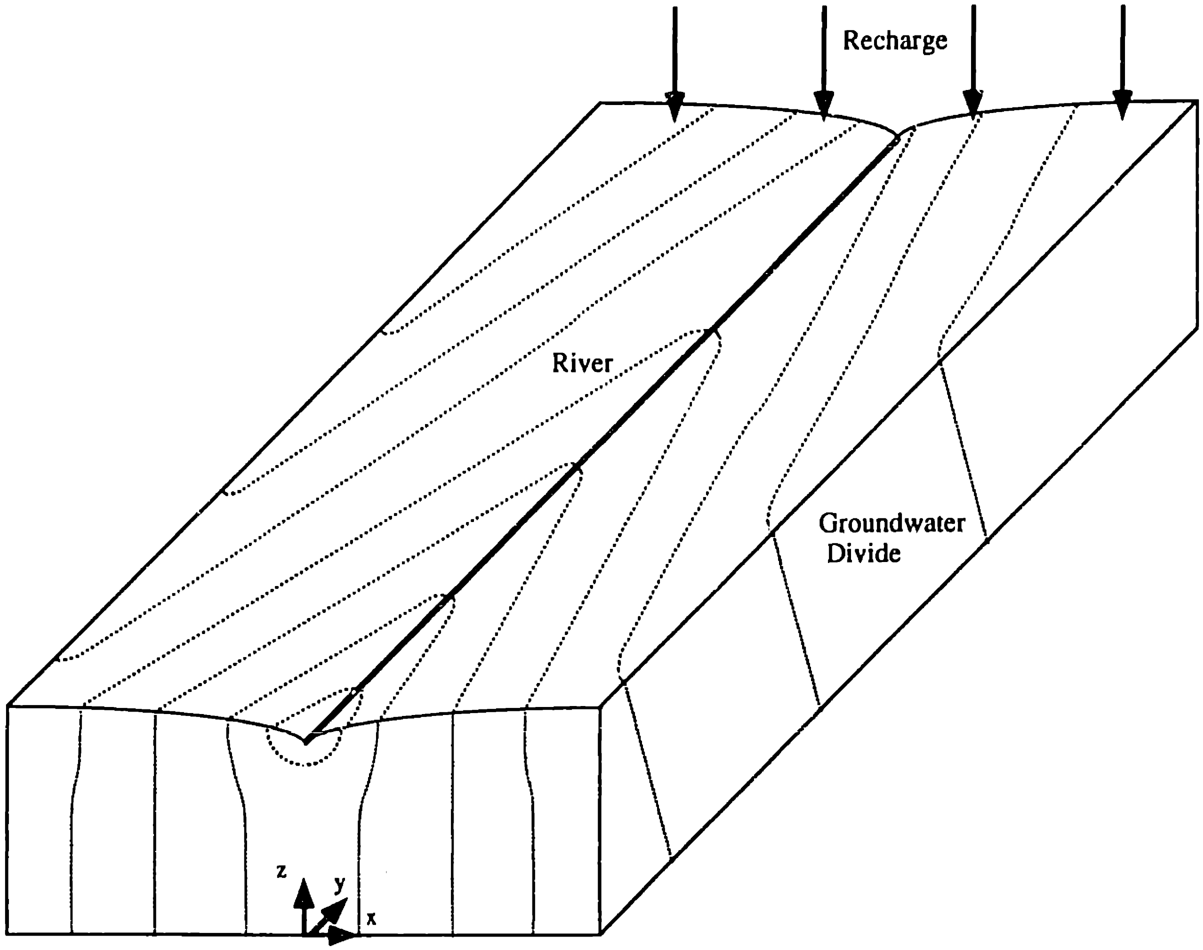

Figure 29. Schematic of Aquifer with Head Equipotentials

Because of the three-dimensional flow, the actual streamlines would differ from those predicted by a vertically average analysis, and water originating from any source location would enter the stream further downstream than a vertically averaged analysis would indicate. In the following sections, we will analyze the assumptions of two-dimensional analysis, and then develop an analytical solution to determine what parameters cause departure from the vertically averaged case. Next, the results from three-dimensional numerical simulations are compared with the analytical solution to verify the simplifying assumptions of the improved analytical solution. The coordinate system displayed in Figure 29 is used. The origin is located at the bottom of the aquifer with the x-axis perpendicular to the stream, the y-axis parallel to the stream, and z positive upward.

Since flow to partially penetrating streams is analogous to flow to agricultural drains, a review of agricultural drainage research provides useful background for the problem of transport. Drainage of agricultural areas by parallel horizontal drains is a similar problem as flow to partially penetrating streams, since the converging flow in the vicinity of the drains affects the flow. Although research on agricultural drainage focuses only on the elevation of the phreatic surface, some of the simplifications are useful for analyzing groundwater transport. The problem of steady flow through saturated homogeneous isotropic soil is complex because of the complicated boundaries including the nonlinear phreatic surface, and a number of approximations have been applied to the analysis.

In 1940, Hooghoudt [Bear, 1972] solved for the maximum elevation of the phreatic surface located midway between drains by assuming radial confined flow in the vicinity of the drain and horizontal Dupuit flow in the remainder of the region. At a distance of $h_r/\sqrt{2}$, where h_r is the saturated thickness at the drain, Hooghoudt assumed that the equipotentials are essentially vertical, and consequently the flow is horizontal. The boundaries of the aquifer bottom and the phreatic surface were accounted for by the use of image sinks in the derivation of the radial flow to the drain.

Kirkham [1958] solved for the elevation of the phreatic surface at any location in the domain without using Hooghoudt's assumption of purely radial and horizontal flow regions by the use of Fourier series. The solution is more exact than Hooghoudt's, but is cumbersome because of the calculation of the infinite Fourier series. Dagan [1966] extended Hooghoudt's analysis using the assumptions of radial and horizontal flow regions to calculate the elevation of the phreatic surface at any location. He assumed a horizontal phreatic surface in the radial flow region and neglected higher order terms in the solution. Dagan assumed that hydrostatic conditions exist at a distance of $2h_r$ from the drain, and assembled the two solutions at that location. The concept of a region of radial flow and a region of essentially horizontal flow is a useful approximation of the physical system, and will be used to analyze groundwater transport.

4.2 Vertically Averaged Analysis

Two-dimensional vertically averaged analysis, which includes graphically created flow nets, is often used to estimate flow paths when analyzing groundwater problems. Observed piezometric heads are contoured, and assuming isotropic hydraulic conductivity, the stream lines are drawn perpendicular to the head equipotentials. The water table is often used as the potential for a phreatic aquifer, with the assumption that the head distribution is hydrostatic in the vertical, and consequently the head throughout the aquifer is independent of the depth. This can be called the hydraulic approach.

Both flow net construction and two-dimensional numerical modeling are based on vertically averaged flow equations. Variations of head in the vertical can usually be neglected because aquifers tend to be very thin in the vertical relative to their large horizontal dimensions. Consequently the flow is largely horizontal [Bear, 1979]. However, significant vertical flow components may occur in the vicinity of partially penetrating wells or streams where the vertically averaged equations are not appropriate.

The hydraulic approach is a powerful and useful tool when solving for the head in many applications, since the errors in the horizontal head distribution introduced by the simplification are often small. But when analyzing flow from a recharge area to a discharge area, continuity constraints require that there will be non-zero vertical components to the flow and consequently there must be a variation of head in the vertical. A vertical cross-section of Figure 29 is analogous to regional groundwater systems as described by Hubbert [1940], with recharge areas located on the hill slopes and discharge areas in the valleys. The streamlines circulate to varying depths into the aquifer, with the depth increasing for source areas closer to the groundwater divide. As the water flows horizontally towards the discharge area, the vertical gradients reverse and the water rises to the stream.

The presence of nonhydrostatic conditions indicates that flow nets drawn from water table data would differ from those drawn from potentials measured at depth. Figure 30 is a representation of this, with a partially penetrating stream along the left boundary. Streamlines are drawn using equipotentials from the surface and the bottom of the aquifer. Streamlines drawn from the two different sets of equipotentials represent the two limiting cases of the possible flow paths, with the surface streamline underestimating the horizontal travel. The actual flow path would be located between these two extreme cases, with the exact location depending on the depth of the source area. An example of the correct streamline is also shown. The surface streamline would underestimate the location where the contaminant enters the stream by a distance d_y.

4.3 Analytical Derivations

An analytical solution can be derived for contaminant transport in the groundwater system depicted in Figure 29 to determine the amount by which analysis using the hydraulic approach would underestimate the distance travelled by a contaminant. The goal is to predict the path of a contaminant from a source area to the point where it would enter the stream. Radial flow is assumed near the stream, and the Dupuit approximation is used for the remainder of the aquifer.

The solution is composed of two components, the depth of circulation caused by the downward recharge flux and the horizontal distance travelled parallel to the stream. The two components are patched together to form the complete solution. Far from the stream the head will be essentially hydrostatic, and the Dupuit approximation may be used for the analysis. The distributed recharge will determine the streamlines, and the depth to which a contaminant will travel. Near the stream the flow will be radial towards the stream. Since there is a gradient parallel to the stream, the contaminant will travel parallel to the stream while it rises vertically to discharge into the stream. The effect of the vertical travel is neglected by the hydraulic approach. The combination of the gradient parallel to the stream and the vertical travel time will determine the value of d_y, which is the horizontal travel distance parallel to the stream neglected by two-dimensional analysis. The two components of the solution should be matched at a distance from the stream where the potential is essentially hydrostatic.

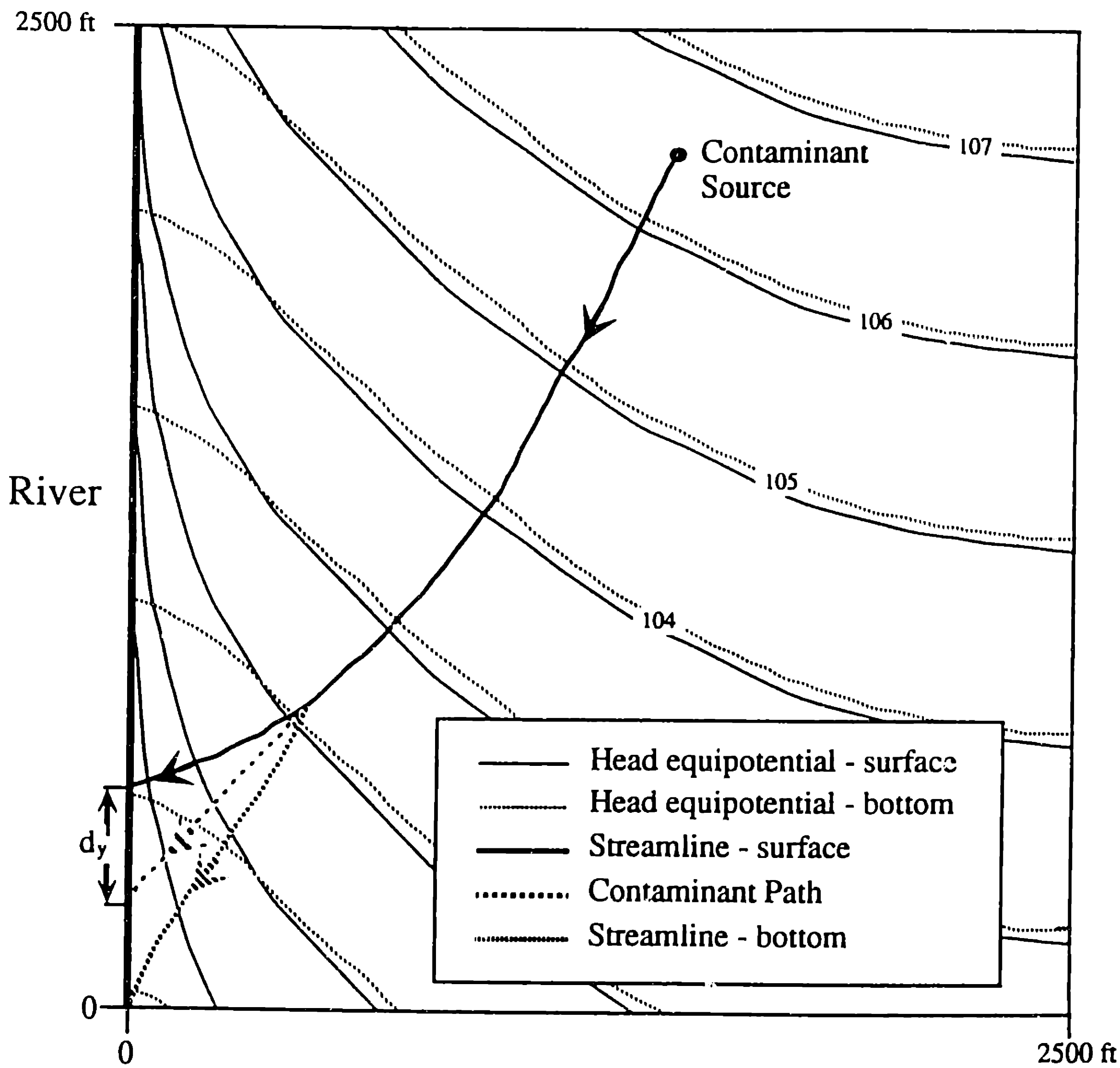

Figure 30. Flow Paths at the Surface and the Bottom of the Aquifer

The relationship between the depth of flow as a particle reaches the stream and the horizontal and vertical source area location can be determined from the Dupuit approximation [Gelhar and Wilson, 1974] applied to a stream connected phreatic aquifer [Figure 31]. The stream is assumed to be fully penetrating, and is represented as a fixed head boundary condition. The potential at the phreatic surface, ϕ, is simply equal to the elevation head, h, since the pressure head equals zero. The steady flow equation is

$$\frac{d}{dx}\left(Kh\frac{dh}{dx}\right)=-\varepsilon \qquad (14)$$

with h(x) representing the elevation of the phreatic surface as a function of horizontal position, h_r is the stream surface, K is the horizontal hydraulic conductivity and ε is the recharge rate. Using the no flux boundary condition at x=W, and the fixed head condition at x=0, the solution of Equation 14 is

$$h^2 - h_r^2=\varepsilon x(2W-x)/K \qquad (15)$$

which can be approximated by

$$h - h_r=\varepsilon x(2W-x)/(2h_rK) \qquad (16)$$

when the slope of the phreatic surface is small ($h - h_r << h_r$).

Using the steady flow field, the kinematics of the contaminant movement can be described. The horizontal specific discharge is

$$q_x=-K\frac{dh}{dx}=-\frac{\varepsilon(W-x)}{h_r}=\frac{\partial\Psi}{\partial z} \qquad (17)$$

where Ψ is the stream function. Solving by integration

$$\Psi=-\frac{\varepsilon(W-x)}{h_r}z \qquad (18)$$

The flow path of a particle will be along a constant streamline. To analyze the path of a particle originating at the surface, consider the streamline passing through the point (x_0,z_0).

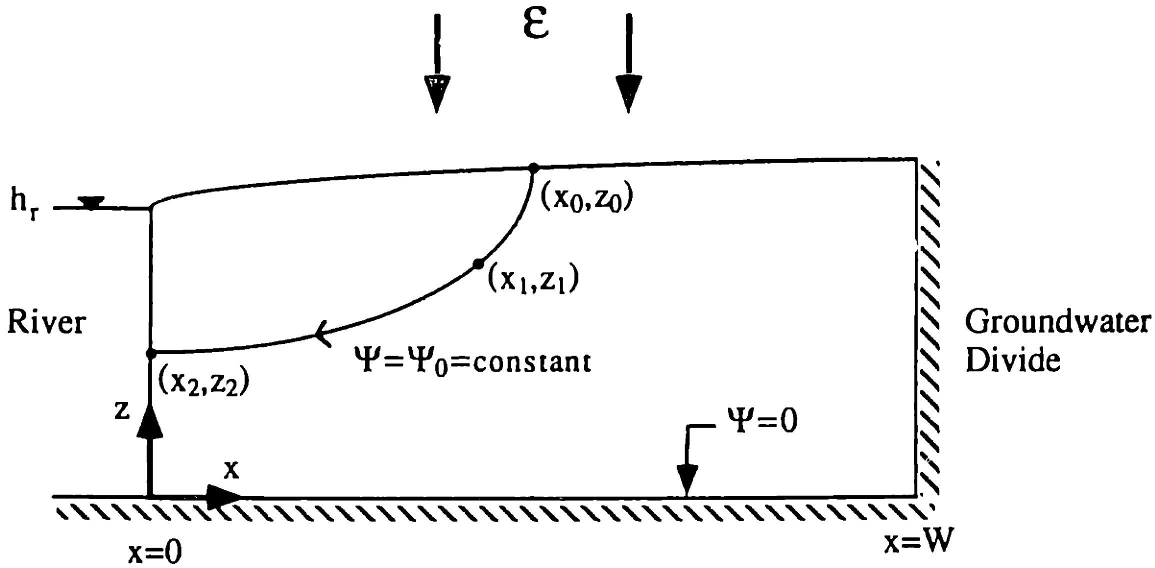

Figure 31. Flow with Dupuit Approximation

$$\Psi=\text{constant}=\Psi_0=-\frac{\varepsilon(W-x_0)}{h_r}z_0 \tag{19}$$

The vertical location of the particle evaluated at x=0 may be determined by equating Equations 18 and 19 with x=0

$$\frac{\varepsilon W}{h_r}z_2=\frac{\varepsilon(W-x_0)}{h_r}z_0 \tag{20}$$

which leads to

$$z_2=z_0\left(\frac{W-x_0}{W}\right) \tag{21}$$

Equation 21 states that for a particle originating at the phreatic surface, there is a linear relation between the depth of the particle when it reaches the fixed head boundary and the source distance from the stream.

The effect of moving the source some depth beneath the surface is to increase the depth at which the particle arrives at the fixed head boundary. Consequently, the flow path for a particle originating at a depth below the surface is equivalent to the flow path of a particle originating at the surface, but at a greater distance from the fixed head boundary. The effective surface source location for a particle originating at depth may be determined by analyzing the streamline with $\Psi=\Psi_0$ passing through the location (x_1,z_1)

$$\frac{\varepsilon(W-x_1)}{h_r}z_1=\frac{\varepsilon(W-x_0)}{h_r}z_0 \tag{22}$$

which after rearranging yields the effective surface source location

$$x_0=x_1+\frac{(W-x_1)(h_r-z_1)}{h_r} \tag{23}$$

Equation 23 relates the effective source location, x_0, at the phreatic surface for a source located beneath the surface.

The second component of the analysis is the horizontal distance which a particle travels parallel to the stream while it rises from depth to discharge into the stream. In the vicinity of the stream, the flow is radial towards the stream [Figure 32], with the stream treated as a line sink. The figure depicts the equivalent isotropic system which has been horizontally distorted to account for an anisotropy of $K_h/K_v=10/1$. K_h and K_v are the principal components of the hydraulic conductivity tensor representing the horizontal and vertical hydraulic conductivity respectively. The system is horizontally isotropic. Streamlines representing stream tubes of equal flux are shown. The statement of conservation of mass and Darcy's equation is

$$K_h \frac{\partial^2 \phi}{\partial x^2} + K_v \frac{\partial^2 \phi}{\partial z^2} = 0 \tag{24}$$

for steady flow in a homogeneous anisotropic media, where ϕ is the potential. Converting to an equivalent isotropic system by coordinate transformation yields

$$\frac{\partial^2 \phi}{\partial x'^2} + \frac{\partial^2 \phi}{\partial z'^2} = 0 \tag{25}$$

where $x'=x(K_v/K_h)^{1/2}$ and $z'=z$.

Since the solution for the potential is linear in the flux, the method of images may be used to account for geometry of the aquifer. Both the aquifer bottom and the phreatic surface are treated as no flux boundaries. The exact solution for the potential with the two no flux boundaries requires the use of an infinite number of image sinks located along the z-axis, and located a distance 2b apart, with b the thickness of the aquifer. Using a conformal transformation, the solution in the equivalent isotropic aquifer [Lamb, 1945] is

$$\phi = C_1 \ln\left[\cosh\left(\frac{\pi}{b}x'\right) - \cos\left(\frac{\pi}{b}(z-b)\right)\right] + C_2 \tag{26}$$

with the stream located at (0,b). In the original anisotropic coordinate system the solution is

$$\phi = C_1 \ln\left[\cosh\left(\frac{\pi}{b}\sqrt{K_v/K_h}\,x\right) - \cos\left(\frac{\pi}{b}(z-b)\right)\right] + C_2 \tag{27}$$

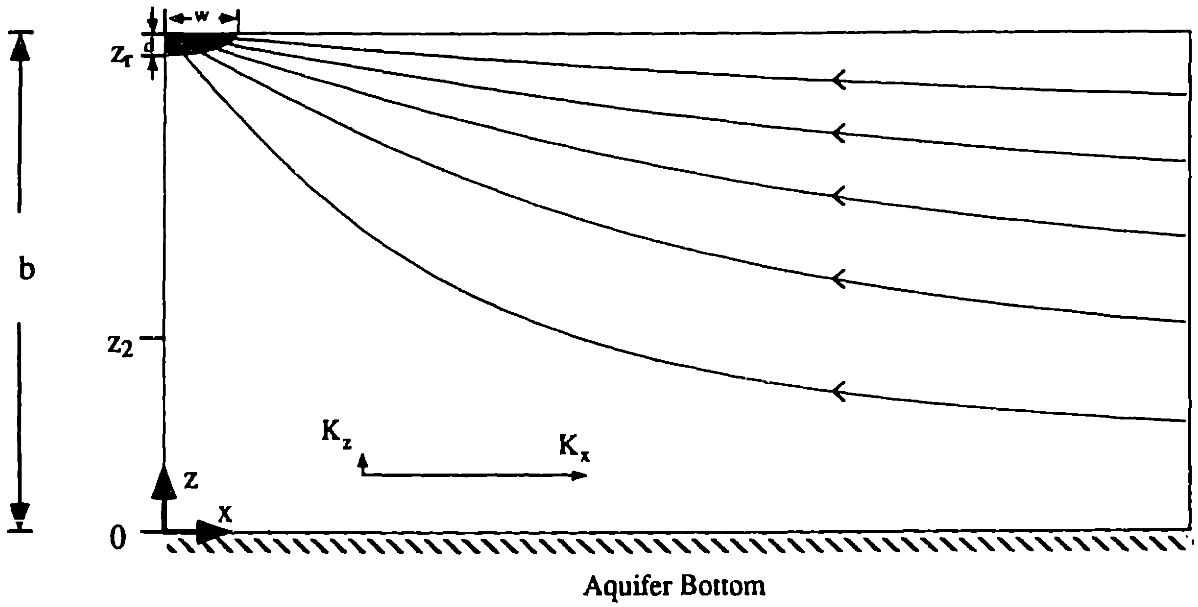

Figure 32. Radial Flow to the River

The constant C_1 is dependent on the flux and C_2 is dependent on the potential at the perimeter of the stream. The coefficient C_1 may be evaluated from the flux to the stream Q, which is equal to εW, the product of the recharge rate and the distance from the stream to the groundwater divide. The horizontal specific discharge equals

$$q_x = -K_h \frac{\partial \phi}{\partial x} = -C_1 K_h \frac{\frac{\pi}{b}\sqrt{K_v/K_h}\sinh\left(\frac{\pi}{b}\sqrt{K_v/K_h}\,x\right)}{\cosh\left(\frac{\pi}{b}\sqrt{K_v/K_h}\,x\right) - \cos\left(\frac{\pi}{b}(z-b)\right)} \tag{28}$$

Integrating the vertical specific discharge over the thickness of the aquifer yields the total flux. The integral is evaluated as x approaches infinity, and consequently the specific discharge is independent of z.

$$C_1 = \frac{-Q}{\pi\sqrt{K_h K_v}} = \frac{-\varepsilon W}{\pi\sqrt{K_h K_v}} \tag{29}$$

The constant C_2 in Equation 28 accounts for a finite stream width, and may be evaluated from the boundary condition $\phi = \phi_r$ at $x = x_r$ and $z = z_r$, along the perimeter of the stream. At the point where the stream perimeter intersects the vertical axis x is equal to zero, and the depth of the river, d, is equal to $b - z_r$. Using the boundary condition to solve for C_2 yields

$$\phi = \phi_r + \frac{\varepsilon W}{\pi\sqrt{K_h K_v}} \ln\left[\frac{1-\cos\left(\frac{\pi}{b}d\right)}{\left[\cosh\left(\frac{\pi}{b}\sqrt{K_v/K_h}\,x\right) - \cos\left(\frac{\pi}{b}(z-b)\right)\right]}\right] \tag{30}$$

The perimeter of the stream, defined as a curve of constant potential, will not be circular. This is because of the distortion induced to account for the anisotropy, and the influence of the image sinks used to account for the boundaries. It is useful to relate the half-width of the stream, w, which is readily observable in the field, to the depth of the stream, d. For a stream with a depth much less than the aquifer thickness, the stream perimeter will be an ellipse; and the half-width and depth of the stream are related by the anisotropy

$$d = \sqrt{K_v/K_h}\, w \tag{31}$$

The travel time for a particle starting at some initial elevation to rise vertically and reach the stream is evaluated as the integral of the distance divided by the vertical velocity. The specific discharge is the derivative of the head with respect to z

$$q_z=-K_v\frac{\partial\phi}{\partial z}=\frac{\varepsilon W}{b\sqrt{K_hK_v}}\left(\frac{\sin\left(\frac{\pi}{b}(z-b)\right)}{\cosh\left(\frac{\pi}{b}\sqrt{K_v/K_h}\,x\right)-\cos\left(\frac{\pi}{b}(z-b)\right)}\right) \tag{32}$$

which is dependent on both x and y. To develop an analytical solution for the travel time, since q_z cannot be solved for directly with dependence on both x and z, the specific discharge directly beneath the stream may be used

$$q_z\,\big|_{x=0}=\frac{\varepsilon W}{b\sqrt{K_hK_v}}\left(\frac{\frac{\pi}{b}\sin\left(\frac{\pi}{b}(z-b)\right)}{1-\cos\left(\frac{\pi}{b}(z-b)\right)}\right) \tag{33}$$

By evaluating the vertical specific discharge at x=0, the horizontal and radial solutions are patched together at x=0. Equation 32 shows that the vertical specific discharge has a maximum value at x=0, therefore the use of Equation 33 for the vertical travel time will yield the solution for the limiting case of the minimum travel time.

Figure 33 displays a vertical cross section of the aquifer taken through the stream. The path of a particle is shown as it travels parallel to the stream , while rising vertically to the point of discharge into the stream. The travel time from a starting vertical location z_2, to the perimeter of the stream, z_r, is equal to

$$t=n\int_{z_2}^{z_r}\frac{dz}{q_z}=\frac{2nb^2\sqrt{K_h/K_v}}{\pi\varepsilon W}\ln\left[\frac{\cos\left(\frac{\pi}{2b}(z_r-b)\right)}{\cos\left(\frac{\pi}{2b}(z_2-b)\right)}\right] \tag{34}$$

where n is the effective porosity. The value of z_r depends on the vertical dimension of the stream, which differs from the width of the stream because of the distortion. With a constant gradient parallel to the stream, a conservative contaminant will travel horizontally beneath the stream as it rises to the stream a distance

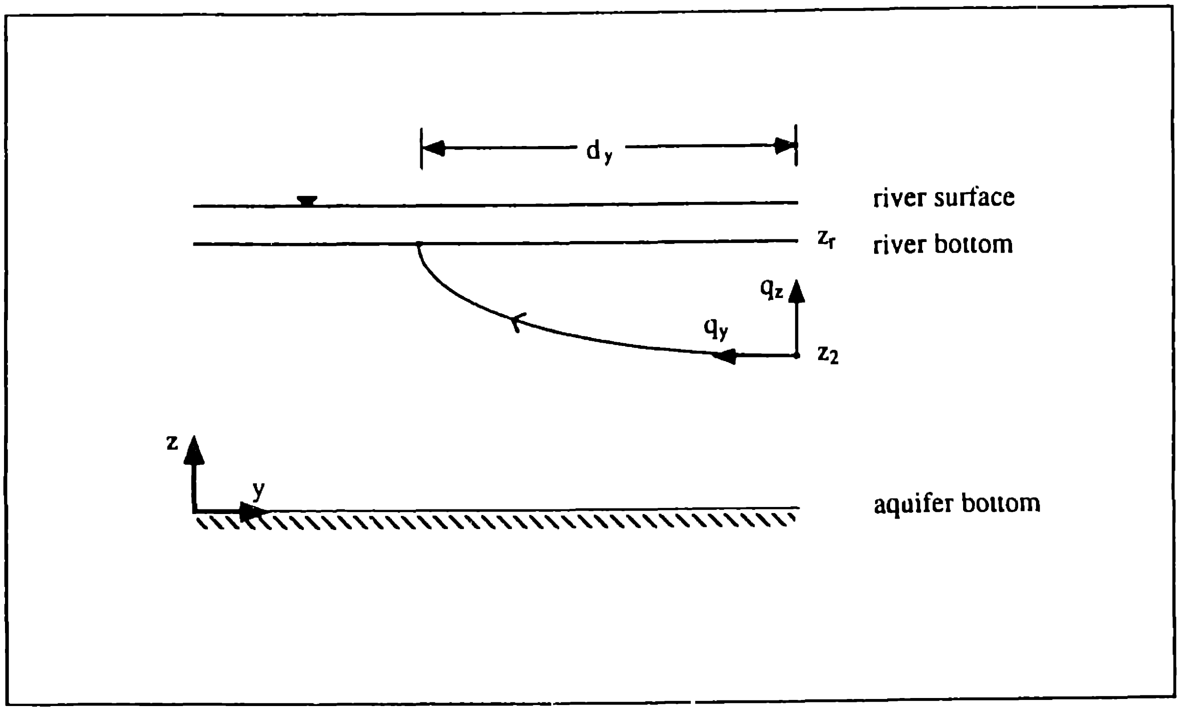

Figure 33. Horizontal Travel Parallel to the River

$$d_y = \frac{q_y}{n}t = \frac{K_h J_y}{n}t = \frac{2K_h J_y b^2\sqrt{K_h/K_v}}{\pi\varepsilon W}\ln\left[\frac{\cos\left(\frac{\pi}{2b}(z_T-b)\right)}{\cos\left(\frac{\pi}{2b}(z_2-b)\right)}\right] \tag{35}$$

with J_y the hydraulic slope of the stream. And d_y is the additional horizontal travel distance. Equation 35 relates the parameters determining the horizontal travel caused by vertical flow, and the importance of the parameters affecting vertical flow on contaminant flow paths. For a small stream the solution has only minor dependence on the width of the stream. Equation 35 may be rearranged in terms of physically significant parameters. Using Equation 21, which relates the source area location to the depth of circulation in the aquifer, with z_0=b gives

$$\frac{z_2-b}{b} = -\frac{x_0}{W} \tag{36}$$

The term z_T-b in Equation 36 may be replaced by z_T-b=-d, where d is the depth of the stream. Rearranging Equation 35 into dimensionless groups yields

$$\frac{d_y}{\beta} = \ln\left[\frac{\cos\left(\frac{\pi}{2}\frac{d}{b}\right)}{\cos\left(\frac{\pi}{2}\frac{x_0}{W}\right)}\right] \quad ; \quad \beta = \frac{2K_h J_y b^2\sqrt{K_h/K_v}}{\pi\varepsilon W} \tag{37}$$

The variable d_y is the distance which hydraulic analysis will underestimate the contaminant travel. The constant β is determined by the properties of the aquifer, and is fixed for a given field situation. The ratio d/b is determined by the stream dimensions, and x_0/W is determined by the source area location.

4.4 Numerical Simulations

Numerical simulations were performed to verify the simplifications made in the analytical solutions. The simulations utilized three-dimensional flow and transport codes. The parameters used in the simulations are representative of a buried valley aquifer.

The fully three-dimensional groundwater flow model uses the finite element method [Camp Dresser & McKee, 1984a]. The horizontal domain is discretized with triangular elements, with the same horizontal grid used at all levels of vertical discretization. The three-dimensional elements are tetrahedrons formed by dividing each vertical triangular prism into three tetrahedrons. To account for the phreatic surface, the nodes in the top horizontal level represent the phreatic surface and are free to move vertically. The model iterates to solve the nonlinear equations for the position of the phreatic surface. The transport model uses a particle tracking algorithm [Camp Dresser & McKee, 1984b]. Streamlines are identified as a particle travels from its source to a fixed head node at the stream.

An idealized aquifer, characteristic of a glacial buried valley, was used for simulations. Due to symmetry about the stream, only one half of the aquifer was modeled as shown in Figure 34. The aquifer has a thickness, b, of 100 feet beneath the stream, and a width, W, of 2500 feet to the groundwater divide. The porous medium is homogeneous and anisotropic with a horizontal hydraulic conductivity of 50 feet/day. Simulations were made for three hydraulic conductivity anisotropy ratios, with K_h/K_v equal to 5, 20, and 80. The recharge rate, ε, is 0.005 feet/day, which is equivalent to 22 inches/year. The stream has a slope of 0.002 ft/ft. The stream is represented as a fixed head boundary condition at the nodes along the top left edge of the domain. The domain is extended to a length, L, of 10,000 feet parallel to the stream to reduce the influence on the groundwater flow of the two vertical boundaries perpendicular to the stream.

The domain was discretized with the goals of having sufficient resolution near the stream, limiting distortion of the grid, and reducing the total number of nodes. The plan view grid is shown in Figure 35. The length of the horizontal discretization at the stream is 50 feet, and becomes progressively greater towards the groundwater divide. Since the theoretical error of the Galerkin method is related to the minimum angle of any element and the ratio of the length of the sides of adjacent elements [Prenter, 1975], the elements are kept near equilateral and the ratio of the lengths of the side of adjacent elements is less than two to one.

Figure 36 displays the vertical discretization used, which decreases in resolution from ten nodes beneath the stream, to five nodes at the groundwater divide. The discretization was chosen to minimize distortion of the equivalent isotropic system. The distortion of horizontal to vertical lengths, x'/z' or y'/z', varies from 2:1 at the stream to 4:1 at the groundwater divide. The vertical discretization is constant along the length of the domain with the elevations of the nodes increasing in the direction parallel to the stream at the same rate as the stream gradient.

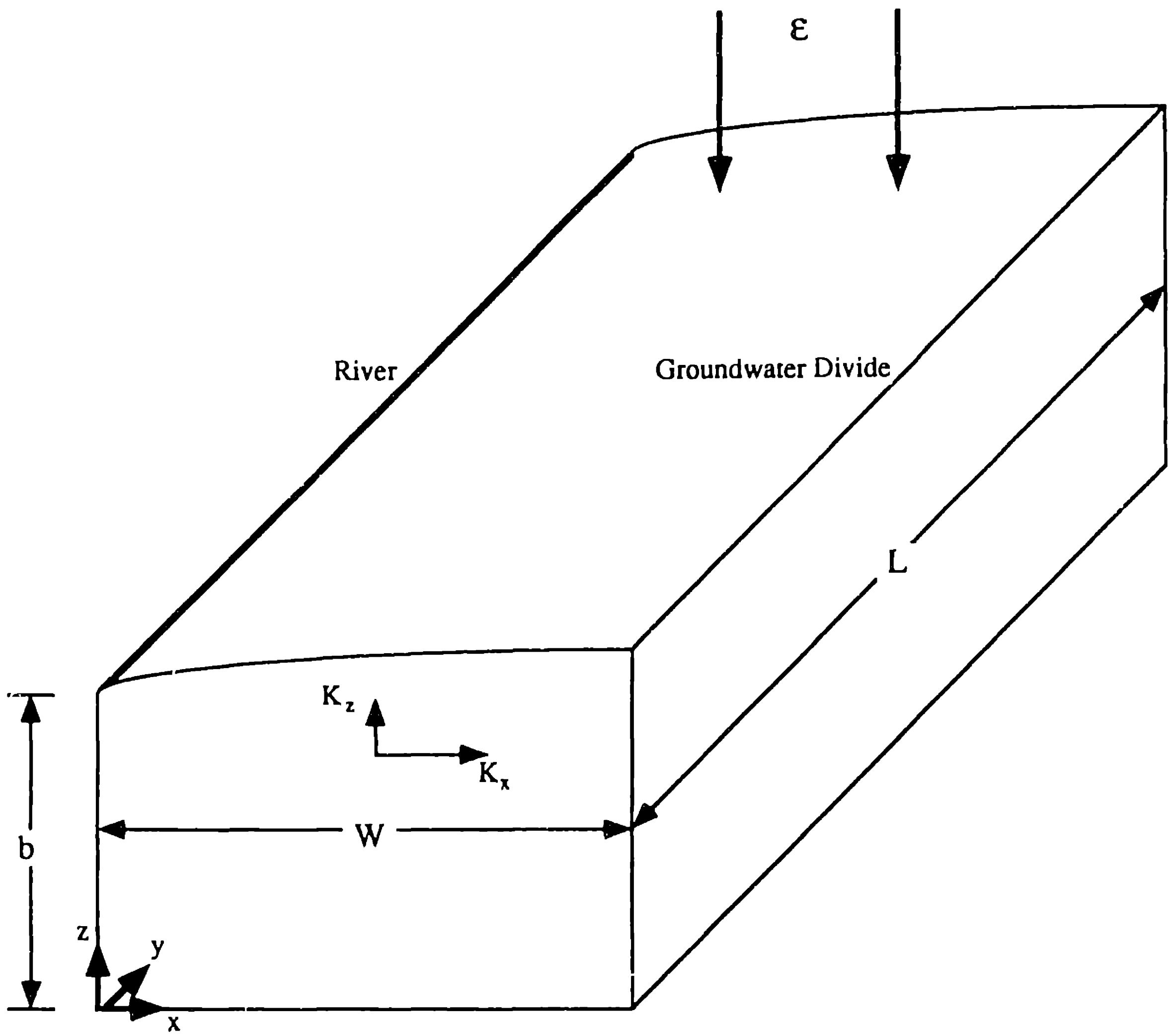

Figure 34. Schematic of Aquifer for Numerical Simulations

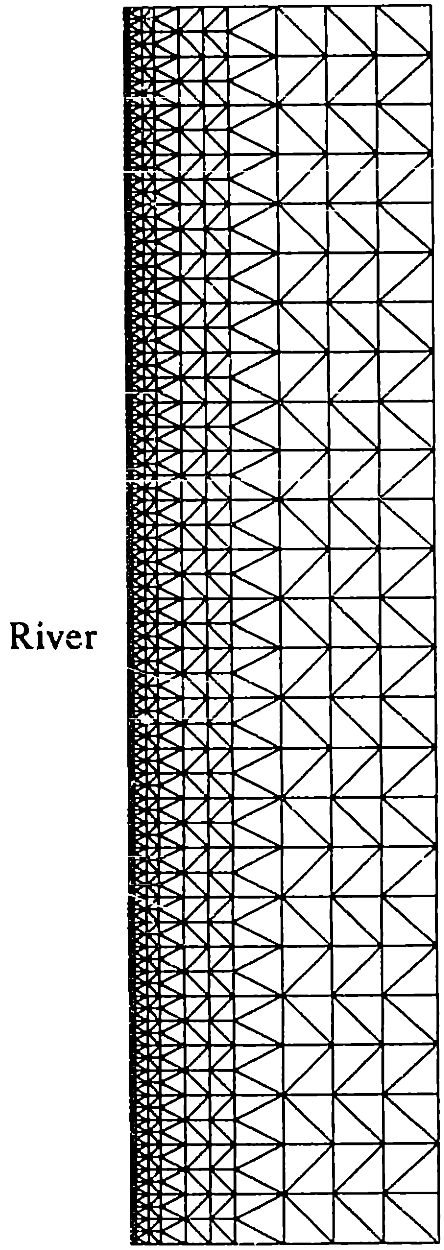

Figure 35. Plan View of Grid

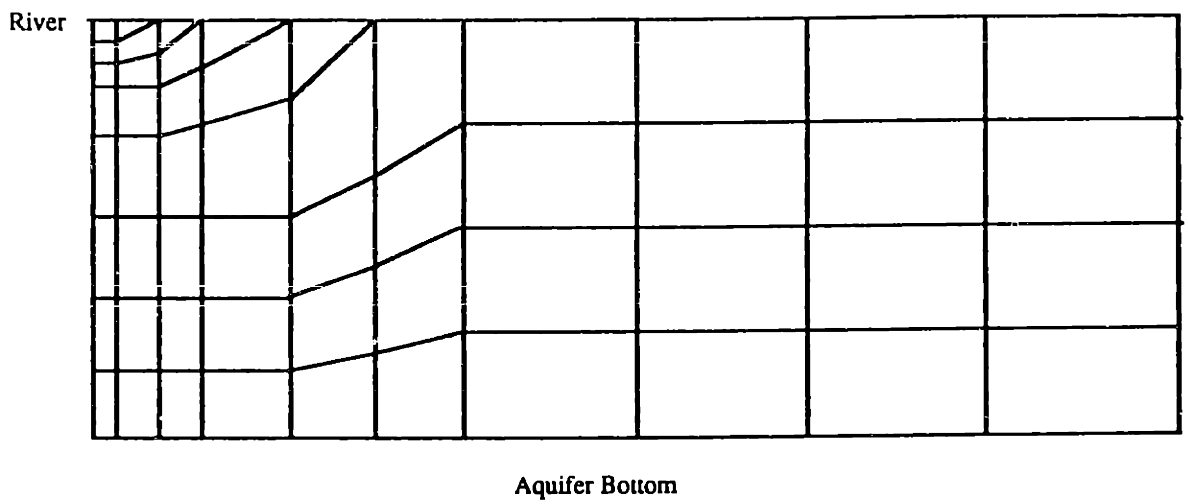

Figure 36. Cross Section of Grid

The two vertical boundaries perpendicular to the stream were treated as fixed head boundaries, and the remaining boundaries were no flux boundaries. Head distributions were imposed on the fixed head boundaries to represent an infinite length aquifer parallel to the stream, and consequently eliminate the influence of the boundaries. To determine the head distributions to use for the fixed head boundaries, a simulation was first made with the boundaries treated as no flux. Next, the potential distribution taken from a cross section through the center of the domain was used for the potential distribution at the fixed head boundaries. This process was repeated for each of the anisotropy cases.

The potentials from the simulations for the three anisotropy ratios are shown in Figure 37. The equipotentials at the bottom of the aquifer and at the phreatic surface are displayed. The potentials throughout the domain deviate from hydrostatic conditions, with the greatest vertical gradients near the stream. The vertical gradients increase for greater degrees of anisotropy, showing the importance of anisotropy on vertical flow.

4.5 Results

Using the potentials from the groundwater flow model and the particle tracking algorithm, flow paths were calculated from the numerical simulations. The numerical results were used to verify the analytic solution for the flow path to the stream. To test the dependence of the discharge location on the vertical location of the source as well as to the anisotropy ratio, numerical simulations were made with the sources located 60% of the distance from the stream to the groundwater divide and distributed vertically throughout the aquifer for the three anisotropy ratios. The additional horizontal travel, d_y, was determined as the difference between the simulated discharge location into the stream and the discharge location predicted by using flow net analysis of the simulated phreatic surface.

The results calculated from the numerical simulations are plotted with the analytical predictions from Equation 37 in dimensionless form in Figure 38. The y-axis is d_y/β. Since the value of β is constant for an aquifer, increasing x_0/W will increase the value of d_y. The analytical curves display a geometric relationship between the dimensionless source location and the dimensionless discharge location, indicating a large effect when the source is near the aquifer bottom or the groundwater divide.

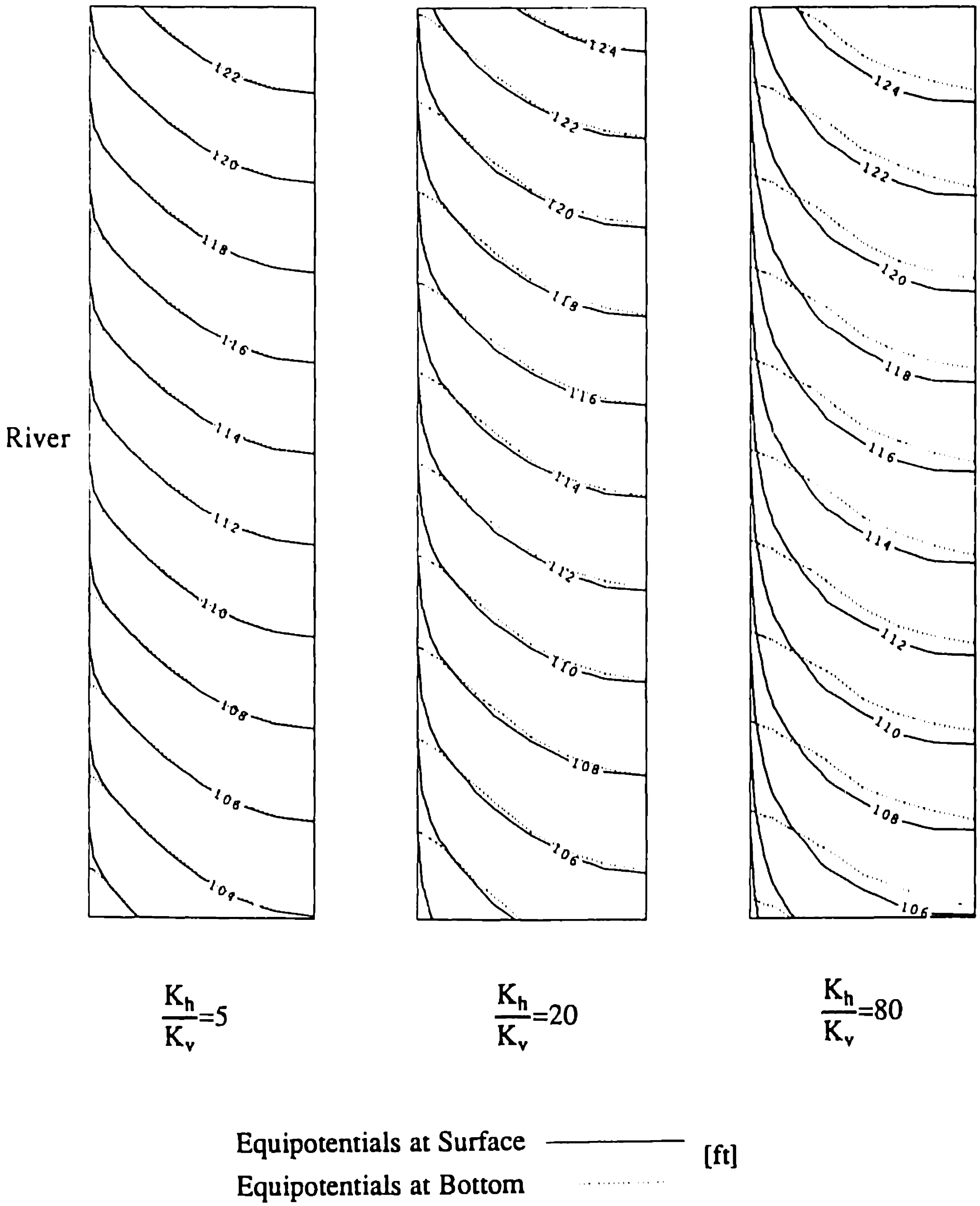

Figure 37. Numerical Simulation with Fixed Head Boundaries

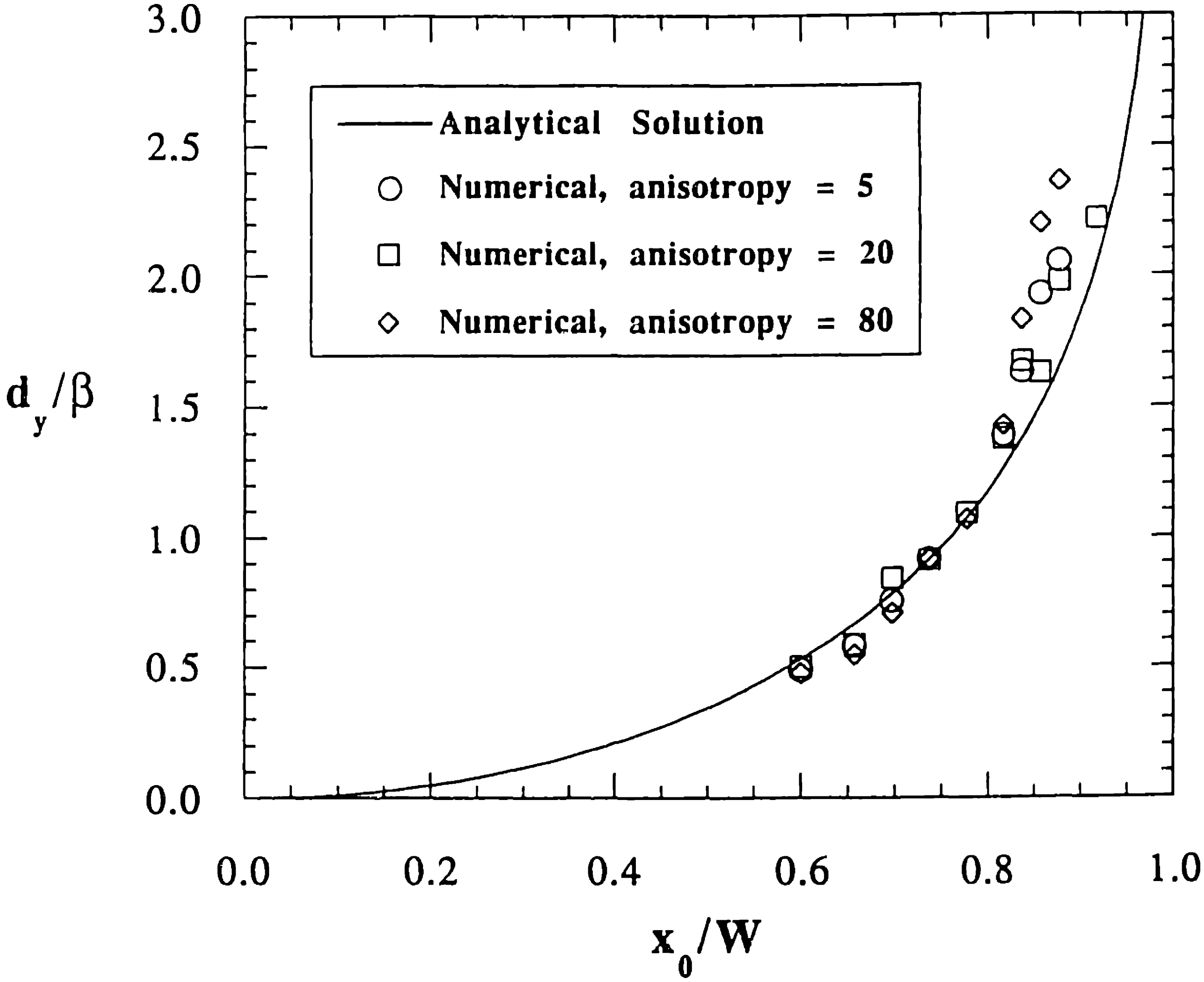

Figure 38. Analytical and Numerical Results

The plotted numerical results follow the shape of the analytical curve. At large values of x_0/W the analytical solution underestimates the value of d_y, which is caused by a mathematical simplification of the analytical solution. The vertical velocity of a particle rising to the stream was evaluated directly beneath the stream, which yields a smaller vertical velocity than if the vertical velocity was calculated along the streamline to the stream. Consequently, the analytical solution gives a lower limit of d_y.

A more exact mathematical representation could have been formulated, but the equations would have to be solved numerically for any set of aquifer parameters. The more exact solution would require determining the distance from the stream where radial flow becomes significant, and then numerically integrating along the streamline to the stream to solve for the vertical travel time. The simplifications used in this paper, with the magnitude of the vertical specific discharge evaluated only directly beneath the stream, allows the results to be generalized and easily applied to a variety of field settings.

Implementing the numerical model showed the importance of both the choice of boundary conditions and the degree of discretization on accurately simulating three-dimensional flow and transport. The initial procedure for the numerical simulations was to use no flux boundaries for the two boundaries perpendicular to the stream. But even with the domain greatly extended parallel to the stream the effect of the upstream and downstream boundaries was evident throughout the domain [Figure 39]. The no flux boundaries have a strong influence on the flow in the top right corner of the domain, where there is a downward gradient of 0.001 ft/ft. The imposition of no flux boundaries in conjunction with recharge force the downward flow. The effect of the boundaries is apparent for the simple geometry of the aquifer which was modeled, and indicates the need for a cautious approach to the imposition of boundary conditions in modeling.

Ten levels of discretization were used in the vertical near the stream and five at the groundwater divide, which is more than is normally used in three-dimensional modeling. The discretization was sufficient to provide a smooth description of the piezometric head, but was not sufficient to describe the vertical gradients near the aquifer bottom. The vertical gradients should be zero at the no flux boundary representing the aquifer bottom, but a nonzero gradient was predicted by the model. In the recharge areas, this caused the particles created by the particle tracking model to be driven into the aquifer bottom, and therefore contaminant sources located near the aquifer bottom or the groundwater divide could not be accurately represented. The use of a finer discretization should solve this problem, but was not possible because of computer storage limitations.

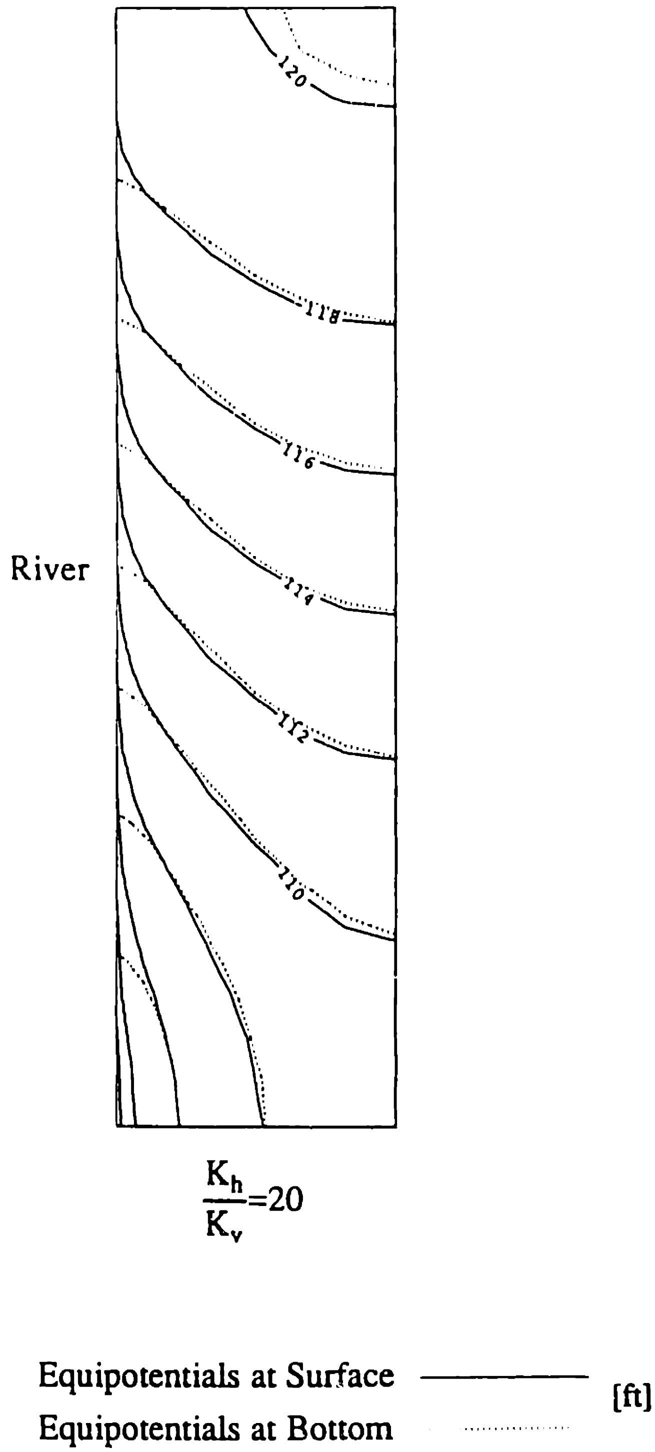

Figure 39. Numerical Simulation with No Flux Boundaries

4.6 Application

The analytical solution, Equation 37, may be used to estimate the location where contamination originating from a known source will enter a partially penetrating stream. The field setting for this example is the same as used for the numerical simulations. Flow net analysis of the numerically simulated water table data, which is equivalent to field water table data, gives an estimate of the discharge location. The analytical solution will be used to provide a correction to the estimated discharge location by accounting for the influence of vertical flow. The parameters are:

$W = 2500$ ft	aquifer width
$b = 100$ ft	aquifer thickness
$w = 3$ ft	stream horizontal half-width
$K_h = 50$ ft/day	horizontal hydraulic conductivity
$K_v = 2.5$ ft/day	vertical hydraulic conductivity
$K_h/K_v = 20/1$	anisotropy ratio
$J_y = 0.002$	stream slope
$\varepsilon = 0.005$ ft/day	recharge rate
$x_1 = 1500$ ft	source distance from stream
$z_1 = 35$ ft	source elevation above aquifer bottom

The stream depth would be

$$d = w\sqrt{\frac{K_v}{K_h}} = 0.67 \text{ ft}$$

The effective source location for a source on the phreatic surface is calculated with Equation 23

$$x_0 = x_1 + \frac{(W-x_1)(h_r - z_1)}{h_r} = 2150 \text{ ft}$$

The value of d_y, the error of the two-dimensional estimate, is calculated using Equation 37

$$\frac{d_y}{\beta}=\ln\left[\frac{\cos\left(\frac{\pi}{2}\frac{d}{b}\right)}{\cos\left(\frac{\pi}{2}\frac{x_0}{W}\right)}\right] \quad ; \quad \beta=\frac{2K_hJ_yb^2\sqrt{K_h/K_v}}{\pi\varepsilon W}$$

$$d_y=342 \text{ ft}$$

The graphical analysis estimates that the contamination will enter the stream 1721 ft downstream from the source location.The correct discharge location into the stream would equal the two dimensional estimate plus the analytical solution for the effect of vertical flow, or 1721+342=2063 ft. The error is relatively small, and increases the horizontal travel distance by only 20%. The magnitude of the error of the discharge location into the stream calculated using vertically averaged analysis may be acceptable for the intentions of the analysis. The sensitivity of the value of d_y to estimates of the parameters describing the aquifer may be readily determined. For example, if $K_h = 200$ ft/day and $K_h/K_v = 100/1$, $x_1=2300$ ft and $z_1=10$ ft, then $d_y = 4420$ ft. This error is almost equal to a mile, and three-dimensional modeling would be warranted.

Another application is to determine the location of a source area starting with field data of chemical analysis of samples collected along a stream. Volatile organic compounds will rapidly dissipate after discharging from the groundwater into a stream, and a short reach of the stream with elevated concentrations originating from a localized source area can be identified. Flow net analysis would be used to estimate the flow path of the contaminant working upgradient from the stream. Assuming a homogeneous flow field, the flow path would be shifted parallel to the stream to account for the influence of vertical flow. The value of d_y would be calculated for different distances from the stream, x_0, assuming a source on the phreatic surface. The values of d_y would be used to shift the flow path at each corresponding x_0 location. The created curve represents a line through source areas located on the surface which discharge into the stream at the desired location.

4.7 Application to the Wells G&H Site

In the vicinity of the Aberjona River at the Wells G & H site, there are vertical gradients (Chapter 2) which would influence contaminant transport. The analytical solution will be applied to determine the discharge location into the river by correcting a flow path drawn from water table contours. The application is useful since field data is analyzed and also because the limitations of the analysis may be examined.

The EPA has located five source areas at the Wells G& H site. The Unifirst property will be examined here. Pure phase tetrachlorethene (PCE) has been found in the bedrock in Well UC8 beneath the building on the Unifirst property. During the downward migration of the PCE, quantities representing residual saturation from the multiphase flow would remain in the soil of the saturated zone. These residual quantities would act as sources for dissolution into the groundwater.

Water table data from December 4, 1985 was contoured to create equipotentials of the phreatic surface (Figure 40). Well UC8 is located under the east end of the building on as shown in the figure. A flow path to the river is also displayed, which travels almost perpendicularly towards the river.

Figure 41 is a cross section of the geology along the flow path. The cross section was interpreted from well logs. Figure 41 is distorted to account for for a hydraulic conductivity anisotropy of $K_h/K_v = 20/1$. The result is to shorten the horizontal dimension by a factor of 0.32. Streamlines are drawn to show flow paths.

From the USGS pumping test, estimates of the horizontal hydraulic conductivity range from 125-300 ft/day. The value of 200 ft/day is an intermediate value. The Unifirst property is located in the glacial outwash, as are Wells G & H used for the pumping test. Analysis of falling head and grain size data leads to an anisotropy of 100/1, which is quite large. The anisotropy may also be estimated from the use of Equation 37 describing the potential in the vicinity of the radial flow region of the partially penetrating river, and field data of the potentials. On April 13,1990, there was a head drop of 0.464 feet between Well S89 finished at the medium depth and the river, which is over a distance of 56 feet. Using Equation 37, with K_h=200 ft/day yields an anisotropy of 17.4. A value of $K_h/K_v = 20/1$ will be used for the calculations.

Well UC8 is located 1720 ft from the river, and the local groundwater divide is located a distance 2500 ft from the river. The river has a width of 3 ft. Some judgement is required to choose the thickness of the aquifer, since it varies from 10 ft at Well UC8 to over 100 ft at the river. The streamlines of Figure 41 indicate that an effective thickness of 75 ft is appropriate. The source will be analyzed as originating at the surface.

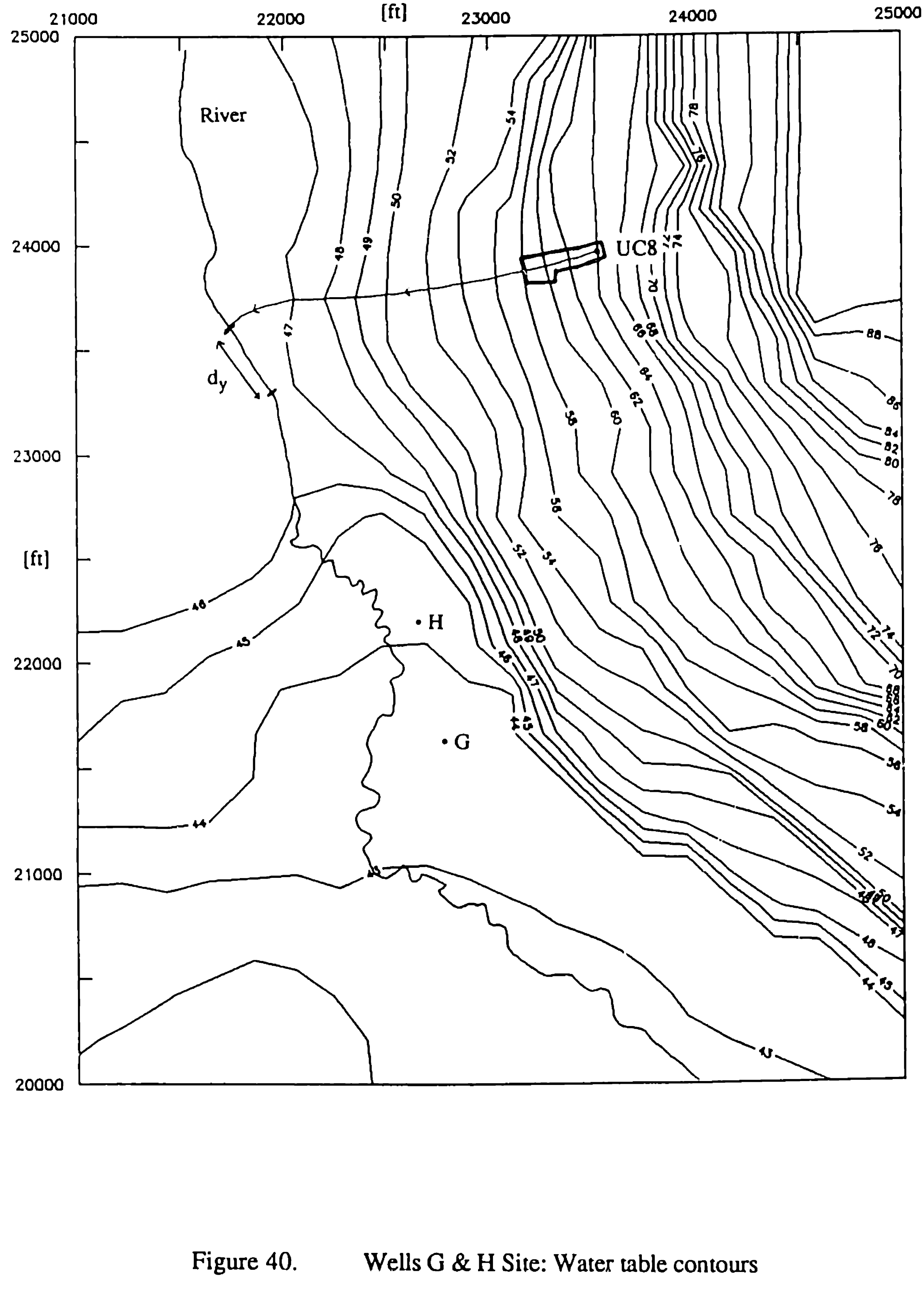

Figure 40. Wells G & H Site: Water table contours

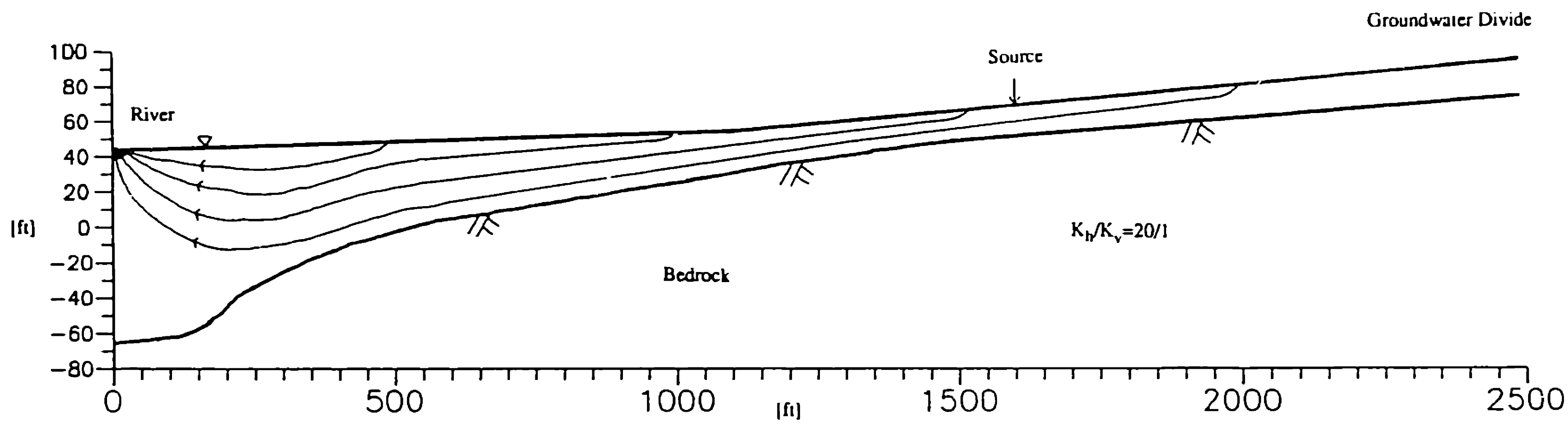

Figure 41. Wells G & H Site: Cross section

$W = 2500$ ft	aquifer width
$x_0=1720$ ft	source distance from river, located at the surface
$b = 75$ ft	aquifer thickness
$w = 3$ ft	river horizontal half-width
$K_h = 200$ ft/day	horizontal hydraulic conductivity
$K_v = 10$ ft/day	vertical hydraulic conductivity
$K_h/K_v = 20/1$	anisotropy ratio
$J_y = 0.002$	river slope
$\varepsilon = 0.005$ ft/day	recharge rate

Using Equation 37, d_y is equal to 389 ft. The corrected discharge location is shown in Figure 41.

There is some uncertainty concerning the values of the parameters used to calculate d_y , and an estimate of the range of possible values for d_y is illustrative. For the following parameter values:

$W = 2500$ ft	aquifer width
$x_0 = 2400$ ft	source distance from river, located at the surface
$b = 100$ ft	aquifer thickness
$w = 3$ ft	river horizontal half-width
$K_h = 400$ ft/day	horizontal hydraulic conductivity
$K_v = 4$ ft/day	vertical hydraulic conductivity
$K_h/K_v = 100/1$	anisotropy ratio
$J_y = 0.002$	river slope
$\varepsilon = 0.005$ ft/day	recharge rate

d_y will be equal to 11,270 feet, which is more than two miles. For a source located close to the groundwater divide, and using greater values for the horizontal hydraulic conductivity and anisotropy, there is a very large influence on the discharge location. Consequently depending on the source location, there is the possibility of contaminant migration over significant distances along the valley.

Two aspects of this application show limitations of the analytical solution for the influence of vertical flow on contaminant transport. Both limitations have to do with irregular aquifer geometry. For the Wells G & H site, the thickness of the unconsolidated material varies significantly between the river and the groundwater divide. The kinematics of the groundwater flow with the distributed recharge create vertical flow. But the relationship between the source area depth and the flow paths is more complex than analyzed in this work. Increasing the source area depth will increase the influence of vertical flow, but not in as simple a manner as analyzed using the Dupuit aquifer.

The changing aquifer geometry also influences the potentials as viewed in plan. The analysis assumes no variation of potentials parallel to the river, in other words an infinite aquifer parallel to the river is assumed. This is definitely not the situation as displayed in Figure 40, where the valley narrows in the vicinity of the Unifirst property. With a small perturbation of the source area, the flow path drawn on Figure 40 would have discharged into the river near Well H. Consequently the influence of the uncertainty of the field data is as great as the influence of vertical flow on the flow paths. Density driven flow and flow in the fractured bedrock may also be important for this field location.

Although there is uncertainty concerning the actual flow paths for the Wells G & H site, analysis of the influence of vertical flow does aid in the understanding of the flow paths. The influence of vertical flow will be greatest for source areas near the groundwater divide, and decrease for source areas near the river. The influence also is greater for sources located at depth. For the case analyzed, with the source located at the surface at the Unifirst property, the influence of vertical flow was not great.

4.8 Conclusions

Vertical flow induced by recharge from precipitation and discharge to a partially penetrating stream can have a significant impact on contaminant transport, which should be considered when utilizing two-dimensional analysis. A simple conceptual model, of radial flow near the stream and horizontal flow far from the stream, is used to derive an analytical solution which predicts the deviation of the flow paths from those derived by two dimensional analysis. The straight forward conceptual and mathematical analysis successfully captures the important aspects of the complicated three-dimensional flow. The analytical solution may be readily applied to estimate a correction to augment flow net analysis or flow paths calculated from two-dimensional numerical models. The analytical solution presented may also be used as a screening tool to determine the importance of vertical flow for a particular field location.

5. SUMMARY AND CONCLUSIONS

This thesis is comprised of three major sections dealing with the physics of groundwater flow. The research is part of a larger project studying the transport, transformations, and health effects of hazardous waste. The first section analyzes hydrogeological information describing the Aberjona watershed. Hydrogeological data is presented while forming a conceptual description of groundwater flow. The second section contains two-dimensional modeling of groundwater flow for the Aberjona River sub-basin containing approximately half of the entire watershed. The modeling process provides a method to organize and evaluate the existing hydrogeological data, as well as to develop a conceptual description and understanding of the groundwater flow.

The third section of the thesis involves a detailed examination of vertical flow, which is neglected in two-dimensional modeling. Vertical flow is particularly important when considering contaminant transport. An analytical solution analyzing the effect of vertical flow on contaminant flow paths is presented. The analytical solution quantifies the effect of vertical flow on contaminant transport, and the influence of parameters such as anisotropy of the hydraulic conductivity and the contaminant source location are included in the analysis. Consequently the analytical solution may be used either as a screening tool to determine the importance of vertical flow for a specific field location, or as a correction to apply to flow paths predicted by vertically averaged two-dimensional analysis.

The field location of interest is the Aberjona watershed, which is located ten miles north of Boston. The watershed includes the seven towns of Woburn, Reading, Wilmington, Burlington, Lexington, Winchester, and Stoneham. The total area is 24.3 square miles, with the town of Woburn located in the center of the watershed and occupying the majority of the area. The Aberjona River drains the watershed, and discharges into the Mystic Lakes.

Woburn has a long and extensive industrial history, which essentially began in 1803 with the construction of the Middlesex Canal. During the initial industrial period, the dominant industry was leather processing and related industries. The related industries included machine shops and chemical companies supporting the tanning industry. The tanning and chemical industries grew over time, and most waste disposal occurred on site. Beginning in approximately 1940, Woburn experienced diversification of its industrial base into light manufacturing. In 1989 there were more than 135 manufacturing firms, with the area having experienced similar growth as did the rest of the Route 128 area.

There is considerable evidence of chemical contamination in the watersheds. There are two sites, Industriplex-128 and Wells G & H, on the EPA's Superfund list of uncontrolled hazardous waste sites. In addition, in 1989 there were 40 potential hazardous waste sites under investigation by the state. The documented contamination involves a wide range of chemicals including metals and organic compounds. The two Superfund sites, as well as the majority of the state-identified sites, are located in the Aberjona sub-basin.

The surficial geology of the watershed is characterized by glacial outwash and till deposits. There are two major buried valleys, filled with glacial outwash, which form the transmissive regions of the aquifer. One trough runs beneath the main branch of the Aberjona River, and the other runs to the west under Horn Pond. The two buried valleys connect near Wedge Pond and the combined trough runs south beneath the Mystic Lakes. The outwash material has a large hydraulic transmissivity, with areas greater than 4000 ft ^{2}/day, and is used for industrial and municipal water supplies. The water sorted outwash material contains lenses of gravel and clay. The hill slopes are covered with a mantle of till. The till is thickest near the valley floors and thins towards the hilltops. In areas there are numerous bedrock outcrops. Glacial tills are directly deposited by glacial ice and consequently poorly sorted, with low hydraulic conductivities.

Data on hydraulic conductivity are available from both water supply investigations and studies of hazardous waste sites. The data consists of pumping tests, specific capacity data, slug tests, and grain size analysis. Using these sources of information estimates can be made concerning the hydraulic conductivity of the outwash and till regions of the watershed, and also the anisotropy of the hydraulic conductivity.

Specific capacity is the measure of the drawdown of a pumping well for a given yield, and an estimate of the transmissivity can be made from specific capacity values. The geometric mean of the transmissivity for all except the bedrock wells for the watershed is 4614 ft^2/day, which represents a very transmissive aquifer. Using an average aquifer thickness of 80 ft, the hydraulic conductivity would equal 58 ft/day. The USGS performed a pumping test at Wells G & H to determine aquifer characteristics and the area contributing to the water supply wells. The estimated values for the hydraulic conductivity assuming an 80-ft saturated thickness range from 125 to 350 ft/day. The hydraulic conductivity calculated for the Wells G & H area is approximately three times that calculated from the specific capacity data. This is primarily because the Wells G & H transmissivity has been corrected for the influence of the partially penetrating pumping wells.

Slug test data from three locations in the till yield hydraulic conductivities ranging from 2.6 to 4.6 ft/day. Slug tests and one pumping test of shallow bedrock give hydraulic conductivities ranging from 0.86 to 1.5 ft/day. In summary the glacial outwash, located along the central portions of the valleys, has a very large hydraulic conductivity. While the till, located in the upland areas, has a hydraulic conductivity almost two orders of magnitude less. The bedrock is essentially impermeable compared to the glacial outwash material.

Estimates were made for hydraulic conductivity for many wells at the Wells G & H site using grain size analysis and falling head slug tests. This data can be used to calculate the hydraulic conductivity anisotropy. Assuming perfect horizontal layering of the porous media, the horizontal hydraulic conductivity would be the arithmetic mean, and the vertical hydraulic conductivity would be the harmonic mean. The ratio is an estimate for the anisotropy, which equals 100:1 for this data.

The transient water level data shows seasonal variations of the head with the variations dependent on the location of the well and the hydraulic properties of the geological material. Seasonal water level variations of ten feet occur in the low conductivity glacial till. In the glacial outwash, the water levels vary much less. The seasonal variations of water levels in the swamps, located at the head of the Aberjona River, are only 1-2 feet. Seasonal water level variations are dependent on the conductivity of the geological material, and are significant in the till regions of the aquifer.

Directly beneath the river at the Wells G & H site, the gradients are upward towards the river. The magnitude of the gradients is dependent on the river stage, with the gradients decreasing during flood periods when the river stage increases. The influence of the river stage on potentials beneath the river decreases with increased depth beneath the river.

A mass balance may be performed on the watershed to estimate the magnitude of the various fluxes. An annual mass balance assuming steady state conditions was done. There are four components to the mass balance: the input from precipitation, groundwater withdrawal, discharge through the Aberjona River, and evapotranspiration. For precipitation, the long-term average value at Logan Airport was used, and a watershed area of 24.3 square miles. In 1987 the groundwater withdrawals accounted for 14% of the precipitation, down from a very sizable fraction of 27% in 1967. The discharge of the Aberjona River accounts for 49% of the total flux in 1987, leaving an evapotranspiration flux of 37%. The reduction of groundwater withdrawal over the period was compensated by a corresponding increase in the discharge of the river.

A hydraulic time constant may be calculated for the aquifer from the discharge of the Aberjona River. The time constant describes the response time of the watershed for varying precipitation inputs. The low time constant calculated, approximately 15 days, indicates that the aquifer responds quickly to changes in recharge. The watershed has a small time constant because of the relatively small size of the watershed, and the high transmissivity of the glacial outwash.

A numerical groundwater flow model was calibrated for the Aberjona River sub-basin, which encompasses approximately one half of the Aberjona watershed. The groundwater flow model AQUIFEM was used, which is a two-dimensional finite-element model developed at MIT. The model uses triangular elements and linear interpolation functions. The aquifer was modeled as steady state and phreatic, with the water level rising to the ground surface at discharge areas. The flow is primarily through the unconsolidated material overlying the bedrock, with the low-permeability bedrock acting as a boundary to flow. The area of interest was primarily the regions adjacent to the river, since the majority of the data available for calibration and the known hazardous waste sites are located in the high-transmissivity glacial outwash along the center of the valley. The till regions along the boundaries were included to supply the correct flux from precipitation to the areas of interest and to extend the domain to the the no-flux boundary of the groundwater divide. Horizontal no-flux boundaries corresponded to a groundwater divide, which was assumed to coincide with the surface water divide. Rivers and streams were approximated as fixed head boundary conditions.

The model was calibrated by varying the hydraulic conductivity in order to minimize the error of the calculated heads at locations where well water level data were available. The hydraulic conductivity zones were based on the surficial geology, with two zones representing glacial till and outwash used initially. Six conductivity zones were used in the final runs, with the hydraulic conductivity ranging from 0.1 to 75 ft/day. The correlation to the measured water level data could have been improved by increasing the number of different conductivity zones. Considering that both the recharge and the conductivity are unknown, the solution is not unique, and it was not warranted to use many zones of different conductivities to exactly match the measured water level data.

The predicted water table is a smoothed version of the land surface. The shape of the phreatic surface follows the shape of the land surface because the surface streams and rivers are the groundwater discharge locations. These discharge locations control the groundwater potential. The smoothing of the phreatic surface is mainly a product of the resolution of the coarse finite element grid used. The general flow path is perpendicular to the the river in the till regions, and turns parallel to the river in the outwash region. This refraction of the flow paths is a result of the varying hydraulic conductivities. The groundwater flow is refracted as it crosses from the low transmissivity till to the high transmissivity outwash in the vicinity of the river.

The third component of the research was the analysis of the importance of vertical flow on contaminant transport. The assumption of hydrostatic head conditions, implicit in two-dimensional analysis, is not correct for situations where there is vertical flow such as near a partially penetrating river. Vertical flow is particularly important when predicting flow paths for contaminant transport. A simple conceptual model, of radial flow near the river and horizontal flow far from the river, was used to derive an analytical solution which predicts the deviation of the flow paths from those derived by two dimensional analysis.

The derivations include the influence of hydraulic conductivity anisotropy. The analytical solution may be used as a correction to apply to the calculation of flow paths generated by two-dimensional analysis. The analytical solution is also useful as a screening tool to determine the magnitude of errors created when vertical flow is neglected by two-dimensional analysis. The goal of the analysis was to predict the path of a contaminant from a source area to the point where it would enter the river. Radial flow is assumed near the river, and the Dupuit approximation is used for the remainder of the aquifer.

Numerical simulations were performed to verify the simplifications made in the analytical solutions. The simulations utilized three-dimensional flow and transport codes. The analytical solution agreed well with results from the numerical simulations. The analytical solution showed that for contaminant sources located near the groundwater divide or near the aquifer bottom, there is a large influence of vertical flow on flow paths and the discharge location into the river.

Developing the steady state, two-dimensional groundwater flow model satisfied the goal of better understanding the regional groundwater flow. The initial plan of using a single model to describe both the regional groundwater flow and to accurately describe the flow for small areas located along the river was overly optimistic. Combining these two goals caused calibration of the model to be excessively time consuming. An alternative and more efficient procedure would have been to develop a regional groundwater flow model accepting the resolution limitations of a coarse grid, and possibly using linear equations for the potential. Next, a detailed model would have been developed for a specific area of interest, using results from the regional model to prescribe boundary conditions.

Transient water level data from wells located in the glacial till show large seasonal variations. Consequently, seasonal variations of flow paths are of concern, and could be investigated with the use of transient simulations. The smoothing, which was evident from the regional groundwater model, indicated that to accurately describe groundwater flow, future work should focus on a small area of particular interest. Another consideration for transient analysis is that transient water level data, necessary for calibration, is very limited.

The evidence of transient behavior, evident even in the vertical gradients beneath the Aberjona River, indicates that flow paths may vary significantly with seasonal recharge variations. Seasonal variations may impact the interpretation of river water samples collected to analyze groundwater/surface water interactions, since discharge locations of groundwater into surface streams would vary with time. There is the possibility that gradients near the river may reverse seasonally, and river reaches would alternate between gaining and losing water to the aquifer.

The analysis of the influence of vertical flow on contaminant transport provided significant insight, including the limitations of vertically averaged models to accurately describe transport. For source areas located near the groundwater divide or deep in the aquifer, the contamination may travel more than a mile before discharging into surface waters. With two Superfund sites and many other known hazardous waste sites all located along the same aquifer, contaminant travel over large distances at depth could greatly complicate the analyses of contamination sources as well as remediation projects. A field sampling scheme could be developed to investigate this question.

The analysis of the influence of vertical flow shows a large influence of source location on the point of discharge of contamination into a river. The effect of vertical flow could be misinterpreted as hydrodynamic dispersion when interpreting field data. An example is a surface spill of a dense nonaqueous phase liquid (DNAPL). As the DNAPL migrated downward through the water column, a residual saturation would remain in the soil. This residual saturation would act as a source distributed in the vertical as the contaminant dissolved into the groundwater. A source distributed throughout the thickness of the aquifer would discharge into the river along a reach of considerable length, because of the varying influence of vertical flow on the transport. Analysis of water samples collected from the river would show a diffuse peak of contamination entering the river, which could be interpreted as originating from a large source area or the effect of hydrodynamic dispersion diluting the contaminant. Consequently vertical flow can have a significant impact on contaminant transport, and must be considered when studying groundwater transport.

6. REFERENCES

Bear, Jacob. 1972. *Dynamics of Fluids in Porous Media.* Dover Publications, Inc., New York.

Bear, Jacob. 1979. *Hydraulics of Groundwater.* McGraw-Hill, New York.

Camp Dresser & McKee, Inc. 1984a. Dynflow: A Three Dimensional Finite Element Groundwater Flow Model. Boston.

Camp Dresser & McKee, Inc. 1984b Dyntrack: A Three Dimensional Contaminant Transport Model for Groundwater Studies. Boston.

Camp, Dresser & McKee. 1967. Winchester, Massachusetts, Aberjona River Watershed Committee, Report on Aberjona River. Boston.

Cherry, John A., Martin L. Johnson, Rudolph J. Jaeger. 1989. Technical Report of the Woburn, Mass., Wells G & H site.

Chute, Newton E. 1949. Glacial geology of the Mystic Lakes-Fresh Pond areas, Massachusetts. *U.S. Geological Survey. Bulletin 1061-F*, 187-216.

Dagan, Gedeon. 1964. Spacing of Drains by an Approximate Method. *Proc. Amer. Soc. Civil Eng. Irrigation and Drainage Div. IR1, 90.*, 41-66.

Delaney, F. D., F. B. Gay. 1980. Hydrology and water resources of the coastal drainage basins of northeastern Massachusetts, from Castle Nash River, Ipswich, to Mystic River, Boston. *U.S. Geological Survey Hydrologic Investigations Atlas No. 489.*

Department of Environmental Quality Engineering, Massachusetts. 1989. List of confirmed disposal sites to be investigated.

Ecology and Environment. 1982. Evaluation of the hydrogeology and groundwater quality of East and North Woburn, Mass. Final Report TDD No. F1-8109-02.

Freeze, R. Allan, John, A. Cherry. 1979. *Groundwater.* Prentice-Hall.

Gelhar, L.W., J.L. Wilson. 1974. Groundwater Quality Modeling. *Groundwater. 12*, 399-408.

GeoEnvironmental Consultants, Inc. 1983. W. R. Grace Co., Cryovac Division, Woburn Plant, Field investigation and remedial measures, Interim report. Port Chester, N.Y.

Goldberg-Zoino and Associates, Inc. 1986. Environmental assessment/remedial studies, North Woburn Industrial Park, Woburn, Mass. Newton Upper Falls, Mass.

Hubbert, M.K. 1940. The Theory of Ground-Water Motion. *Journal of Geology. 48*, 785-944.

Kirkham, Dan. 1958. Seepage of Steady Rainfall through Soil into Drains. *Transactions American Geophysical Union. 39*, 892-908.

Metropolitan Area Planning Council. 1988. Woburn land use 1971, 1985. Boston.

Myette, Charles F., Julio C. Olimpio, David G. Johnson. 1987. Area of influence and zone of contribution to Superfund-site Wells G & H, Woburn, Mass. *U.S. Geological Survey, Water Resources Investigation Report* 87-4100.

NUS Corp. 1986. Wells G & H site remedial investigation report, Part I, Woburn, Mass. TDD No. F1-8607-07.

Prenter, P.M. 1975. *Splines and Variational Methods*. John Wiley & Sons. New York.

Pye, Veronica, Jocelyn Kelley. 1984. The extent of groundwater contamination in the United States. In *Groundwater contamination*. National Academy Press, Washington.

Roy, Steven P. 1988. Long-range water supply planning and management in Massachusetts. *Journal NEWWA*, June, 117-120.

Stouffer Chemical Company. 1983. Woburn environmental studies Phase I report. Roux Associates, Inc.

Tarr, Joel. 1987. History of pollution in Woburn, Massachusetts. In Review of EPA report "Wells G & H site remediation Investigation Report, Part 1, Woburn, Massachusetts." GeoTrans, Boxborough, Mass.

Townley, L. R., J, L. Wilson, 1980. Description of user's manual for a finite element aquifer flow model AQUIFEM-1. Technical Report No. 252. R. M. Parsons Laboratory for Water Resources and Hydrodynamics. MIT.

United States Geological Survey. 1962. Surficial geology of the Reading quadrangle, Massachusetts. Map 5Q-168.

United States Geological Survey. 1962. Surficial geology of the Wilmington quadrangle, Massachusetts. Map 5Q-122.

United States Geological Survey. 1975. Water resources data for Massachusetts and Rhode Island, Water Year 1975. *U.S. Geological Survey Water-Data Report* MA-RI-75-1.

Walton, W. C. 1970. *Groundwater resource evaluation*. McGraw-Hill.

Wehran Engineering Corp. 1987. Site investigation report of the Weyerhaeuser Site, Woburn, Mass. Methuen, Mass.

Wilson, John L., L. R. Townley, A. Sa da Costa. 1979. Mathematical development and verification of a finite element aquifer flow model AQUIFEM-1. Technical Report No. 248, R. M. Parsons Laboratory for Water Resources and Hydrodynamics, MIT.

Woodward-Clyde Consultants. 1984. Phase II groundwater investigation, J. J. Riley Site, Woburn, Mass. Wayne, N.J.

7. APPENDICES

Appendix 1. Wells used for calibration

well #	model node #	original name	town	Date of measurement Mon	Day	Yr	Reference	Owner	Land elev (ft)	Water elev (ft)	Bedrock elev (ft)	Location X (ft)	Location Y (ft)
1	251	W1	WOB	10	30	81	1	EPA	75.0	73.0	43.0	18864.65	32779.64
2	236	W2	WOB	10	30	81	1	EPA	76.0	72.1	48.0	22839.51	30398.68
3	229	W3	WOB	10	30	81	1	EPA	79.0	65.4	45.0	17679.56	30204.98
4	186	W4	WOB	10	30	81	1	EPA	53.5	48.5	-30.5	21552.10	24712.26
5	188	W5	WOB	10	30	81	1	EPA	54.0	51.1	-0.6	22100.12	24422.72
6	176	W6	WOB	10	30	81	1	EPA	57.5	49.3	-26.5	22919.91	23741.65
7	177	W7	WOB	10	30	81	1	EPA	91.0	89.9	73.0	25216.10	23748.90
8	154	W8	WOB	10	30	81	1	EPA	45.0	43.0	-79.0	22718.76	21892.69
9	112	W9	WOB	10	30	81	1	EPA	43.0	41.1	-17.0	22666.09	18669.27
10	120	W10	WOB	10	30	81	1	EPA	82.5	42.1	5.5	22881.89	19655.13
11		W11	WOB	10	30	81	1	EPA	43.0	41.0	-32.5	23601.44	20054.76
12	128	W12	STO	10	30	81	1	EPA	41.0	38.1	-10.0	24461.08	19794.29
13	118	W13	STO	10	30	81	1	EPA	79.0	70.2	69.0	29978.04	18341.05
14	95	W14	WOB	10	30	81	1	EPA	48.0	39.1	-6.0	27477.98	15978.85
15	93	W15	WOB	10	30	81	1	EPA	39.0	31.7	8.0	25840.37	16242.85
16	80	W16	WOB	10	30	81	1	EPA	37.0	30.4	-71.0	25638.96	14747.55
17	57	W17	WIN	10	30	81	1	EPA	40.0	14.3	-71.0	22988.67	13184.53
18	49	W18	WIN	10	30	81	1	EPA	27.0	24.0	-134.0	22447.97	12010.45
19	214	W19	WOB	10	30	81	1	EPA	65.0	51.9	16.0	19558.46	27571.97
20	92	W20	WOB	10	30	81	1	EPA	65.0	51.9	-76.0	24055.83	16661.21
21		W21	WOB	10	30	81	1	EPA	77.0	57.1	56.0	23697.70	23133.07
23	261	GW2	WIL	3	2	81	1	OLIN CHEM	88.0	77.0	73.0	17186.66	34548.73
24	258	GW10	WIL	11	12	80	1	OLIN CHEM	87.0	78.4	63.0	16648.18	33714.15
25	249	GW5	WIL	11	12	80	1	OLIN CHEM	76.0	71.9	64.0	17833.51	33369.00
26		GZ3	WOB	1	19	81	1	JAMPET ASSOC	68.5	63.1	37.5	19517.74	30963.16
27	233	GZ2	WOB	1	12	81	1	JAMPET ASSOC	68.5	65.1	48.5	19526.21	30881.06
28		GZ6	WOB	1	16	81	1	JAMPET ASSOC	69.0	57.3	24.0	19507.97	29976.17
29		GZ5	WOB	1	14	81	1	JAMPET ASSOC	69.0	56.5	52.5	19438.23	29938.96
30		E30	WOB				1			?		22138.39	29760.58
31	226	E29	WOB				1	MARSHALL'S FIELD		?		21650.54	29161.32
32	205	E9	WOB				1	INSULTAB	55.0	?	55.0	20319.65	27061.61
33	206	E26	WOB			79	1	SOLAR POWER	70.0	63.0	20.0	21416.81	26803.14
34	189	E4	WOB	10	30	81	1	KOALA INN	61.0	53.5	?	22536.73	24991.13
35		E12	WOB				1					20916.88	26423.85
36	164	E3	WOB				1	MCSHEFFREY		?		18728.90	22221.09
37	166	E27	WOB				1	ROHSTEIN		?		20938.83	23079.07
38		E11	WOB			?	1	NE RIFLE ASSOC		?		22999.68	22419.70
39	157	420	WOB	12	4	85	1	WOBURN H	45.0	43.7	-39.0	22637.17	22165.30
40	150	419	WOB	12	4	85	1	WOBURN G	45.0	43.9	-43.0	22770.77	21592.94
41	151	436	WOB	2		62	1	NE PLASTICS	60.0	45.0	22.0	23459.46	21828.66
42		E8	WOB			?	1	MIRRA		?		23886.46	22244.30
43		E42	WOB			?	1					22616.08	21812.87
44	159	364	WOB	12	2	80	1	IND. TALLOW	85.0	80.0	51.0	25311.40	22453.33
45	137	422	WOB	10		63	1	WOBURN	45.0	43.0	-13.0	23913.81	20283.27
46	135	6	WOB			58	1	JJ RILEY	50.0	45.0	-1.0	22103.42	20553.09
47		439	WOB			45	1	JJ RILEY	55.0	50.0	35.0	21846.33	20440.11
48		E39	WOB				1					23215.05	17507.53
49	101	E38	WOB				1					23867.15	17637.36
50		424	WOB	2	12	81	1	ATL GELATIN	50.0	36.0	-84.0	24054.56	16782.46
51	91	AG7	WOB			?	1	ATL GELATIN	50.0	?	-65.0	23685.70	16546.48
52		E37	WOB				1					24723.03	16035.91
53		426	WOB	10		60	1	ATL GELATIN	56.0	42.8	-86.0	25192.34	15882.79
54		AG4A	WOB	12	3	57	1	ATL GELATIN	35.0	25.2	-15.0	26067.01	15439.28

55	79	AG6	WOB			58	1	ATL GELATIN	47.0	?	-77.0	24750.21	14874.50
56	81	E25	WOB			?	1	ATL GELATIN		?		23705.21	15079.69
57	71	AG1	WOB			35	1	ATL GELATIN	29.0	?	-38.0	24997.32	13968.36
58	67	AG2	WOB			36	1	ATL GELATIN	32.0	?	-68.0	24681.38	13735.10
59	65	AG5	WOB			57	1	ATL GELATIN	30.0	?	?	24568.66	13638.55
60	190	E41	WOB	10	31	81	1	MDC	122.4	96.2	98.4	23808.78	24562.68
61	191	BW7	WOB			82	1	MDC	104.0	?	83.0	26208.76	24439.48
62	131	BW5	WOB	1	14	82	1	MDC	90.0	74.7	59.5	30469.89	19841.08
63		GW3	WOB	12	6	78	1	OLIN CHEM	85.5	81.3	63.5	17431.62	34149.68
64		GW6	WOB	11	12	80	1	OLIN CHEM	87.0	81.1	69.0	17168.78	33807.86
65		GW1	WOB	11	12	80	1	OLIN CHEM	88.0	76.6	66.8	16954.66	34900.88
66		GW11	WOB	11	12	80	1	OLIN CHEM	86.0	79.7	69.0	16726.17	33350.25
67		GW7	WOB	11	12	80	1	OLIN CHEM	83.0	77.7	69.0	17241.27	33548.97
68		GW8	WOB	11	12	80	1	OLIN CHEM	78.0	72.9	67.8	17418.73	33137.31
69		192	WOB			45	1	ABERJONA PACKING	75.0	?	45.0	17731.64	33145.69
70		GW4	WIL	12	6	78	1	OLIN CHEM	80.0	77.5	66.5	17659.12	33719.48
71		76	WIL			45	1	ABERJONA PACKING	80.0	?	41.5	16519.01	33331.67
72	247	77	WIL	2		45	1	ABERJONA PACKING	80.0	70.0	56.5	15600.87	33133.88
73	248	GW12	WOB	11	12	80	1	OLIN CHEM	82.0	77.4	69.3	16828.98	33002.24
74		190	WIL			45	1	ABERJONA PACKING	75.0	?	46.0	18206.21	33141.48
75	252	191	WIL			45	1	ABERJONA PACKING	75.0	70.0	54.0	18840.83	33297.05
76		168	WOB			45	1	ABERJONA PACKING	70.0	?	51.0	18959.20	32617.58
77		170	WOB			?	1			?		18383.13	32663.08
78		178	WOB			?	1			?		19524.51	32628.76
79	264	119	REA			45	1	ABERJONA PACKING	75.0	70.0	56.0	22249.97	34509.76
80		185	WOB			?	1					21793.85	33329.99
81	253	B16	WOB	8		55	1	MDPW	63.0	62.0	38.0	21461.50	33040.81
82		164	WOB			45	1	ABERJONA PACKING	70.0	?	45.0	19516.26	31510.61
83		176	WOB	2		45	1	ABERJONA PACKING	70.0	?	40.0	17754.59	30663.94
84		183	WOB			45	1	ABERJONA PACKING	70.0	?	39.0	17659.65	30647.14
85	241	GZ1	WOB	1	12	81	1	JAMPET ASSOC	71.0	64.5	58.5	19016.89	31069.45
86		B14A	WOB	1	19	81	1	JAMPET ASSOC	70.0	64.3	59.0	19277.18	30922.59
87		B6A	WOB	1	19	81	1	JAMPET ASSOC	69.0	63.6	46.0	19199.40	30673.99
88		GZ4	WOB	1	16	81	1	JAMPET ASSOC	68.0	59.9	48.0	19696.51	30402.22
89	230	B2A	WOB	1	16	81	1	JAMPET ASSOC	68.5	58.9	36.5	19335.86	30208.64
90	231	B9A	WOB	1	16	81	1	JAMPET ASSOC	68.0	59.0	56.2	19772.08	30225.59
91		306	WOB	11		57	1	STAUFFER CHEM	65.0	61.0	17.0	19771.11	29664.58
92		304	WOB	11		57	1	STAUFFER CHEM	65.0	58.0	1.0	19739.55	29344.59
93	225	305	WOB	11		57	1	STAUFFER CHEM	55.0	51.0	?	19854.13	28828.56
94		B7	WOB	8		55	1	MDPW	63.0	61.0	33.0	22480.73	30323.70
95		E31	WOB			?	1			?		22101.48	29677.80
96		E32	WOB			?	1			?		22163.34	29606.64
97		E33	WOB			?	1			?		22225.21	29449.76
98		E34	WOB			?	1			?		22245.62	29360.38
99		E35	WOB			?	1			?		22278.20	29281.84
100		E36	WOB			?	1			?		22312.89	29211.42
101		371	WOB			57	1	STAUFFER CHEM	70.0	?	39.5	22413.87	29376.25
102		5	WOB	9		39	1					19123.01	28958.82
103		E28	WOB				1					21617.11	29225.06
104		391	WOB	2		58	1	STAUFFER CHEM	55.0	53.0	27.0	22718.75	24500.90
105		382	WOB	8		57	1	STAUFFER CHEM	65.0	61.0	27.0	22864.73	27575.41
106	207	381	WOB	8		57	1	STAUFFER CHEM	65.0	54.0	49.0	22151.76	27398.91
107		374	WOB	6		57	1	STAUFFER CHEM	60.0	57.0	15.5	22471.36	26907.36
108	206	428	WOB	8		59	1	STAUFFER CHEM	65.0	48.0	-27.0	21158.03	26947.45
109		429	WOB	8		59	1	STAUFFER CHEM	60.0	36.0	-36.0	21317.86	26788.22
110		61	WOB	11		34	1	STAUFFER CHEM	70.0	?	31.0	20682.46	26676.39
111		62	WOB			35	1	STAUFFER CHEM	70.0	?	-17.0	20707.03	26473.01
112		55	WOB			52	1	STAUFFER CHEM	70.0	?	-17.0	20815.50	26008.44

113		438	WOB	5	64	1	STAUFFER CHEM	55.0	46.0	-6.0	20982.70	26536.29
114	198	63	WOB		36	1	STAUFFER CHEM	70.0	?	-13.0	20968.30	25612.22
115		64	WOB		37	1	STAUFFER CHEM	70.0	?	-9.0	21032.46	25509.60
116	183	B12	WOB		?	1	MDPW	104.0	?	8.0	16944.45	24131.50
117	184	B11	WOB		49	1	MDPW	91.0	?	19.0	19689.59	24219.26
118		B10	WOB	9	49	1	MDPW	58.0	?	-38.0	21393.05	24455.15
119		B9	WOB		49	1	MDPW	119.0	?	108.5	23532.03	24581.07
120		431	WOB		?	1			?		24482.73	24570.90
121		432	WOB		?	1			?		24021.56	24191.86
122		430	WOB	12	38	1			?		25084.12	24306.33
123		RW2	REA	6	40	1			?		25169.08	25081.26
124		RW4	REA	9	57	1	H.O. HOWE	120.0	105.0	102.0	26675.96	25124.02
125		B1	REA	6	55	1	MDPW	109.0	95.0	72.0	25721.73	24284.49
126	167	435	WOB	5	69	1	LAMONT	50.0	44.0	-40.0	21421.63	23074.39
127		263	WOB		58	1	JOHNSON BROS	75.0	?	15.0	23720.71	22902.58
128		B6	WOB	6	55	1	WOBURN	47.0	38.0	-22.0	26247.62	20356.78
129	123	B5	WOB	6	55	1	WOBURN	47.0	?	69.0	25935.55	19302.26
130		5	STO	8	73	1	GREICO BROS	90.0	86.0	-62.0	29816.65	17211.92
131	110	B15	WOB	7	41	1	WOBURN	37.0	?	-70.0	25416.37	18301.70
132	113	416	WOB		51	1	WOBURN	45.0	?	-24.4	23215.53	18547.81
133		415	WOB		51	1	WOBURN	45.0	?	-8.0	22752.17	18360.14
134		E40	WOB		?	1	?		?		22684.03	18178.58
135		E40A	WOB		?	1	?		?		22738.16	18102.10
136	98	414	WOB	10	51	1	WOBURN	45.0	?	9.4	22362.64	17592.82
137	100	412	WOB		51	1	WOBURN	50.0	?	9.4	22992.68	17668.70
138		417	WOB	1	52	1	WOBURN	45.0	?	-6.0	22915.25	17970.73
139		427	WOB		66	1	ATL GELATIN	45.0	?	17.0	23437.58	17592.82
140		413	WOB		51	1	WOBURN	50.0	?	15.5	23441.92	16822.64
141		425	WOB	3	61	1	ATL GELATIN	55.0	23.0	-83.0	24285.82	16102.27
142		187	STO	10	60	1	ATL GELATIN	55.0	40.0	-85.0	24417.56	16142.51
143		B5	WOB		58	1	MDPW	58.0	?	44.0	26846.51	16594.68
144		B4	STO	1	58	1	MDPW	54.0	40.0	13.0	27138.18	15990.15
145		4	STO		41	1	ATL GELATIN	50.0	?	24.0	27399.33	16073.23
146	84	B1	WOB	1	58	1	MDPW	77.0	75.0	52.0	27122.68	15090.04
147		X3	WOB		23	1	UNKNOWN	150.0	?	138.0	30666.41	15633.07
148	86	X1	WOB		25	1	UNKNOWN	145.0	?	107.0	30874.36	15450.47
149	74	27	WOB		?	1			?		25582.64	13983.33
150	68	14	WIN		?	1	USGS #14	116.0			26275.59	13433.21
151	75	B1	WIN		58	1	MDPW (DRY)	162.0	99.0	99.0	27742.52	13684.34
152	54	B13	WIN		34	1	MDPW	33.0	27.0	18.2	23777.06	12717.13
153	51	153	WIN	10	67	1	WINWAKE CORP	40.0	25.0	-57.5	22269.61	12406.50
154		152	WIN	8	67	1	WINWAKE CORP	35.0	18.0	-12.5	21365.37	12479.11
155	48	154	WIN	10	67	1	WINWAKE CORP	40.0	22.0	-10.0	20986.48	12369.83
156		10	WOB		?	1	WIN CRUSHED STON	80.0	?	80.0	20569.62	13363.23
157	45	9	WIN		?	1	JO WHITTEN	25.0	20.0	-35.0	22353.19	11423.20
158	42	X2	WIN	4	51	1	MDPW	32.0	18.0	-70.0	21582.29	10603.63
159	38	X1	WIN	4	51	1	MDPW	30.0	18.0	-77.2	21555.76	9970.42
160	36	24	WIN	8	65	1	BERNDT REALTY	45.0	30.0	-35.0	20048.60	9664.72
161	34	B14	WIN	4	51	1	MDPW	37.0	17.0	-83.6	21079.97	9423.22
162	30	X3	WIN	11	51	1	MDPW	28.0	18.0	-74.2	21068.42	8907.03
163	27	B3	WIN	2	54	1	MDPW	26.0	10.0	-94.0	20747.20	7937.12
164	24	B2	WIN	10	51	1	MDPW	18.0	14.0	-92.5	20999.80	7756.90
165	23	B15	WIN	4	35	1	MDPW	22.0	21.0	-34.0	20280.65	7679.56
166		B2	STO		58	1	MDPW	164.0	?	121.0	29933.48	8637.03
167		B3	STO	1	58	1	MDPW	154.0	153.0	131.7	28351.73	12351.80
168		E10	WOB		79	1	WOB NAT BANK	60.0	51.0	45.0	22854.91	25478.15
169		X4	WOB		?	1	WOBURN	55.0	?	33.5	22673.23	25271.80
170	178	340	REA	11	65	1	ADDISON WESLEY	130.0	117.0	117.0	28271.31	24325.80

171	179	B2	REA			?	1	MDPW	150.0	?	129.0	29285.11	24251.83
172	246	120	REA	8		69	1	READING	110.0	106.0	80.0	27018.58	33030.32
173	239	188	WOB	9		56	1	W GAUVIN	145.0	68.0	142.0	15418.35	32712.42
174		E44	WOB	8	11	81	1	MCD	106.2	95.5	101.2	23801.96	24716.40
175		E45	WOB	8	14	81	1	MCD	122.8	99.8	107.8	23799.94	24853.36
176	260	GW9	WIL			77	1	OLIN CHEM	90.0	?	87.0	16504.62	34586.31
177	202	W40	WOB	6		40	2	TABBUTT DAIRY	115.0	113.0	95.0	13620.37	26104.56
178		W262	WOB	6		56	2	L.A. DONAVAN	125.0	118.0	69.0	13361.68	27750.18
179		W23	WOB	3		41	2	WOBURN	96.0	95.0	?	15318.15	24344.89
180	180	B3	BUR	8		56	2	MDPW	124.0	120.0	?	9946.93	22497.87
181		W37	BUR	11		67	2	BURLINGTON	125.0	123.0	?	11227.97	23420.59
182	182	B13	WOB	9		49	2	MDPW	97.0	95.0	59.0	15437.07	23716.74
183	283	W53	REA	10		55	2	J KOPTUK	130.0	126.0	115.0	27352.31	39976.22
184								NOT USED					
185		W3	REA	6		40	2	FARR MERLE	160.0	157.0	?	25764.40	28061.55
186		W13	REA	6		32	2	L.G.HAWES	145.0	137.0	?	25037.40	27222.12
187	228	W41	WOB	6		40	2	JOSEPH RAY	85.0	78.0	76.0	15541.93	30705.32
188		W3	WOB	8		39	2	N.E. POULTRY	73.0	72.0	?	16653.32	30065.04
189	196	W30	WOB	6		40	2	THORNTON	95.0	86.0	83.0	18563.50	25641.02
190		W4	WOB	9		39	2	STAUFFER CHEM	65.0	63.0	?	18458.51	31280.87
191	90	W17	WOB	6		40	2	JD COAKLEY	175.0	168.0	163.0	20657.70	17304.30
192		W29	WOB				2	?		?			
193	25	W3	WIN	8		39	2	I BRINE	45.0	43.0	41.0	22315.27	7661.09
194	9	W22	WIN	6		40	2	WC WHITMAN	180.0	162.0	176.0	22496.10	4291.14
195		W30	WIN	5		66	2	B+M RR	25.0	17.0	?	20134.85	5707.12
196		W155	WIN	7		73	2	PURITY SUPREME	30.0	22.0	?	20847.45	6632.63
197	12	X5	WIN	11		51	2	MDPW	16.0	10.0	-11.0	20074.13	4463.05
198		B11	WIN	4		51	2	MDPW	15.0	9.0	?	19678.13	3806.99
199	6	B10	WIN	11		51	2	MDPW	15.0	9.0	-39.0	19405.95	3479.91
200		W1	STO	12	4	85	3	McDONALD	160.0	155.0	?	27577.82	14236.77
201	153	S79	WOB	12	4	85	3	EPA		44.0		21861.88	21823.02
202	174	S73	WOB	12	4	85	3	EPA		48.2		22321.65	23899.21
203		S74	WOB	12	4	85	3	EPA		46.7		21757.22	23809.84
204	146	S78	WOB	12	4	85	3	EPA		43.3		22053.15	21366.00
205	161	S87	WOB	12	4	85	3	EPA		44.9		22625.25	22343.85
206	152	S91	WOB	12	4	85	3	EPA		44.0		22675.96	21895.67
207	147	S92	WOB	12	4	85	3	EPA		43.3		22352.00	21442.86
208	143	S95	WOB	12	4	85	3	EPA		43.2		22366.40	21109.47
209		S97	WOB	12	4	85	3	EPA		45.2		22902.75	22409.28
210	156	S88	WOB	12	4	85	3	EPA		44.2		22290.19	22118.56
211		S63	WOB	12	4	85	3	EPA		57.9		23341.19	23108.96
212	170	S67	WOB	12	4	85	3	EPA		69.1		24213.91	22928.28
213		S70	WOB	12	4	85	3	EPA		56.8		23095.64	23825.72
214		S71	WOB	12	4	85	3	EPA		61.4		23394.57	23690.84
215		S72	WOB	12	4	85	3	EPA		45.0		22356.60	22718.86
216		S85	WOB	12	4	85	3	EPA		44.2		22630.78	22473.42
217	145	S86	WOB	12	4	85	3	EPA		43.6		23048.47	21237.24
218	148	S93	WOB	12	4	85	3	EPA		43.5		22614.93	21543.58
219	144	S96	WOB	12	4	85	3	EPA		43.1		22717.18	21181.18
220		S81	WOB	12	4	85	3	EPA		52.0		22924.45	23349.04
221		G3S	WOB	12	4	85	3	GRACE		71.3		24126.01	23488.71
222		G24S	WOB	12	4	85	3	GRACE		86.2		24531.87	23470.01
223		G2S	WOB	12	4	85	3	GRACE		91.2		24757.35	23940.68
224		GZA1	WOB	12	17	85	4	3 C COMPANY		49.4		19972.87	28067.25
225		GZA2/2A	WOB	12	17	85	4	3 C COMPANY		46.7		19631.53	27765.68
226		GZA3	WOB	12	17	85	4	3 C COMPANY		45.1		19847.09	28363.25
227		GZA4	WOB	12	17	85	4	3 C COMPANY		51.7		19499.20	28251.41
228		B81	WOB	6	7	81	5	DUNDEE PARK		66.2		19162.62	31813.67

229		BB2	WOB	6	7	81	5	DUNDEE PARK		66.6			
230		B3	WOB	6	7	81	5	DUNDEE PARK		66.6		19125.62	32146.99
231		BB4	WOB	6	7	81	5	DUNDEE PARK		68.7			
232		BB5	WOB	6	7	81	5	DUNDEE PARK		67.2			
233	242	BB6	WOB	6	7	81	5	DUNDEE PARK	69.8	66.4	48.3	19586.53	32032.15
234		BB7	WOB	6	7	81	5	DUNDEE PARK		68.4			
235		B8	WOB	6	7	81	5	DUNDEE PARK		LAKE			
236		BB9	WOB	6	7	81	5	DUNDEE PARK		LAKE		18640.68	33075.54
237		BB10	WOB	6	7	81	5	DUNDEE PARK		LAKE			
238		GZ1	WOB	11	9	81	6	UTILITY LINE		60.0		18842.30	30398.94
239		GZ1A	WOB				6	UTILITY LINE		61.9			
240		GZ3	WOB				6	UTILITY LINE		65.6			
241		GZ5	WOB	11	13	81	6	UTILITY LINE		70.2		18509.51	31776.94
242		GZ7B	WOB				6	UTILITY LINE		72.5		18305.59	32275.70
243		GZ8	WOB	11	17	81	6	UTILITY LINE		73.0		18359.31	32717.35
244		GZ11	WOB	9	28	81	6	UTILITY LINE		66.0		19001.25	29627.59
245		GZ12	WOB	9	28	81	6	UTILITY LINE		65.8		19156.91	29121.76
246	204	GZA1A	WOB	3	21	86	7	N WOBURN IND P	84.3	80.8	73.3	18635.69	26845.07
247		GZA2	WOB	3	21	86	7	N WOBURN IND P	78.0	76.0		17843.86	27322.06
248		GZA3	WOB	3	21	86	7	N WOBURN IND P	78.8	76.9		18315.99	27313.51
249		GZA5	WOB	3	21	86	7	N WOBURN IND P	77.4	71.2		18169.08	27833.73
250		GZA6	WOB	3	21	86	7	N WOBURN IND P	81.0	77.3		18416.03	27070.45
251		GZA7	WOB	3	21	86	7	N WOBURN IND P	78.0	75.2		18623.45	27553.94
252		GZA8	WOB	3	21	86	7	N WOBURN IND P	79.9	77.0		18051.93	27209.86
253		GZA9	WOB	3	21	86	7	N WOBURN IND P	76.7	74.0		18213.24	27533.65
254	213	GZA10	WOB	3	21	86	7	N WOBURN IND P	78.7	73.4	68.7	18823.94	27857.87
255		GZA11	WOB	3	21	86	7	N WOBURN IND P	78.0	74.0		18484.24	27662.20
256		WE1	WOB	2	2	87	8	WEYERHAEUSER		48.4		21270.76	23724.54
257		WE2	WOB	2	2	87	8	WEYERHAEUSER		48.9		21350.98	23676.40
258	172	WE3	WOB	2	2	87	8	WEYERHAEUSER	53.6	47.2	31.6	21431.47	23638.69
259	218	B2	WOB	5	17	85	9	CHROMERICS	65.1	57.4	32.6	22442.29	28414.49
260		B4	WOB	5	17	85	9	CHROMERICS	65.7	57.4	31.2	22458.42	28547.83
261		B5	WOB	5	17	85	9	CHROMERICS	64.8	57.3		22471.20	28323.84
262	96	MW101	STO	4	29	88	10	21 MAPLE ST 21E	70.0	64.5	50.0	27772.01	16089.63
263		S40 G		12	4	85	3	EPA		43.9		22773.73	21600.35
264		S39 H		12	4	85	3	EPA		43.7		22633.12	22173.08
265		S5		12	4	85	3	EPA		46.4		22100.15	24423.50
266		S6		12	4	85	3	EPA		54.9		22941.49	23785.06
267		S11		12	4	85	3	EPA		42.4		23520.24	20137.47
275		S76		12	4	85	3	EPA		47.3		21687.39	22642.59
276		S77		12	4	85	3	EPA		42.6		22694.34	20886.56
280		S84		12	4	85	3	EPA		44.1		22985.27	21919.32
285		S89		12	4	85	3	EPA		44.0		22536.57	22163.74
286		S90		12	4	85	3	EPA		44.5		22771.45	22182.33
290		S94		12	4	85	3	EPA		43.7		22903.35	21661.96
294		BSW1		12	4	85	3	BEATRICE		44.5		22035.02	21375.47
295		BW4		12	4	85	3	BEATRICE		41.8		21989.28	20511.11
296		W8		12	4	85	3	BEATRICE		42.9		22278.83	20855.05
297		W9		12	4	85	3	BEATRICE		42.6		22060.59	20888.63
298		W10		12	4	85	3	BEATRICE		43.5		22171.47	21095.40
299		W12		12	4	85	3	BEATRICE		43.7		22069.84	21523.75
300		W13		12	4	85	3	BEATRICE		43.6		22113.78	21210.45
301		W14		12	4	85	3	BEATRICE		43.6		22184.61	21305.74
302		GW01		12	4	85	3	GRACE		59.3		23642.24	23193.08
305		GW4		12	4	85	3	GRACE		85.2		24482.95	23496.06
306		GW5		12	4	85	3	GRACE		86.7		24840.11	23517.07
307		GW9		12	4	85	3	GRACE		90.7		24890.47	23674.78
308		GW10		12	4	85	3	GRACE		91.6		24602.61	23672.46

309	GW11	WOB	12	4	85	3	GRACE		75.6	24306.09	23418.46
310	GW12	WOB	12	4	85	3	GRACE		74.6	24111.25	23608.79
311	GW13	WOB	12	4	85	3	GRACE		78.6	24364.83	23591.17
312	GW14	WOB	12	4	85	3	GRACE		82.6	24430.84	23599.45
313	GW21	WOB	12	4	85	3	GRACE		75.3	24097.55	23724.68
314	GW22	WOB	12	4	85	3	GRACE		74.4	24139.20	23564.17
316	GW26	WOB	12	4	85	3	GRACE		92.1	24663.31	23760.13
317	GW27	WOB	12	4	85	3	GRACE		95.2	24591.83	23754.19
318	GW28	WOB	12	4	85	3	GRACE		72.6	24256.22	23569.32
319	TP3	WOB	8	13	86	11		125.0	118.5	19263.65	16058.29
320	TP4	WOB	8	13	86	11		130.0	125.0	19162.39	15925.87
321	B13	WOB	9		46	2	Woburn	97.0	95.0	15292.47	23737.13
322	W38	WOB	6		40	2	P Flowers	52.0	43.0	14592.52	11479.71
323	W53	WOB	7		40	2	Woburn	115.0	107.0	15099.43	19129.26
324	W54	WOB	9		36	2	Woburn	42.0	42.0	11921.11	13957.42
325	W66	WOB	10		48	2	Woburn	52.0	31.0	15857.78	10842.72
326	W67	WOB	8		36	2	Woburn	54.0	23.0	15824.46	10622.14
327	W71	WOB				2	Woburn	51.0	46.0	15001.38	11969.78
328	W72	WOB				2	Woburn	95.0	95.0	15082.32	19975.50
329	W73	WOB				2	Woburn	50.0	45.0	15595.37	11753.77
330	W98	WOB				2	Woburn	95.0	90.0	12544.57	9975.46
331	W107	WOB				2	Woburn	45.0	40.0	16753.84	11509.56
332	W119	WOB			31	2	Woburn	54.0	50.0	15267.88	14401.33
333	W306	WOB	11		57	2	Sylvania Electric	95.0	90.0	14465.32	23309.30
334	W339	WOB	8		34	2	Sylvania Electric	95.0	91.0	14790.46	23314.60
335	W366	WOB	8		58	2	Woburn	50.0	37.0	15936.01	10962.86
336	W421	WOB	1		60	2	Woburn	44.0	40.0	12754.03	13664.15
337	W434	WOB	10		64	2	Johnson Bros	105.0	103.0	13597.31	20512.42
338	W437	WOB	9		60	2	William Tarkey	95.0	45.0	8984.35	12786.56
339	X2	WOB			29	2	Woburn	170.0	166.0	18803.55	17446.32
340	B3	BUR	9		49	2	MDPW	124.0	120.0	9875.39	22520.63
341	B4	BUR	8		56	2	MDPW	221.0	204.0	4821.87	18725.00
342	W6	BUR	6		61	2	Burlington	105.0	104.0	11761.15	20935.92
343	W10	BUR	6		40	2	James Ray	110.0	110.0	7375.53	17475.83
344	W11	BUR	7		42	2	Lynch	115.0	52.0	11082.44	21675.80
345	W32	BUR			62	2	Burlington	100.0	99.0	9954.36	18700.05
346	W4	WIN	8		39	2	Winchester	50.0	34.0	17021.92	9641.93
347	W17	WIN	1		38	2	Winchester	46.0	39.0	16991.20	10146.53
348	W18	WIN	7		40	2	Thomas Vinson	250.0	239.0	10336.38	3581.71
349	W20	WIN				2	Eastern Felt Co	30.0	20.0	18282.06	9573.91
350	W29	WIN	6		60	2	Boadakian Kako	85.0	71.0	18174.67	11242.06

References

1 E+E 1982
2 USGS HDR 21
3 USGS WELLS G+H
4 3C COMPANY 21E
5 DUNDEE PARK 21E
6 UTILITY LINE ASSESMENT
7 NORTH WOBURN INDUSTRIAL PARK 21E
8 WEYERHAEUSER 21E
9 CHROMERIC 21E
10 21 MAPLE ST, STONEHAM 21E
11 SHAMROCK SCHOOL 21E

Appendix 2. Specific capacity data

Well	Town	Owner	Year	Diameter (inches)	Depth (ft)	Bedrock (ft)	Yield (gpm)	Drawdown (ft)	Time (hr)	Q/s (gpm/ft)	T (ft^2/day)	Location X (ft)	Location Y (ft)
76	WIL	Aberjona Packing	1945	2	38		72.0	4.0	4.0	18.0	3798	16140	33119
24	WIN	Berndt Realty	1965	18	80		250.0	10.0	66.0	25.0	5275	19748	9552
26	WIN	Atlantic Gelatin	1936	18	93		1000.0	8.0		125.0	26375	24620	13741
27	WIN	Atlantic Gelatin	1935	18	62		1000.0	15.0		66.7	14067	26187	14109
29	WIN	Koko Boadakian	1966	2	45		40.0	1.0	10.0	40.0	8440	17918	11063
151	WIN	JO Whitten	1971	16	129		2000.0	37.0	24.0	54.1	11405	22058	11212
152	WIN	Win-Wake Co	1967	2	42		25.0	3.0	1.0	8.3	1758	20903	12452
2	WOB	Stauffer Chemical	1934	18	62		600.0	54.0		11.1	2344	19026	27292
10	WOB	Win Crushed Stone		6	50	0	100.0	7.0	8.0	14.3	[illegible]	20060	12921
54	WOB	Woburn	1937	24	40		833.0	10.0		83.3	17576	11630	13818
66	WOB	Woburn	1931	18	63		349.0	33.0	6.0	10.6	2231	15740	10614
67	WOB	Woburn	1931	14	70		175.0	8.0	117.0	21.9	4616	15668	10301
68	WOB	Woburn	1931	18	53		842.0	26.0	14.0	32.4	6833	14951	11147
69	WOB	Woburn	1937	18	84		1750.0	14.0		125.0	26375	16601	10669
72	WOB	Woburn	1936	6	45		120.0	4.0	48.0	30.0	6330	15051	19852
85	WOB	Woburn	1936	2	42		75.0	2.0	24.0	37.5	7913	25578	19503
176	WOB	Aberjona Packing		2	28		92.0	9.0	3.0	10.2	2157	18239	30616
183	WOB	Aberjona Packing	1945	2	28		100.0	8.0	5.0	12.5	2638	17957	30486
262	WOB	Donovan L A Co	1956	6	315	56	50.0	100.0	16.0	0.5	106	13155	27933
264	WOB	Atlantic Gelatin	1658	18	124		400.0	46.0		8.7	1835	24537	14748
271	WOB	Atlantic Gelatin	1957	18	50		300.0	28.0		10.7	2261	25740	15415
335	WOB	Sylvania Electric	1952	16	46		210.0	27.0		7.8	1641	14259	23289
336	WOB	Sylvania Electric	1952	10	40		201.0	26.0		7.7	1631	14521	23267
337	WOB	Sylvania Electric	1952	10	38		239.0	12.0		19.9	4202	14976	23223
338	WOB	Sylvania Electric	1954	8	40		20.0	15.0		1.3	281	14422	23350
339	WOB	Sylvania Electric	1954	8	36		65.0	22.0		3.0	623	14732	23144
366	WOB	Woburn	1958	24	80		1388.0	16.0	216.0	86.8	18304	15801	10790
374	WOB	Woburn	1957	2	35		67.0	2.0	2.0	33.5	7069	22301	26934
382	WOB	Woburn	1957	2	32		63.0	1.0	3.0	63.0	13293	20932	24979
415	WOB	Woburn	1951	2	51		60.0	2.0	4.0	30.0	6330	22241	18555
417	WOB	Woburn	1951	2	444		70.0	1.0	4.0	70.0	14770	22397	18010
419	WOB	Woburn G	1985	24	85		483.0	17.3		27.9	5891	22513	21684
420	WOB	Woburn H	1985	24	84		358.8	12.3		29.1	6140	22313	22184
421	WOB	Woburn	1959	24	35		350.0	10.0	120.0	35.0	7385	12576	13431
422	WOB	Woburn	1963	2	40		40.0	1.0	3.0	40.0	8440	23840	20201
424	WOB	Atlantic Gelatin	1961	8	134	134	80.0	73.0		1.1	231	23444	16700
434	WOB	Johnson Bros	1964		725	28	80.0	575.0	6.0	0.1	29	13354	20553
438	WOB	Stauffer Chemical	1964	24	61		720.0	9.0	92.0	80.0	16880	20808	26290
37	BUR	Burlington	1965	2	48		180.0	15.0	168.0	12.0	2532	11500	24000

Arithmetic-Mean 7496.4
Geometric-Mean 4613.5
Harmonic-Mean 2085.1

Appendix 3. Falling head data

Well	Screen depth [ft]	K [ft/day]	Ground elev [ft]	Bedrock depth [ft]
S 64	9.0	4.4182	57.6	
S 64	19.0	0.2913	57.6	
S 64	31.5	4.2545	57.6	
S 74	39.0	65.4545	48.2	
S 74	54.0	327.2727	48.2	
S 74	66.0	0.5007	48.2	
S 76	20.0	0.0861	53.0	130.0
S 76	60.0	0.1613	53.0	130.0
S 76	126.0	0.1217	53.0	130.0
S 77	30.0	0.1276	44.9	130.0
S 77	73.0	0.4156	44.9	130.0
S 84	16.0	0.0861	46.2	81.5
S 84	78.0	0.3600	46.2	81.5
S 85	15.0	1.7345	46.1	>70
S 85	35.0	0.6905	46.1	>70
S 86	50.0	0.4909	44.7	

Appendix 4. Grain size data

Well	Sample depth [ft]	d10 [mm]	d25 [mm]	d60 [mm]	K (d10) [ft/day]	Ground elev [ft]	Bedrock depth [ft]
S 63	13.0	0.15	0.23	1.40	73.6364	69.5	22.0
S 64 M	9.0	0.01	0.07	0.32	0.2651	57.6	
S 64 M	32.0	0.01	0.12	0.31	0.2095	57.6	
S 66 D	10.0	0.01	0.05	0.42	0.1604	57.6	
S 67	15.0	0.01	0.09	0.84	0.2363	83.3	54.0
S 67	40.0	0.08	0.15	0.25	18.3927	83.3	54.0
S 70	15.0	0.06	0.30	2.80	11.7818	69.4	62.0
S 70 D	35.0	0.01	0.05	0.99	0.0818	69.4	62.0
S 70 D	55.0	0.15	0.35	1.50	73.6364	69.4	62.0
S 71	0.0	0.07	1.40	5.00	16.0364	71.4	16.5
S 71	2.0	0.08	0.48	5.00	20.9455	71.4	16.5
S 71	4.0	0.08	0.26	5.00	23.6291	71.4	16.5
S 71	6.0	0.03	0.20	3.60	2.9455	71.4	16.5
S 71	8.0	0.02	0.15	3.20	1.7313	71.4	16.5
S 71	10.0	0.06	0.25	5.00	11.7818	71.4	16.5
S 71	12.0	0.06	0.18	1.20	11.7818	71.4	16.5
S 71	14.0	0.23	0.80	5.00	173.1273	71.4	16.5
S 72 D	35.0	0.01	0.03	0.12	0.7364	50.2	116.0
S 72 D	55.0	0.01	0.03	0.15	0.5531	50.2	116.0
S 72 D	80.0	0.15	0.26	0.58	73.6364	50.2	116.0
S 74 M	34.0	0.01	0.04	0.20	0.7364	48.2	
S 74 M	39.0	0.07	0.16	0.42	16.0364	48.2	
S 75 D	10.0	0.20	0.48	1.00	130.9091	57.0	
S 75 D	40.0	0.06	0.26	0.40	11.7818	57.0	
S 75 D	65.0	0.02	0.04	0.04	1.3091	57.0	
S 76	21.0	0.02	0.04	0.20	1.0604	53.0	130.0
S 76 M	60.0	0.05	0.12	0.20	6.6109	53.0	130.0
S 77	20.0	0.15	0.24	0.26	73.6364	44.9	130.0
S 77 D	70.0	0.22	0.29	0.84	158.4000	44.9	130.0
S 77 D	120.0	0.00	0.01	0.02	0.0334	44.9	130.0
S 78	17.0	0.08	0.19	0.25	20.9455	45.8	90.5
S 78	63.0	0.00	0.03	0.12	0.0399	45.8	90.5
S 79	14.0	0.17	0.25	0.26	94.5818	47.4	107.5
S 79	69.0	0.07	0.12	0.90	13.8109	47.4	107.5
S 80	8.0	0.01	0.04	0.13	0.7364	48.7	
S 82	10.0	0.05	0.14	0.99	8.1318	57.0	
S 82	20.0	0.08	0.23	0.24	18.3927	57.0	
S 82	35.0	0.00	0.05	0.50	0.0524	57.0	
S 83	40.0	0.17	0.24	0.89	94.5818	48.1	
S 83	60.0	0.25	0.48	0.90	204.5455	48.1	
S 83	80.0	0.03	0.07	0.15	2.9455	48.1	
S 84	10.0	0.25	0.89	5.00	204.5455	46.2	81.5
S 84	40.0	0.15	0.28	1.80	73.6364	46.2	81.5
S 84	65.0	0.10	0.60	5.00	32.7273	46.2	81.5
S 85 D	25.0	0.20			130.9091	46.1	>70
S 85	34.0	0.28	0.68	5.00	256.5818	46.1	>70
S 85	59.0	0.02	0.13	2.50	1.5840	46.1	>70
S 86	25.0	0.20	0.90	5.00	173.1273	44.7	
S 86 D	50.0	0.23	0.30	0.32	173.1273	44.7	

Appendix 5. AQUIFEM output

```
*****************************************************************************************************

                                        AQUIFEM-1
                                        =========
*****************************************************************************************************

                              TWO DIMENSIONAL FINITE ELEMENT MODEL
                                   OF GROUNDWATER FLOW WITH
                                  LINEAR TRIANGULAR ELEMENTS

                                DEPARTMENT OF CIVIL ENGINEERING
                             MASSACHUSETTS INSTITUTE OF TECHNOLOGY
                                CAMBRIDGE, MASSACHUSETTS, 02139

                                                                        NOVEMBER 1979 VERSION

*****************************************************************************************************

            WOBURN 13C RUN 1- 12/18/89 RISING HEAD, K=75,50,10,5,1,.75 MAXIT=50, ERROR=.5

*****************************************************************************************************


PROBLEM DESCRIPTION
===================

TYPE OF AQUIFER.....................................................................LINEAR=      .F.
   LINEAR=.T.  LINEAR (CONFINED) OR LINEARIZED AQUIFER
   LINEAR=.F.  NONLINEAR (UNCONFINED OR MIXED) AQUIFER

TYPE OF PROBLEM.....................................................................STEADY=      .T.
   STEADY=.T.  STEADY STATE PROBLEM
   STEADY=.F.  UNSTEADY OR TRANSIENT PROBLEM

INITIAL CONDITIONS/GUESSES PARAMETER................................................INITAL=      .F.
   INITAL=.T.  COMPUTE LINEAR SOLUTION AS A FIRST GUESS FOR A NONLINEAR PROBLEM
               AND/OR INITIAL STEADY STATE SOLUTION FOR AN UNSTEADY PROBLEM
   INITAL=.F.  READ INITIAL CONDITIONS OR GUESSES

FINAL STEADY STATE SOLUTION PARAMETER................................................FINAL=      .F.
   FINAL=.T.  COMPUTE FINAL STEADY STATE SOLUTION WITH BOUNDARY CONDITIONS AT TIME=ENDTIM
   FINAL=.F.  DO NOT COMPUTE FINAL STEADY STATE SOLUTION

DATA CHECK PARAMETER.................................................................CHECK=      .F.
   CHECK=.T.  CHECK DATA THEN STOP
   CHECK=.F.  EXECUTE PROGRAM NORMALLY


FINITE ELEMENT GRID PARAMETERS
==============================

NUMBER OF ELEMENTS...................................................................NUMEL=      494

NUMBER OF NODE POINTS................................................................NUMNP=      282

FLAG FOR PRINTING GEOMETRIC DATA....................................................PRGEOM=      .F.
   PRGEOM=.T.  PRINT GEOMETRIC DATA
```

```
   PRGEOM=.F.  DO NOT PRINT GEOMETRIC DATA

FLAG FOR PRINT-PLOTTING GEOMETRIC DATA...............................................PLGEOM=        .F.
   PLGEOM=.T.  PLOT GEOMETRIC DATA
   PLGEOM=.F.  DO NOT PLOT GEOMETRIC DATA

SCALING FACTOR FOR X-COORDINATES.....................................................XSCALE=     1.000

SCALING FACTOR FOR Y-COORDINATES.....................................................YSCALE=     1.000

LARGEST ELEMENT IDENTIFICATION NUMBER................................................MAXELT=       499

LARGEST NODE IDENTIFICATION NUMBER...................................................MAXNOD=       284


AQUIFER PROPERTY PARAMETERS
===========================

NUMBER OF REGIONS WITH REGIONALLY DEFINED AQUIFER PROPERTIES...........................NAQR=         0

NUMBER OF INDIVIDUAL ELEMENTS OR NODES WITH SPECIALLY DEFINED AQUIFER PROPERTIES.....NSPEC=       282

METHOD BY WHICH AQUIFER PROPERTIES ARE GIVEN.................................... ....BYNODE=        .T.
   BYNODE=.T.  BY NODES
   BYNODE=.F.  BY ELEMENTS

METHOD BY WHICH HYDRAULIC PROPERTIES ARE GIVEN..........................................PERM=        .T.
   PERM=.T.  PERMEABILITIES KXX,KYY ARE GIVEN
   PERM=.F.  TRANSMISSIVITIES TXX,TYY ARE GIVEN
```

```
BOUNDARY CONDITION PARAMETERS
=============================

NUMBER OF PRESCRIBED BOUNDARY HEAD NODES............................................NHNODE=       90

NUMBER OF TIMES WHEN PRESCRIBED HEAD BOUNDARY CONDITIONS ARE SET.......................NTBH=        1

NUMBER OF NODES WHERE GROUND LEVELS ARE SPECIFIED.....................................NGRD=      192

NUMBER OF TIMES WHEN GROUND LEVELS ARE SET...........................................NTGRD=        1

NUMBER OF FLUX ELEMENTS.............................................................NFLXE=      494

NUMBER OF TIMES WHEN PRESCRIBED BOUNDARY FLUXES ARE SET.............................NTFLXE=        1

NUMBER OF REGIONS WITH REGIONAL ELEMENT FLUX..........................................NEFR=        1

NUMBER OF FLUX SIDES................................................................NFLXS=        0

NUMBER OF TIMES WHEN PRESCRIBED SIDE FLUXES ARE SET.................................NTFLXS=        0

NUMBER OF FLUX NODES................................................................NFLXN=        0

NUMBER OF TIMES WHEN PRESCRIBED NODE FLUXES ARE SET.................................NTFLXN=        0


NUMBER OF 3RD-TYPE BOUNDARY SIDES.....................................................NBC3=        0

NUMBER OF TIMES WHEN 3RD-TYPE BOUNDARY HEADS ARE SET.................................NTBC3=        0

NUMBER OF NODES ON THE 3RD-TYPE BOUNDARY SIDES.......................................NNOD3=        0

3RD-TYPE BOUNDARY PARAMETER.........................................................BEDBC3=      .F.
   BEDBC3=.T.  USE RIVER BED LEVELS TO MODIFY 3RD-TYPE INFLOWS
   BEDBC3=.F.  DO NOT USE RIVER BED LEVELS

NUMBER OF NODES WHERE HEADS IN ADJACENT AQUIFER ARE GIVEN............................NHADJ=        0

NUMBER OF TIMES WHEN HEADS IN ADJACENT AQUIFER ARE SET..............................NTHADJ=        0

ADJACENT AQUIFER PARAMETER...........................................................ATTOP=      .F.
   ATTOP=.T.  ADJACENT AQUIFER IS ABOVE AQUIFER UNDER STUDY
   ATTOP=.F.  ADJACENT AQUIFER IS NOT AT TOP

METHOD OF SUPPLYING ADJACENT HEADS..................................................HAVARY=      .F.
   HAVARY=.T.  ADJACENT HEADS VARY IN SPACE
   HAVARY=.F.  ADJACENT HEADS ARE CONSTANT

TYPE OF INITIAL CONDITIONS/GUESSES IF INITAL=.F.....................................ICVARY=      .T.
   ICVARY=.T.  INITIAL CONDITIONS VARY IN SPACE
   ICVARY=.F.  INITIAL CONDITIONS ARE CONSTANT
```

SOLUTION STRATEGY
================

START TIME..STRTIM= 0.0000

END TIME..ENDTIM= 1.0000

TOLERANCE FOR CONVERGENCE..TOL= 0.5000

INDICATOR FOR CONVERGENCE CRITERION...ITOL= 1
ITOL=0 ROOT MEAN SQUARE ERROR CRITERION
ITOL=1 MAXIMUM ABSOLUTE ERROR CRITERION

MAXIMUM NUMBER OF ITERATIONS...MAXIT= 50

TIME STEP..DT= 0.00000

ALPHA PARAMETER FOR TIME INTEGRATION SCHEME...................................ALPHA= 0.5000

TIME STEP PARAMETER...DTPARM= 0.0000

INDICATOR FOR CHANGING TIME STEP...IDT= 0
IDT=0 NO CHANGE OF TIME STEP
IDT=1 DT=DT*DTPARM AFTER NDT TIME STEPS
IDT=2 DT=DT+DTPARM AFTER NDT TIME STEPS

NUMBER OF CONSTANT LENGTH TIME STEPS BEFORE CHANGING ACCORDING TO IDT..........NDT= 1

NUMBER OF ITERATIONS WITH SAME LEFT HAND SIDE SYSM MATRIX....................NSYS= 1
NSYS=999 REFORM SYSM ONCE EACH TIME STEP

OUTPUT CONTROL
==============

FIRST TIME STEP FOR PRINTED OUTPUT..ISTPRT= 0

NUMBER OF TIME STEPS BETWEEN PRINTED OUTPUTS.................................NDTPRT= 1

NUMBER OF SPECIAL PRINTED OUTPUT TIMES...NOUT= 0

FIRST TIME STEP FOR PLOTTED OUTPUT..ISTPLT= 0

NUMBER OF TIME STEPS BETWEEN PLOTTED OUTPUTS.................................NDTPLT= 1

NUMBER OF SPECIAL PLOTTED OUTPUT TIMES...NPLT= 0

PLOT SCALING FACTOR...PSCALE= 100.00

INCREMENT FOR LABELLING PLOT AXES..PDELTA= 100.00

ROTATION PARAMETER..NRFLAG= 2
NRFLAG=0 ROTATION OF PLOT IS ALLOWED
NRFLAG=1 NO ROTATION IS ALLOWED, X-AXIS ACROSS THE PAGE
NRFLAG=2 ROTATION IS FORCED, Y-AXIS ACROSS THE PAGE

NUMBER OF ROWS/COLUMNS AROUND PLOT BOUNDARY..................................NBOUND= 3

```
NUMBER OF DECIMAL PLACES IN PLOTTED VALUES OF HEAD.....................................NDP=        1



NUMBER OF ELEMENTS (NK) IN SYMMETRIC COMPACTED MATRIX IS 3063

BANDWIDTH OF MATRIX IN FULL FORM WOULD BE   95

53710 WORDS OF STORAGE HAVE BEEN USED OUT OF A TOTAL ALLOCATION OF  55000

CALCULATIONS ARE IN DOUBLE PRECISION
```

AQUIFER CHARACTERISTICS

=====================

NODE NO	BOTTOM ELEVATION	AQUIFER THICKNESS	STORATIVITY	SPECIFIC YIELD	CONF.LAYER K'/B'
1	-25.00	100.00	0.000E+00	0.000E+00	0.000E+00
2	-56.00	100.00	0.000E+00	0.000E+00	0.000E+00
3	-30.00	100.00	0.000E+00	0.000E+00	0.000E+00
4	20.00	120.00	0.000E+00	0.000E+00	0.000E+00
5	-120.00	128.50	0.000E+00	0.000E+00	0.000E+00
6	-120.00	129.20	0.000E+00	0.000E+00	0.000E+00
7	-119.50	129.50	0.000E+00	0.000E+00	0.000E+00
8	-25.00	100.00	0.000E+00	0.000E+00	0.000E+00
9	0.00	180.00	0.000E+00	0.000E+00	0.000E+00
10	40.00	120.00	0.000E+00	0.000E+00	0.000E+00
11	-100.00	150.00	0.000E+00	0.000E+00	0.000E+00
12	-118.80	129.50	0.000E+00	0.000E+00	0.000E+00
13	-95.00	150.00	0.000E+00	0.000E+00	0.000E+00
14	-118.10	129.50	0.000E+00	0.000E+00	0.000E+00
15	-65.00	110.00	0.000E+00	0.000E+00	0.000E+00
16	30.00	200.00	0.000E+00	0.000E+00	0.000E+00
17	-85.00	140.00	0.000E+00	0.000E+00	0.000E+00
18	-120.00	132.20	0.000E+00	0.000E+00	0.000E+00
19	-120.00	132.90	0.000E+00	0.000E+00	0.000E+00
20	-95.00	150.00	0.000E+00	0.000E+00	0.000E+00
21	-120.00	133.60	0.000E+00	0.000E+00	0.000E+00
22	-60.00	100.00	0.000E+00	0.000E+00	0.000E+00
23	-120.00	142.00	0.000E+00	0.000E+00	0.000E+00
24	-120.00	134.40	0.000E+00	0.000E+00	0.000E+00
25	-60.00	100.00	0.000E+00	0.000E+00	0.000E+00
26	30.00	200.00	0.000E+00	0.000E+00	0.000E+00
27	-94.40	108.90	0.000E+00	0.000E+00	0.000E+00
28	-105.00	150.00	0.000E+00	0.000E+00	0.000E+00
29	-120.00	135.80	0.000E+00	0.000E+00	0.000E+00
30	-74.00	104.00	0.000E+00	0.000E+00	0.000E+00
31	-55.00	100.00	0.000E+00	0.000E+00	0.000E+00
32	-67.00	120.00	0.000E+00	0.000E+00	0.000E+00
33	-120.00	136.60	0.000E+00	0.000E+00	0.000E+00
34	-113.00	150.00	0.000E+00	0.000E+00	0.000E+00
35	10.00	200.00	0.000E+00	0.000E+00	0.000E+00
36	-105.00	150.00	0.000E+00	0.000E+00	0.000E+00
37	-90.00	107.30	0.000E+00	0.000E+00	0.000E+00
38	-120.00	150.00	0.000E+00	0.000E+00	0.000E+00
39	-110.00	150.00	0.000E+00	0.000E+00	0.000E+00
40	-20.00	80.00	0.000E+00	0.000E+00	0.000E+00
41	-100.00	118.00	0.000E+00	0.000E+00	0.000E+00
42	-120.00	138.80	0.000E+00	0.000E+00	0.000E+00
43	0.00	100.00	0.000E+00	0.000E+00	0.000E+00
44	-120.00	139.50	0.000E+00	0.000E+00	0.000E+00
45	-120.00	140.60	0.000E+00	0.000E+00	0.000E+00
46	-90.00	133.00	0.000E+00	0.000E+00	0.000E+00
47	32.00	120.00	0.000E+00	0.000E+00	0.000E+00
48	-10.00	50.00	0.000E+00	0.000E+00	0.000E+00
49	-120.00	141.30	0.000E+00	0.000E+00	0.000E+00
50	30.00	120.00	0.000E+00	0.000E+00	0.000E+00

51	-70.00	110.00	0.000E+00	0.000E+00	0.000E+00
52	-95.00	117.80	0.000E+00	0.000E+00	0.000E+00
53	-120.00	143.90	0.000E+00	0.000E+00	0.000E+00
54	-120.00	145.10	0.000E+00	0.000E+00	0.000E+00
55	-5.00	44.00	0.000E+00	0.000E+00	0.000E+00
56	30.00	120.00	0.000E+00	0.000E+00	0.000E+00
57	-65.00	105.00	0.000E+00	0.000E+00	0.000E+00
58	-120.00	146.20	0.000E+00	0.000E+00	0.000E+00
59	-55.00	83.00	0.000E+00	0.000E+00	0.000E+00
60	-40.00	100.00	0.000E+00	0.000E+00	0.000E+00
61	40.00	120.00	0.000E+00	0.000E+00	0.000E+00
62	-40.00	74.50	0.000E+00	0.000E+00	0.000E+00
63	-85.00	137.00	0.000E+00	0.000E+00	0.000E+00
64	-90.00	117.30	0.000E+00	0.000E+00	0.000E+00
65	-120.00	150.00	0.000E+00	0.000E+00	0.000E+00
66	-80.00	108.40	0.000E+00	0.000E+00	0.000E+00
67	-95.00	127.00	0.000E+00	0.000E+00	0.000E+00
68	16.00	100.00	0.000E+00	0.000E+00	0.000E+00
69	-115.00	167.00	0.000E+00	0.000E+00	0.000E+00
70	-65.00	94.50	0.000E+00	0.000E+00	0.000E+00
71	-55.00	84.00	0.000E+00	0.000E+00	0.000E+00
72	-50.00	80.50	0.000E+00	0.000E+00	0.000E+00
73	-72.00	103.20	0.000E+00	0.000E+00	0.000E+00
74	-25.00	105.00	0.000E+00	0.000E+00	0.000E+00
75	42.00	120.00	0.000E+00	0.000E+00	0.000E+00
76	70.00	93.00	0.000E+00	0.000E+00	0.000E+00
77	28.00	40.00	0.000E+00	0.000E+00	0.000E+00
78	-70.00	113.00	0.000E+00	0.000E+00	0.000E+00
79	-85.00	132.00	0.000E+00	0.000E+00	0.000E+00
80	-50.00	81.00	0.000E+00	0.000E+00	0.000E+00
81	-80.00	132.00	0.000E+00	0.000E+00	0.000E+00
82	-25.00	57.50	0.000E+00	0.000E+00	0.000E+00
83	69.00	100.00	0.000E+00	0.000E+00	0.000E+00
84	-23.00	100.00	0.000E+00	0.000E+00	0.000E+00
85	60.00	108.00	0.000E+00	0.000E+00	0.000E+00
86	45.00	100.00	0.000E+00	0.000E+00	0.000E+00
87	80.00	100.00	0.000E+00	0.000E+00	0.000E+00
88	-66.00	99.50	0.000E+00	0.000E+00	0.000E+00
89	-11.00	55.00	0.000E+00	0.000E+00	0.000E+00
90	65.00	110.00	0.000E+00	0.000E+00	0.000E+00
91	-80.00	127.00	0.000E+00	0.000E+00	0.000E+00
92	-85.00	150.00	0.000E+00	0.000E+00	0.000E+00
93	-15.00	49.50	0.000E+00	0.000E+00	0.000E+00
94	15.00	40.00	0.000E+00	0.000E+00	0.000E+00
95	-5.00	54.00	0.000E+00	0.000E+00	0.000E+00
96	-30.00	100.00	0.000E+00	0.000E+00	0.000E+00
97	-22.00	100.00	0.000E+00	0.000E+00	0.000E+00
98	5.00	40.00	0.000E+00	0.000E+00	0.000E+00
99	5.00	45.00	0.000E+00	0.000E+00	0.000E+00
100	5.00	45.00	0.000E+00	0.000E+00	0.000E+00
101	-20.00	67.50	0.000E+00	0.000E+00	0.000E+00
102	-64.00	99.50	0.000E+00	0.000E+00	0.000E+00
103	-30.00	99.50	0.000E+00	0.000E+00	0.000E+00
104	-20.00	99.50	0.000E+00	0.000E+00	0.000E+00
105	90.00	100.00	0.000E+00	0.000E+00	0.000E+00
106	-50.00	120.00	0.000E+00	0.000E+00	0.000E+00
107	-60.00	96.50	0.000E+00	0.000E+00	0.000E+00
108	-20.00	68.00	0.000E+00	0.000E+00	0.000E+00

109	0.00	100.00	0.000E+00	0.000E+00	0.000E+00
110	-45.00	82.50	0.000E+00	0.000E+00	0.000E+00
111	65.00	107.00	0.000E+00	0.000E+00	0.000E+00
112	-5.00	48.00	0.000E+00	0.000E+00	0.000E+00
113	0.00	45.00	0.000E+00	0.000E+00	0.000E+00
114	-30.00	79.00	0.000E+00	0.000E+00	0.000E+00
115	-30.00	68.50	0.000E+00	0.000E+00	0.000E+00
116	-52.00	100.00	0.000E+00	0.000E+00	0.000E+00
117	30.00	100.00	0.000E+00	0.000E+00	0.000E+00
118	0.00	99.50	0.000E+00	0.000E+00	0.000E+00
119	70.00	80.00	0.000E+00	0.000E+00	0.000E+00
120	5.00	77.50	0.000E+00	0.000E+00	0.000E+00
121	-30.00	70.00	0.000E+00	0.000E+00	0.000E+00
122	-30.00	69.50	0.000E+00	0.000E+00	0.000E+00
123	-53.00	100.00	0.000E+00	0.000E+00	0.000E+00
124	-30.00	70.20	0.000E+00	0.000E+00	0.000E+00
125	-30.00	70.00	0.000E+00	0.000E+00	0.000E+00
126	-30.00	79.00	0.000E+00	0.000E+00	0.000E+00
127	-20.00	60.80	0.000E+00	0.000E+00	0.000E+00
128	-15.00	55.30	0.000E+00	0.000E+00	0.000E+00
129	-32.00	100.00	0.000E+00	0.000E+00	0.000E+00
130	35.00	100.00	0.000E+00	0.000E+00	0.000E+00
131	10.00	99.50	0.000E+00	0.000E+00	0.000E+00
132	70.00	100.00	0.000E+00	0.000E+00	0.000E+00
133	100.00	47.00	0.000E+00	0.000E+00	0.000E+00
134	30.00	75.00	0.000E+00	0.000E+00	0.000E+00
135	0.00	50.00	0.000E+00	0.000E+00	0.000E+00
136	-25.00	66.50	0.000E+00	0.000E+00	0.000E+00
137	-15.00	60.00	0.000E+00	0.000E+00	0.000E+00
138	30.00	42.00	0.000E+00	0.000E+00	0.000E+00
139	96.00	44.00	0.000E+00	0.000E+00	0.000E+00
140	-40.00	85.00	0.000E+00	0.000E+00	0.000E+00
141	-45.00	87.20	0.000E+00	0.000E+00	0.000E+00
142	-10.00	58.00	0.000E+00	0.000E+00	0.000E+00
143	-40.00	84.20	0.000E+00	0.000E+00	0.000E+00
144	-65.00	107.80	0.000E+00	0.000E+00	0.000E+00
145	-40.00	83.60	0.000E+00	0.000E+00	0.000E+00
146	-40.00	84.30	0.000E+00	0.000E+00	0.000E+00
147	-55.00	98.50	0.000E+00	0.000E+00	0.000E+00
148	-70.00	114.50	0.000E+00	0.000E+00	0.000E+00
149	-5.00	54.00	0.000E+00	0.000E+00	0.000E+00
150	-80.00	125.00	0.000E+00	0.000E+00	0.000E+00
151	20.00	40.00	0.000E+00	0.000E+00	0.000E+00
152	-75.00	119.20	0.000E+00	0.000E+00	0.000E+00
153	-30.00	75.00	0.000E+00	0.000E+00	0.000E+00
155	-20.00	69.00	0.000E+00	0.000E+00	0.000E+00
156	-70.00	114.00	0.000E+00	0.000E+00	0.000E+00
157	-90.00	136.00	0.000E+00	0.000E+00	0.000E+00
158	-20.00	92.00	0.000E+00	0.000E+00	0.000E+00
159	-15.00	100.00	0.000E+00	0.000E+00	0.000E+00
160	-24.00	75.00	0.000E+00	0.000E+00	0.000E+00
161	-74.00	119.50	0.000E+00	0.000E+00	0.000E+00
162	-75.00	123.00	0.000E+00	0.000E+00	0.000E+00
163	100.00	40.00	0.000E+00	0.000E+00	0.000E+00
164	65.00	40.00	0.000E+00	0.000E+00	0.000E+00
165	22.00	40.00	0.000E+00	0.000E+00	0.000E+00
166	0.00	63.00	0.000E+00	0.000E+00	0.000E+00
167	-35.00	85.00	0.000E+00	0.000E+00	0.000E+00

168	-70.00	116.20	0.000E+00	0.000E+00	0.000E+00
169	-80.00	126.80	0.000E+00	0.000E+00	0.000E+00
170	-25.00	100.00	0.000E+00	0.000E+00	0.000E+00
171	10.00	52.00	0.000E+00	0.000E+00	0.000E+00
172	-40.00	93.60	0.000E+00	0.000E+00	0.000E+00
173	-65.00	112.50	0.000E+00	0.000E+00	0.000E+00
174	-30.00	80.00	0.000E+00	0.000E+00	0.000E+00
175	-45.00	93.20	0.000E+00	0.000E+00	0.000E+00
176	-25.00	82.50	0.000E+00	0.000E+00	0.000E+00
177	-9.00	100.00	0.000E+00	0.000E+00	0.000E+00
178	30.00	100.00	0.000E+00	0.000E+00	0.000E+00
179	50.00	100.00	0.000E+00	0.000E+00	0.000E+00
180	50.00	45.00	0.000E+00	0.000E+00	0.000E+00
181	75.00	40.00	0.000E+00	0.000E+00	0.000E+00
182	84.00	40.00	0.000E+00	0.000E+00	0.000E+00
183	64.00	40.00	0.000E+00	0.000E+00	0.000E+00
184	19.00	72.00	0.000E+00	0.000E+00	0.000E+00
185	10.00	70.00	0.000E+00	0.000E+00	0.000E+00
186	-30.50	79.30	0.000E+00	0.000E+00	0.000E+00
187	-30.00	79.50	0.000E+00	0.000E+00	0.000E+00
188	-0.60	54.60	0.000E+00	0.000E+00	0.000E+00
189	-39.00	100.00	0.000E+00	0.000E+00	0.000E+00
190	22.00	100.00	0.000E+00	0.000E+00	0.000E+00
191	4.00	100.00	0.000E+00	0.000E+00	0.000E+00
192	120.00	40.00	0.000E+00	0.000E+00	0.000E+00
193	78.00	40.00	0.000E+00	0.000E+00	0.000E+00
194	78.00	40.00	0.000E+00	0.000E+00	0.000E+00
195	47.00	46.50	0.000E+00	0.000E+00	0.000E+00
196	55.00	40.00	0.000E+00	0.000E+00	0.000E+00
197	40.00	40.00	0.000E+00	0.000E+00	0.000E+00
198	-10.00	62.00	0.000E+00	0.000E+00	0.000E+00
199	1.00	100.00	0.000E+00	0.000E+00	0.000E+00
200	105.00	40.00	0.000E+00	0.000E+00	0.000E+00
201	79.00	40.00	0.000E+00	0.000E+00	0.000E+00
202	75.00	40.00	0.000E+00	0.000E+00	0.000E+00
203	72.00	40.00	0.000E+00	0.000E+00	0.000E+00
204	44.30	40.00	0.000E+00	0.000E+00	0.000E+00
205	15.00	39.50	0.000E+00	0.000E+00	0.000E+00
206	20.00	50.00	0.000E+00	0.000E+00	0.000E+00
207	18.00	39.50	0.000E+00	0.000E+00	0.000E+00
208	55.00	100.00	0.000E+00	0.000E+00	0.000E+00
209	120.00	80.00	0.000E+00	0.000E+00	0.000E+00
210	80.00	40.00	0.000E+00	0.000E+00	0.000E+00
211	45.00	39.50	0.000E+00	0.000E+00	0.000E+00
212	28.00	39.50	0.000E+00	0.000E+00	0.000E+00
213	15.00	63.70	0.000E+00	0.000E+00	0.000E+00
214	25.00	40.00	0.000E+00	0.000E+00	0.000E+00
215	5.00	52.00	0.000E+00	0.000E+00	0.000E+00
216	-10.00	76.00	0.000E+00	0.000E+00	0.000E+00
217	20.00	41.50	0.000E+00	0.000E+00	0.000E+00
218	25.10	40.00	0.000E+00	0.000E+00	0.000E+00
219	16.00	100.00	0.000E+00	0.000E+00	0.000E+00
220	60.00	100.00	0.000E+00	0.000E+00	0.000E+00
221	82.00	80.00	0.000E+00	0.000E+00	0.000E+00
222	58.00	39.50	0.000E+00	0.000E+00	0.000E+00
223	65.00	40.00	0.000E+00	0.000E+00	0.000E+00
224	23.00	39.50	0.000E+00	0.000E+00	0.000E+00
225	-10.00	69.50	0.000E+00	0.000E+00	0.000E+00

226	24.00	39.50	0.000E+00	0.000E+00	0.000E+00
227	70.00	80.00	0.000E+00	0.000E+00	0.000E+00
228	45.00	40.00	0.000E+00	0.000E+00	0.000E+00
229	39.00	40.00	0.000E+00	0.000E+00	0.000E+00
230	24.00	39.50	0.000E+00	0.000E+00	0.000E+00
231	20.00	48.00	0.000E+00	0.000E+00	0.000E+00
232	26.00	38.00	0.000E+00	0.000E+00	0.000E+00
233	28.50	40.00	0.000E+00	0.000E+00	0.000E+00
234	27.00	39.50	0.000E+00	0.000E+00	0.000E+00
235	45.00	40.00	0.000E+00	0.000E+00	0.000E+00
236	36.00	36.80	0.000E+00	0.000E+00	0.000E+00
237	38.00	39.50	0.000E+00	0.000E+00	0.000E+00
238	30.00	100.00	0.000E+00	0.000E+00	0.000E+00
239	65.00	80.00	0.000E+00	0.000E+00	0.000E+00
240	49.00	40.00	0.000E+00	0.000E+00	0.000E+00
241	28.00	39.50	0.000E+00	0.000E+00	0.000E+00
242	33.00	40.00	0.000E+00	0.000E+00	0.000E+00
243	55.00	65.00	0.000E+00	0.000E+00	0.000E+00
244	45.00	40.00	0.000E+00	0.000E+00	0.000E+00
245	39.00	39.50	0.000E+00	0.000E+00	0.000E+00
246	70.00	40.00	0.000E+00	0.000E+00	0.000E+00
247	40.00	40.00	0.000E+00	0.000E+00	0.000E+00
248	42.00	40.00	0.000E+00	0.000E+00	0.000E+00
249	40.00	39.50	0.000E+00	0.000E+00	0.000E+00
250	32.00	39.50	0.000E+00	0.000E+00	0.000E+00
251	42.00	40.00	0.000E+00	0.000E+00	0.000E+00
252	42.00	40.00	0.000E+00	0.000E+00	0.000E+00
253	33.00	39.50	0.000E+00	0.000E+00	0.000E+00
254	38.00	40.00	0.000E+00	0.000E+00	0.000E+00
255	50.00	40.00	0.000E+00	0.000E+00	0.000E+00
256	40.00	39.50	0.000E+00	0.000E+00	0.000E+00
257	55.00	40.00	0.000E+00	0.000E+00	0.000E+00
258	47.00	40.00	0.000E+00	0.000E+00	0.000E+00
259	55.00	40.00	0.000E+00	0.000E+00	0.000E+00
260	50.00	40.00	0.000E+00	0.000E+00	0.000E+00
261	41.30	39.50	0.000E+00	0.000E+00	0.000E+00
262	42.00	48.00	0.000E+00	0.000E+00	0.000E+00
263	68.00	40.00	0.000E+00	0.000E+00	0.000E+00
264	35.00	39.50	0.000E+00	0.000E+00	0.000E+00
265	41.70	39.50	0.000E+00	0.000E+00	0.000E+00
266	45.00	40.00	0.000E+00	0.000E+00	0.000E+00
267	43.30	40.00	0.000E+00	0.000E+00	0.000E+00
268	47.00	40.00	0.000E+00	0.000E+00	0.000E+00
269	64.00	40.00	0.000E+00	0.000E+00	0.000E+00
270	75.00	40.00	0.000E+00	0.000E+00	0.000E+00
271	85.00	40.00	0.000E+00	0.000E+00	0.000E+00
272	45.00	40.00	0.000E+00	0.000E+00	0.000E+00
273	38.00	39.50	0.000E+00	0.000E+00	0.000E+00
274	60.00	40.00	0.000E+00	0.000E+00	0.000E+00
275	55.00	40.00	0.000E+00	0.000E+00	0.000E+00
276	45.00	39.50	0.000E+00	0.000E+00	0.000E+00
278	108.00	40.00	0.000E+00	0.000E+00	0.000E+00
279	48.00	39.50	0.000E+00	0.000E+00	0.000E+00
280	65.00	40.00	0.000E+00	0.000E+00	0.000E+00
281	95.00	40.00	0.000E+00	0.000E+00	0.000E+00
282	49.00	39.50	0.000E+00	0.000E+00	0.000E+00
283	85.00	40.00	0.000E+00	0.000E+00	0.000E+00
284	85.00	40.00	0.000E+00	0.000E+00	0.000E+00

AQUIFER CHARACTERISTICS

ELEMENT NO	BOTTOM ELEVATION	AQUIFER THICKNESS	TXX	TYY	STORATIVITY	SPECIFIC YIELD	CONF.LAYER K'/B'
1	-35.00	100.00	5.000E+00	5.000E+00	0.000E+00	0.000E+00	0.000E+00
2	-11.67	106.67	5.000E+00	5.000E+00	0.000E+00	0.000E+00	0.000E+00
3	-96.67	119.23	5.000E+01	5.000E+01	0.000E+00	0.000E+00	0.000E+00
4	-96.50	119.57	5.000E+01	5.000E+01	0.000E+00	0.000E+00	0.000E+00
5	-66.50	109.83	5.000E+01	5.000E+01	0.000E+00	0.000E+00	0.000E+00
6	-3.33	133.33	1.000E+00	1.000E+00	0.000E+00	0.000E+00	0.000E+00
7	20.00	140.00	1.000E+00	1.000E+00	0.000E+00	0.000E+00	0.000E+00
8	-113.33	135.90	5.000E+01	5.000E+01	0.000E+00	0.000E+00	0.000E+00
9	-113.17	136.23	5.000E+01	5.000E+01	0.000E+00	0.000E+00	0.000E+00
10	-58.17	109.83	5.000E+01	5.000E+01	0.000E+00	0.000E+00	0.000E+00
11	-18.33	126.67	1.000E+00	1.000E+00	0.000E+00	0.000E+00	0.000E+00
12	23.33	166.67	1.000E+00	1.000E+00	0.000E+00	0.000E+00	0.000E+00
13	-112.30	136.33	5.000E+01	5.000E+01	0.000E+00	0.000E+00	0.000E+00
14	-87.77	119.67	5.000E+01	5.000E+01	0.000E+00	0.000E+00	0.000E+00
15	-87.30	119.67	5.000E+01	5.000E+01	0.000E+00	0.000E+00	0.000E+00
16	-30.00	130.00	1.000E+00	1.000E+00	0.000E+00	0.000E+00	0.000E+00
17	-104.37	143.17	5.000E+01	5.000E+01	0.000E+00	0.000E+00	0.000E+00
18	-69.37	113.17	5.000E+01	5.000E+01	0.000E+00	0.000E+00	0.000E+00
19	-101.03	123.90	5.000E+01	5.000E+01	0.000E+00	0.000E+00	0.000E+00
20	-41.67	130.00	1.000E+00	1.000E+00	0.000E+00	0.000E+00	0.000E+00
21	-10.00	160.00	1.000E+00	1.000E+00	0.000E+00	0.000E+00	0.000E+00
22	-99.37	139.83	5.000E+01	5.000E+01	0.000E+00	0.000E+00	0.000E+00
23	-107.70	133.90	5.000E+01	5.000E+01	0.000E+00	0.000E+00	0.000E+00
24	-101.67	125.03	5.000E+01	5.000E+01	0.000E+00	0.000E+00	0.000E+00
25	-81.67	114.30	5.000E+01	5.000E+01	0.000E+00	0.000E+00	0.000E+00
26	-100.00	140.73	5.000E+01	5.000E+01	0.000E+00	0.000E+00	0.000E+00
27	-111.67	138.37	5.000E+01	5.000E+01	0.000E+00	0.000E+00	0.000E+00
28	-111.67	138.83	5.000E+01	5.000E+01	0.000E+00	0.000E+00	0.000E+00
29	-100.00	122.17	5.000E+01	5.000E+01	0.000E+00	0.000E+00	0.000E+00
30	0.00	166.67	5.000E+00	5.000E+00	0.000E+00	0.000E+00	0.000E+00
31	-111.67	141.87	5.000E+01	5.000E+01	0.000E+00	0.000E+00	0.000E+00
32	-120.00	136.67	5.000E+01	5.000E+01	0.000E+00	0.000E+00	0.000E+00
33	-100.00	122.67	5.000E+01	5.000E+01	0.000E+00	0.000E+00	0.000E+00
34	-80.00	111.20	5.000E+01	5.000E+01	0.000E+00	0.000E+00	0.000E+00
35	-30.00	133.33	1.000E+00	1.000E+00	0.000E+00	0.000E+00	0.000E+00
36	-111.47	128.43	5.000E+01	5.000E+01	0.000E+00	0.000E+00	0.000E+00
37	-106.47	133.63	5.000E+01	5.000E+01	0.000E+00	0.000E+00	0.000E+00
38	-106.47	131.57	5.000E+01	5.000E+01	0.000E+00	0.000E+00	0.000E+00
39	-96.13	116.23	5.000E+01	5.000E+01	0.000E+00	0.000E+00	0.000E+00
40	-96.13	115.77	5.000E+01	5.000E+01	0.000E+00	0.000E+00	0.000E+00
41	-84.67	112.80	5.000E+01	5.000E+01	0.000E+00	0.000E+00	0.000E+00
42	-63.00	101.33	5.000E+01	5.000E+01	0.000E+00	0.000E+00	0.000E+00
43	-28.33	133.33	1.000E+00	1.000E+00	0.000E+00	0.000E+00	0.000E+00
44	-5.00	166.67	1.000E+00	1.000E+00	0.000E+00	0.000E+00	0.000E+00
45	-115.00	140.80	5.000E+01	5.000E+01	0.000E+00	0.000E+00	0.000E+00
46	-97.33	135.53	5.000E+01	5.000E+01	0.000E+00	0.000E+00	0.000E+00
47	-97.33	135.53	5.000E+01	5.000E+01	0.000E+00	0.000E+00	0.000E+00
48	-105.00	131.30	5.000E+01	5.000E+01	0.000E+00	0.000E+00	0.000E+00
49	-107.67	131.30	5.000E+01	5.000E+01	0.000E+00	0.000E+00	0.000E+00
50	-117.67	140.80	5.000E+01	5.000E+01	0.000E+00	0.000E+00	0.000E+00
51	-102.33	129.93	5.000E+01	5.000E+01	0.000E+00	0.000E+00	0.000E+00

52	-80.67	118.00	5.000E+01	5.000E+01	0.000E+00	0.000E+00	0.000E+00
53	-96.00	133.33	5.000E+01	5.000E+01	0.000E+00	0.000E+00	0.000E+00
54	-95.00	133.33	5.000E+01	5.000E+01	0.000E+00	0.000E+00	0.000E+00
55	-51.67	150.00	1.000E+00	1.000E+00	0.000E+00	0.000E+00	0.000E+00
56	-64.00	116.67	5.000E+01	5.000E+01	0.000E+00	0.000E+00	0.000E+00
57	-41.67	110.00	5.000E+01	5.000E+01	0.000E+00	0.000E+00	0.000E+00
58	-65.00	119.10	5.000E+01	5.000E+01	0.000E+00	0.000E+00	0.000E+00
59	-63.33	108.43	5.000E+01	5.000E+01	0.000E+00	0.000E+00	0.000E+00
60	-36.67	89.33	5.000E+01	5.000E+01	0.000E+00	0.000E+00	0.000E+00
61	-101.00	125.10	5.000E+01	5.000E+01	0.000E+00	0.000E+00	0.000E+00
62	-111.00	139.33	5.000E+01	5.000E+01	0.000E+00	0.000E+00	0.000E+00
63	-113.33	135.60	5.000E+01	5.000E+01	0.000E+00	0.000E+00	0.000E+00
64	-120.00	142.77	5.000E+01	5.000E+01	0.000E+00	0.000E+00	0.000E+00
65	-116.67	146.50	5.000E+01	5.000E+01	0.000E+00	0.000E+00	0.000E+00
66	-106.67	140.83	5.000E+01	5.000E+01	0.000E+00	0.000E+00	0.000E+00
67	-56.00	134.33	1.000E+00	1.000E+00	0.000E+00	0.000E+00	0.000E+00
68	-22.67	156.67	1.000E+00	1.000E+00	0.000E+00	0.000E+00	0.000E+00
69	-76.67	102.27	5.000E+01	5.000E+01	0.000E+00	0.000E+00	0.000E+00
70	-83.33	109.80	5.000E+01	5.000E+01	0.000E+00	0.000E+00	0.000E+00
71	-120.00	139.63	5.000E+01	5.000E+01	0.000E+00	0.000E+00	0.000E+00
72	-110.00	137.70	5.000E+01	5.000E+01	0.000E+00	0.000E+00	0.000E+00
73	6.67	90.00	5.000E+00	5.000E+00	0.000E+00	0.000E+00	0.000E+00
74	-16.67	93.33	5.000E+00	5.000E+00	0.000E+00	0.000E+00	0.000E+00
75	-66.67	100.43	1.000E+01	1.000E+01	0.000E+00	0.000E+00	0.000E+00
76	-83.33	110.63	5.000E+01	5.000E+01	0.000E+00	0.000E+00	0.000E+00
77	-95.00	123.03	7.500E+01	7.500E+01	0.000E+00	0.000E+00	0.000E+00
78	-101.67	130.70	7.500E+01	7.500E+01	0.000E+00	0.000E+00	0.000E+00
79	-110.00	138.30	5.000E+01	5.000E+01	0.000E+00	0.000E+00	0.000E+00
80	-101.67	131.57	5.000E+01	5.000E+01	0.000E+00	0.000E+00	0.000E+00
81	-110.00	140.67	5.000E+01	5.000E+01	0.000E+00	0.000E+00	0.000E+00
82	-71.67	107.37	5.000E+01	5.000E+01	0.000E+00	0.000E+00	0.000E+00
83	-21.00	99.00	1.000E+00	1.000E+00	0.000E+00	0.000E+00	0.000E+00
84	19.00	94.67	1.000E+00	1.000E+00	0.000E+00	0.000E+00	0.000E+00
85	-35.00	111.57	5.000E+00	5.000E+00	0.000E+00	0.000E+00	0.000E+00
86	1.67	115.00	5.000E+00	5.000E+00	0.000E+00	0.000E+00	0.000E+00
87	-76.67	110.93	7.500E+01	7.500E+01	0.000E+00	0.000E+00	0.000E+00
88	-93.33	122.23	5.000E+01	5.000E+01	0.000E+00	0.000E+00	0.000E+00
89	-101.67	131.33	7.500E+01	7.500E+01	0.000E+00	0.000E+00	0.000E+00
90	-101.67	132.10	7.500E+01	7.500E+01	0.000E+00	0.000E+00	0.000E+00
91	-81.67	111.77	7.500E+01	7.500E+01	0.000E+00	0.000E+00	0.000E+00
92	-71.67	102.50	7.500E+01	7.500E+01	0.000E+00	0.000E+00	0.000E+00
93	-50.00	81.43	7.500E+01	7.500E+01	0.000E+00	0.000E+00	0.000E+00
94	-33.33	75.67	1.000E+00	1.000E+00	0.000E+00	0.000E+00	0.000E+00
95	-5.00	88.00	7.500E-01	7.500E-01	0.000E+00	0.000E+00	0.000E+00
96	2.00	106.67	7.500E-01	7.500E-01	0.000E+00	0.000E+00	0.000E+00
97	29.33	113.33	7.500E-01	7.500E-01	0.000E+00	0.000E+00	0.000E+00
98	-21.67	99.83	5.000E+00	5.000E+00	0.000E+00	0.000E+00	0.000E+00
99	-63.33	105.50	5.000E+00	5.000E+00	0.000E+00	0.000E+00	0.000E+00
100	-90.00	129.40	7.500E+01	7.500E+01	0.000E+00	0.000E+00	0.000E+00
101	-98.33	133.50	7.500E+01	7.500E+01	0.000E+00	0.000E+00	0.000E+00
102	-96.67	140.43	7.500E+01	7.500E+01	0.000E+00	0.000E+00	0.000E+00
103	-95.00	130.90	7.500E+01	7.500E+01	0.000E+00	0.000E+00	0.000E+00
104	-96.67	125.23	7.500E+01	7.500E+01	0.000E+00	0.000E+00	0.000E+00
105	-98.33	128.47	7.500E+01	7.500E+01	0.000E+00	0.000E+00	0.000E+00
106	-80.00	109.97	7.500E+01	7.500E+01	0.000E+00	0.000E+00	0.000E+00
107	-71.67	101.83	7.500E+01	7.500E+01	0.000E+00	0.000E+00	0.000E+00
108	-56.67	86.33	7.500E+01	7.500E+01	0.000E+00	0.000E+00	0.000E+00
109	-59.00	89.23	1.000E+00	1.000E+00	0.000E+00	0.000E+00	0.000E+00

110	-57.33	88.23	1.000E+00	1.000E+00	0.000E+00	0.000E+00	0.000E+00
111	-63.33	103.33	1.000E+00	1.000E+00	0.000E+00	0.000E+00	0.000E+00
112	-63.33	103.67	1.000E+00	1.000E+00	0.000E+00	0.000E+00	0.000E+00
113	-55.67	95.73	1.000E+00	1.000E+00	0.000E+00	0.000E+00	0.000E+00
114	-45.67	102.73	7.500E-01	7.500E-01	0.000E+00	0.000E+00	0.000E+00
115	-16.33	101.67	7.500E-01	7.500E-01	0.000E+00	0.000E+00	0.000E+00
116	11.00	108.33	7.500E-01	7.500E-01	0.000E+00	0.000E+00	0.000E+00
117	9.33	78.17	5.000E+00	5.000E+00	0.000E+00	0.000E+00	0.000E+00
118	-27.33	75.83	1.000E+01	1.000E+01	0.000E+00	0.000E+00	0.000E+00
119	-65.00	108.17	5.000E+00	5.000E+00	0.000E+00	0.000E+00	0.000E+00
120	-90.00	139.00	7.500E+01	7.500E+01	0.000E+00	0.000E+00	0.000E+00
121	-88.33	137.33	7.500E+01	7.500E+01	0.000E+00	0.000E+00	0.000E+00
122	-88.33	131.17	7.500E+01	7.500E+01	0.000E+00	0.000E+00	0.000E+00
123	-66.67	102.33	7.500E+01	7.500E+01	0.000E+00	0.000E+00	0.000E+00
124	-61.67	97.83	7.500E+01	7.500E+01	0.000E+00	0.000E+00	0.000E+00
125	-49.00	96.40	7.500E-01	7.500E-01	0.000E+00	0.000E+00	0.000E+00
126	-33.33	81.17	7.500E-01	7.500E-01	0.000E+00	0.000E+00	0.000E+00
127	-24.33	87.50	7.500E-01	7.500E-01	0.000E+00	0.000E+00	0.000E+00
128	-2.00	108.33	7.500E-01	7.500E-01	0.000E+00	0.000E+00	0.000E+00
129	46.00	84.33	5.000E+00	5.000E+00	0.000E+00	0.000E+00	0.000E+00
130	-40.67	93.33	7.500E+01	7.500E+01	0.000E+00	0.000E+00	0.000E+00
131	-76.67	124.00	7.500E+01	7.500E+01	0.000E+00	0.000E+00	0.000E+00
132	-93.33	143.67	7.500E+01	7.500E+01	0.000E+00	0.000E+00	0.000E+00
133	-63.33	107.17	7.500E+01	7.500E+01	0.000E+00	0.000E+00	0.000E+00
134	-57.00	96.33	7.500E+01	7.500E+01	0.000E+00	0.000E+00	0.000E+00
135	-25.33	65.67	1.000E+00	1.000E+00	0.000E+00	0.000E+00	0.000E+00
136	-7.00	50.83	1.000E+00	1.000E+00	0.000E+00	0.000E+00	0.000E+00
137	-19.67	70.83	7.500E-01	7.500E-01	0.000E+00	0.000E+00	0.000E+00
138	26.33	109.33	7.500E-01	7.500E-01	0.000E+00	0.000E+00	0.000E+00
139	57.00	109.33	7.500E-01	7.500E-01	0.000E+00	0.000E+00	0.000E+00
140	58.00	102.67	1.000E+01	1.000E+01	0.000E+00	0.000E+00	0.000E+00
141	64.67	100.00	1.000E+01	1.000E+01	0.000E+00	0.000E+00	0.000E+00
142	46.67	81.00	5.000E+00	5.000E+00	0.000E+00	0.000E+00	0.000E+00
143	34.33	57.67	5.000E+00	5.000E+00	0.000E+00	0.000E+00	0.000E+00
144	12.67	41.67	1.000E+01	1.000E+01	0.000E+00	0.000E+00	0.000E+00
145	-15.67	70.67	1.000E+01	1.000E+01	0.000E+00	0.000E+00	0.000E+00
146	-23.33	72.33	7.500E+01	7.500E+01	0.000E+00	0.000E+00	0.000E+00
147	-31.67	79.83	7.500E+01	7.500E+01	0.000E+00	0.000E+00	0.000E+00
148	-61.67	114.83	7.500E+01	7.500E+01	0.000E+00	0.000E+00	0.000E+00
149	-51.67	112.50	7.500E+01	7.500E+01	0.000E+00	0.000E+00	0.000E+00
150	-66.33	123.17	7.500E+01	7.500E+01	0.000E+00	0.000E+00	0.000E+00
151	-81.67	136.33	7.500E+01	7.500E+01	0.000E+00	0.000E+00	0.000E+00
152	-77.00	127.17	7.500E+01	7.500E+01	0.000E+00	0.000E+00	0.000E+00
153	-55.33	99.67	7.500E+01	7.500E+01	0.000E+00	0.000E+00	0.000E+00
154	-54.67	99.67	7.500E+01	7.500E+01	0.000E+00	0.000E+00	0.000E+00
155	-21.33	63.00	1.000E+00	1.000E+00	0.000E+00	0.000E+00	0.000E+00
156	-16.33	79.83	1.000E+00	1.000E+00	0.000E+00	0.000E+00	0.000E+00
157	-2.33	80.00	1.000E+00	1.000E+00	0.000E+00	0.000E+00	0.000E+00
158	-6.00	65.00	1.000E+00	1.000E+00	0.000E+00	0.000E+00	0.000E+00
159	-12.67	69.67	1.000E+00	1.000E+00	0.000E+00	0.000E+00	0.000E+00
160	-13.00	69.67	7.500E-01	7.500E-01	0.000E+00	0.000E+00	0.000E+00
161	-19.33	84.67	7.500E-01	7.500E-01	0.000E+00	0.000E+00	0.000E+00
162	2.33	102.67	7.500E-01	7.500E-01	0.000E+00	0.000E+00	0.000E+00
163	-19.00	84.50	1.000E+00	1.000E+00	0.000E+00	0.000E+00	0.000E+00
164	-21.67	84.50	1.000E+00	1.000E+00	0.000E+00	0.000E+00	0.000E+00
165	0.00	102.50	1.000E+01	1.000E+01	0.000E+00	0.000E+00	0.000E+00
166	3.33	102.33	1.000E+01	1.000E+01	0.000E+00	0.000E+00	0.000E+00
167	28.33	102.50	1.000E+01	1.000E+01	0.000E+00	0.000E+00	0.000E+00

168	35.00	99.83	1.000E+01	1.000E+01	0.000E+00	0.000E+00	0.000E+00
169	50.00	99.83	1.000E+01	1.000E+01	0.000E+00	0.000E+00	0.000E+00
170	45.00	85.67	5.000E+00	5.000E+00	0.000E+00	0.000E+00	0.000E+00
171	21.67	65.00	5.000E+00	5.000E+00	0.000E+00	0.000E+00	0.000E+00
172	1.67	44.33	1.000E+01	1.000E+01	0.000E+00	0.000E+00	0.000E+00
173	0.00	46.00	7.500E+01	7.500E+01	0.000E+00	0.000E+00	0.000E+00
174	-5.00	52.50	7.500E+01	7.500E+01	0.000E+00	0.000E+00	0.000E+00
175	-16.67	63.83	7.500E+01	7.500E+01	0.000E+00	0.000E+00	0.000E+00
176	-33.33	88.83	7.500E+01	7.500E+01	0.000E+00	0.000E+00	0.000E+00
177	-36.67	89.17	7.500E+01	7.500E+01	0.000E+00	0.000E+00	0.000E+00
178	-41.67	90.33	7.500E+01	7.500E+01	0.000E+00	0.000E+00	0.000E+00
179	-51.67	99.67	7.500E+01	7.500E+01	0.000E+00	0.000E+00	0.000E+00
180	-41.67	82.33	7.500E+01	7.500E+01	0.000E+00	0.000E+00	0.000E+00
181	-39.00	83.50	7.500E+01	7.500E+01	0.000E+00	0.000E+00	0.000E+00
182	-24.00	89.33	1.000E+00	1.000E+00	0.000E+00	0.000E+00	0.000E+00
183	-7.33	100.00	1.000E+00	1.000E+00	0.000E+00	0.000E+00	0.000E+00
184	0.00	99.83	1.000E+00	1.000E+00	0.000E+00	0.000E+00	0.000E+00
185	-6.67	99.67	1.000E+00	1.000E+00	0.000E+00	0.000E+00	0.000E+00
186	3.33	99.67	1.000E+00	1.000E+00	0.000E+00	0.000E+00	0.000E+00
187	23.33	99.67	1.000E+01	1.000E+01	0.000E+00	0.000E+00	0.000E+00
188	66.67	67.33	1.000E+01	1.000E+01	0.000E+00	0.000E+00	0.000E+00
189	55.00	87.33	5.000E+00	5.000E+00	0.000E+00	0.000E+00	0.000E+00
190	31.67	77.33	5.000E+00	5.000E+00	0.000E+00	0.000E+00	0.000E+00
191	20.00	68.33	5.000E+00	5.000E+00	0.000E+00	0.000E+00	0.000E+00
192	0.00	58.50	7.500E+01	7.500E+01	0.000E+00	0.000E+00	0.000E+00
193	0.00	56.83	7.500E+01	7.500E+01	0.000E+00	0.000E+00	0.000E+00
194	65.00	54.00	1.000E+01	1.000E+01	0.000E+00	0.000E+00	0.000E+00
195	39.00	51.67	1.000E+01	1.000E+01	0.000E+00	0.000E+00	0.000E+00
196	15.67	56.33	1.000E+01	1.000E+01	0.000E+00	0.000E+00	0.000E+00
197	-5.00	71.10	7.500E+01	7.500E+01	0.000E+00	0.000E+00	0.000E+00
198	-3.33	69.77	7.500E+01	7.500E+01	0.000E+00	0.000E+00	0.000E+00
199	-11.67	70.83	7.500E+01	7.500E+01	0.000E+00	0.000E+00	0.000E+00
200	-8.33	67.17	7.500E+01	7.500E+01	0.000E+00	0.000E+00	0.000E+00
201	-30.00	72.33	7.500E+01	7.500E+01	0.000E+00	0.000E+00	0.000E+00
202	-30.00	69.33	7.500E+01	7.500E+01	0.000E+00	0.000E+00	0.000E+00
203	-30.00	72.90	7.500E+01	7.500E+01	0.000E+00	0.000E+00	0.000E+00
204	-30.00	69.83	7.500E+01	7.500E+01	0.000E+00	0.000E+00	0.000E+00
205	-30.00	69.90	7.500E+01	7.500E+01	0.000E+00	0.000E+00	0.000E+00
206	-26.67	70.00	7.500E+01	7.500E+01	0.000E+00	0.000E+00	0.000E+00
207	-21.67	62.10	7.500E+01	7.500E+01	0.000E+00	0.000E+00	0.000E+00
208	-25.00	65.17	7.500E+01	7.500E+01	0.000E+00	0.000E+00	0.000E+00
209	-25.00	68.77	7.500E+01	7.500E+01	0.000E+00	0.000E+00	0.000E+00
210	-20.00	62.43	7.500E+01	7.500E+01	0.000E+00	0.000E+00	0.000E+00
211	-16.67	58.70	7.500E+01	7.500E+01	0.000E+00	0.000E+00	0.000E+00
212	-16.67	61.50	7.500E+01	7.500E+01	0.000E+00	0.000E+00	0.000E+00
213	-36.67	79.57	7.500E+01	7.500E+01	0.000E+00	0.000E+00	0.000E+00
214	-26.67	70.57	7.500E+01	7.500E+01	0.000E+00	0.000E+00	0.000E+00
215	-48.33	92.33	7.500E+01	7.500E+01	0.000E+00	0.000E+00	0.000E+00
216	-50.00	93.33	7.500E+01	7.500E+01	0.000E+00	0.000E+00	0.000E+00
217	-50.00	92.87	7.500E+01	7.500E+01	0.000E+00	0.000E+00	0.000E+00
218	-31.67	76.27	7.500E+01	7.500E+01	0.000E+00	0.000E+00	0.000E+00
219	-45.00	89.00	7.500E+01	7.500E+01	0.000E+00	0.000E+00	0.000E+00
220	-53.33	96.83	7.500E+01	7.500E+01	0.000E+00	0.000E+00	0.000E+00
221	-63.33	106.93	7.500E+01	7.500E+01	0.000E+00	0.000E+00	0.000E+00
222	-58.33	101.97	7.500E+01	7.500E+01	0.000E+00	0.000E+00	0.000E+00
223	-63.33	107.70	7.500E+01	7.500E+01	0.000E+00	0.000E+00	0.000E+00
224	-25.00	71.10	7.500E+01	7.500E+01	0.000E+00	0.000E+00	0.000E+00
225	-41.67	85.93	7.500E+01	7.500E+01	0.000E+00	0.000E+00	0.000E+00

226	-51.67	95.83	7.500E+01	7.500E+01	0.000E+00	0.000E+00	0.000E+00
227	-65.00	109.00	7.500E+01	7.500E+01	0.000E+00	0.000E+00	0.000E+00
228	-71.67	115.90	7.500E+01	7.500E+01	0.000E+00	0.000E+00	0.000E+00
229	-75.00	119.57	7.500E+01	7.500E+01	0.000E+00	0.000E+00	0.000E+00
230	-45.00	94.73	7.500E+01	7.500E+01	0.000E+00	0.000E+00	0.000E+00
231	-25.00	83.73	7.500E+01	7.500E+01	0.000E+00	0.000E+00	0.000E+00
232	-61.67	115.73	7.500E+01	7.500E+01	0.000E+00	0.000E+00	0.000E+00
233	-78.33	123.07	7.500E+01	7.500E+01	0.000E+00	0.000E+00	0.000E+00
234	-24.67	73.00	7.500E+01	7.500E+01	0.000E+00	0.000E+00	0.000E+00
235	-41.33	88.00	7.500E+01	7.500E+01	0.000E+00	0.000E+00	0.000E+00
236	-54.67	101.73	7.500E+01	7.500E+01	0.000E+00	0.000E+00	0.000E+00
237	-71.33	116.57	7.500E+01	7.500E+01	0.000E+00	0.000E+00	0.000E+00
238	-78.00	123.17	7.500E+01	7.500E+01	0.000E+00	0.000E+00	0.000E+00
239	-61.33	115.83	7.500E+01	7.500E+01	0.000E+00	0.000E+00	0.000E+00
240	-56.33	111.50	7.500E+01	7.500E+01	0.000E+00	0.000E+00	0.000E+00
241	-61.67	109.93	7.500E+01	7.500E+01	0.000E+00	0.000E+00	0.000E+00
242	-58.33	106.43	7.500E+01	7.500E+01	0.000E+00	0.000E+00	0.000E+00
243	-26.33	76.33	7.500E+01	7.500E+01	0.000E+00	0.000E+00	0.000E+00
244	-43.00	92.07	7.500E+01	7.500E+01	0.000E+00	0.000E+00	0.000E+00
245	-43.33	95.17	7.500E+01	7.500E+01	0.000E+00	0.000E+00	0.000E+00
246	-73.00	119.57	7.500E+01	7.500E+01	0.000E+00	0.000E+00	0.000E+00
247	-61.67	109.33	7.500E+01	7.500E+01	0.000E+00	0.000E+00	0.000E+00
248	-75.00	122.00	7.500E+01	7.500E+01	0.000E+00	0.000E+00	0.000E+00
249	-26.67	72.83	7.500E+01	7.500E+01	0.000E+00	0.000E+00	0.000E+00
250	-26.67	73.07	7.500E+01	7.500E+01	0.000E+00	0.000E+00	0.000E+00
251	-20.00	76.33	7.500E+01	7.500E+01	0.000E+00	0.000E+00	0.000E+00
252	-16.67	74.33	7.500E+01	7.500E+01	0.000E+00	0.000E+00	0.000E+00
253	-20.00	64.73	7.500E+01	7.500E+01	0.000E+00	0.000E+00	0.000E+00
254	-20.00	64.73	7.500E+01	7.500E+01	0.000E+00	0.000E+00	0.000E+00
255	-45.00	89.50	7.500E+01	7.500E+01	0.000E+00	0.000E+00	0.000E+00
256	-37.67	79.50	7.500E+01	7.500E+01	0.000E+00	0.000E+00	0.000E+00
257	-37.67	80.00	7.500E+01	7.500E+01	0.000E+00	0.000E+00	0.000E+00
258	-38.33	90.00	7.500E+01	7.500E+01	0.000E+00	0.000E+00	0.000E+00
259	-25.67	75.10	7.500E+01	7.500E+01	0.000E+00	0.000E+00	0.000E+00
260	-25.00	100.00	1.000E+00	1.000E+00	0.000E+00	0.000E+00	0.000E+00
261	4.00	100.00	1.000E+01	1.000E+01	0.000E+00	0.000E+00	0.000E+00
262	21.67	99.83	1.000E+01	1.000E+01	0.000E+00	0.000E+00	0.000E+00
263	15.00	99.67	1.000E+01	1.000E+01	0.000E+00	0.000E+00	0.000E+00
264	33.33	99.67	1.000E+01	1.000E+01	0.000E+00	0.000E+00	0.000E+00
265	56.67	99.83	1.000E+01	1.000E+01	0.000E+00	0.000E+00	0.000E+00
266	1.67	53.33	7.500E+01	7.500E+01	0.000E+00	0.000E+00	0.000E+00
267	0.00	52.43	7.500E+01	7.500E+01	0.000E+00	0.000E+00	0.000E+00
268	-5.67	45.77	7.500E+01	7.500E+01	0.000E+00	0.000E+00	0.000E+00
269	-16.67	100.00	7.500E+01	7.500E+01	0.000E+00	0.000E+00	0.000E+00
270	11.00	80.67	7.500E+01	7.500E+01	0.000E+00	0.000E+00	0.000E+00
271	16.67	80.67	7.500E+01	7.500E+01	0.000E+00	0.000E+00	0.000E+00
272	16.67	100.00	1.000E+01	1.000E+01	0.000E+00	0.000E+00	0.000E+00
273	53.67	81.33	1.000E+01	1.000E+01	0.000E+00	0.000E+00	0.000E+00
274	47.00	81.17	1.000E+01	1.000E+01	0.000E+00	0.000E+00	0.000E+00
275	58.67	81.17	1.000E+01	1.000E+01	0.000E+00	0.000E+00	0.000E+00
279	-10.00	60.53	7.500E+01	7.500E+01	0.000E+00	0.000E+00	0.000E+00
280	13.33	46.67	7.500E+01	7.500E+01	0.000E+00	0.000E+00	0.000E+00
281	11.67	60.67	7.500E+01	7.500E+01	0.000E+00	0.000E+00	0.000E+00
282	-40.00	99.17	7.500E+01	7.500E+01	0.000E+00	0.000E+00	0.000E+00
283	-23.33	91.50	5.000E+00	5.000E+00	0.000E+00	0.000E+00	0.000E+00
284	-8.33	77.33	5.000E+00	5.000E+00	0.000E+00	0.000E+00	0.000E+00
285	-6.67	80.00	7.500E+01	7.500E+01	0.000E+00	0.000E+00	0.000E+00
286	-16.33	100.00	5.000E+00	5.000E+00	0.000E+00	0.000E+00	0.000E+00

287	2.00	100.00	1.000E+01	1.000E+01	0.000E+00	0.000E+00	0.000E+00
288	58.67	81.33	1.000E+01	1.000E+01	0.000E+00	0.000E+00	0.000E+00
289	-17.33	99.83	1.000E+00	1.000E+00	0.000E+00	0.000E+00	0.000E+00
290	88.33	42.33	1.000E+01	1.000E+01	0.000E+00	0.000E+00	0.000E+00
291	76.33	40.00	1.000E+01	1.000E+01	0.000E+00	0.000E+00	0.000E+00
292	49.33	50.67	1.000E+01	1.000E+01	0.000E+00	0.000E+00	0.000E+00
293	31.33	54.67	1.000E+01	1.000E+01	0.000E+00	0.000E+00	0.000E+00
294	32.33	44.00	1.000E+01	1.000E+01	0.000E+00	0.000E+00	0.000E+00
295	-1.00	54.33	1.000E+01	1.000E+01	0.000E+00	0.000E+00	0.000E+00
296	0.67	57.33	7.500E+01	7.500E+01	0.000E+00	0.000E+00	0.000E+00
297	-18.33	72.33	7.500E+01	7.500E+01	0.000E+00	0.000E+00	0.000E+00
298	10.67	51.67	7.500E+01	7.500E+01	0.000E+00	0.000E+00	0.000E+00
299	-8.33	66.67	7.500E+01	7.500E+01	0.000E+00	0.000E+00	0.000E+00
300	-21.67	76.87	7.500E+01	7.500E+01	0.000E+00	0.000E+00	0.000E+00
301	-51.67	101.80	7.500E+01	7.500E+01	0.000E+00	0.000E+00	0.000E+00
302	-61.67	110.97	7.500E+01	7.500E+01	0.000E+00	0.000E+00	0.000E+00
303	-33.33	82.87	7.500E+01	7.500E+01	0.000E+00	0.000E+00	0.000E+00
306	-9.33	94.17	5.000E+00	5.000E+00	0.000E+00	0.000E+00	0.000E+00
307	-4.00	100.00	5.000E+00	5.000E+00	0.000E+00	0.000E+00	0.000E+00
308	5.67	100.00	5.000E+00	5.000E+00	0.000E+00	0.000E+00	0.000E+00
309	8.33	100.00	1.000E+01	1.000E+01	0.000E+00	0.000E+00	0.000E+00
310	29.67	100.00	1.000E+01	1.000E+01	0.000E+00	0.000E+00	0.000E+00
311	45.00	100.00	1.000E+01	1.000E+01	0.000E+00	0.000E+00	0.000E+00
312	13.00	64.67	7.500E+01	7.500E+01	0.000E+00	0.000E+00	0.000E+00
313	-6.67	71.87	7.500E+01	7.500E+01	0.000E+00	0.000E+00	0.000E+00
314	-25.00	85.60	7.500E+01	7.500E+01	0.000E+00	0.000E+00	0.000E+00
315	-50.00	99.77	7.500E+01	7.500E+01	0.000E+00	0.000E+00	0.000E+00
316	-46.67	95.23	7.500E+01	7.500E+01	0.000E+00	0.000E+00	0.000E+00
317	-25.20	75.93	7.500E+01	7.500E+01	0.000E+00	0.000E+00	0.000E+00
318	-18.53	72.37	7.500E+01	7.500E+01	0.000E+00	0.000E+00	0.000E+00
319	-21.53	79.03	7.500E+01	7.500E+01	0.000E+00	0.000E+00	0.000E+00
320	-21.83	80.83	7.500E+01	7.500E+01	0.000E+00	0.000E+00	0.000E+00
321	-16.83	76.27	7.500E+01	7.500E+01	0.000E+00	0.000E+00	0.000E+00
322	-10.00	70.50	7.500E+01	7.500E+01	0.000E+00	0.000E+00	0.000E+00
323	-25.37	75.70	7.500E+01	7.500E+01	0.000E+00	0.000E+00	0.000E+00
324	-20.37	71.13	7.500E+01	7.500E+01	0.000E+00	0.000E+00	0.000E+00
325	-23.20	78.03	7.500E+01	7.500E+01	0.000E+00	0.000E+00	0.000E+00
326	-14.00	94.17	1.000E-01	1.000E-01	0.000E+00	0.000E+00	0.000E+00
327	-5.33	100.00	1.000E-01	1.000E-01	0.000E+00	0.000E+00	0.000E+00
328	9.00	100.00	5.000E+00	5.000E+00	0.000E+00	0.000E+00	0.000E+00
329	21.67	100.00	5.020E+00	5.020E+00	0.000E+00	0.000E+00	0.000E+00
330	39.67	100.00	5.020E+00	5.020E+00	0.000E+00	0.000E+00	0.000E+00
331	46.00	50.67	7.500E+01	7.500E+01	0.000E+00	0.000E+00	0.000E+00
332	38.00	50.67	7.500E+01	7.500E+01	0.000E+00	0.000E+00	0.000E+00
333	23.00	60.67	7.500E+01	7.500E+01	0.000E+00	0.000E+00	0.000E+00
334	13.33	57.33	7.500E+01	7.500E+01	0.000E+00	0.000E+00	0.000E+00
335	15.00	47.17	7.500E+01	7.500E+01	0.000E+00	0.000E+00	0.000E+00
336	8.33	50.50	7.500E+01	7.500E+01	0.000E+00	0.000E+00	0.000E+00
337	-6.67	63.83	7.500E+01	7.500E+01	0.000E+00	0.000E+00	0.000E+00
338	2.67	56.33	7.500E+01	7.500E+01	0.000E+00	0.000E+00	0.000E+00
339	-17.00	73.00	7.500E+01	7.500E+01	0.000E+00	0.000E+00	0.000E+00
340	-6.67	79.83	5.000E+00	5.000E+00	0.000E+00	0.000E+00	0.000E+00
341	11.67	79.83	5.000E+00	5.000E+00	0.000E+00	0.000E+00	0.000E+00
342	25.67	100.00	5.020E+00	5.020E+00	0.000E+00	0.000E+00	0.000E+00
343	82.67	41.67	7.500E+01	7.500E+01	0.000E+00	0.000E+00	0.000E+00
344	67.67	41.67	7.500E+01	7.500E+01	0.000E+00	0.000E+00	0.000E+00
345	77.00	40.00	7.500E+01	7.500E+01	0.000E+00	0.000E+00	0.000E+00
346	79.00	40.00	7.500E+01	7.500E+01	0.000E+00	0.000E+00	0.000E+00

347	69.67	42.17	7.500E+01	7.500E+01	0.000E+00	0.000E+00	0.000E+00
348	65.00	42.17	7.500E+01	7.500E+01	0.000E+00	0.000E+00	0.000E+00
349	61.00	42.17	7.500E+01	7.500E+01	0.000E+00	0.000E+00	0.000E+00
350	63.67	40.00	7.500E+01	7.500E+01	0.000E+00	0.000E+00	0.000E+00
351	57.10	40.00	5.000E+00	5.000E+00	0.000E+00	0.000E+00	0.000E+00
352	46.43	40.00	5.000E+00	5.000E+00	0.000E+00	0.000E+00	0.000E+00
353	33.10	39.83	5.000E+00	5.000E+00	0.000E+00	0.000E+00	0.000E+00
354	28.10	39.83	5.000E+00	5.000E+00	0.000E+00	0.000E+00	0.000E+00
355	15.00	43.83	7.500E+01	7.500E+01	0.000E+00	0.000E+00	0.000E+00
356	3.33	55.83	7.500E+01	7.500E+01	0.000E+00	0.000E+00	0.000E+00
357	8.33	55.17	7.500E+01	7.500E+01	0.000E+00	0.000E+00	0.000E+00
358	10.00	55.83	1.000E+01	1.000E+01	0.000E+00	0.000E+00	0.000E+00
359	19.33	43.67	1.000E+01	1.000E+01	0.000E+00	0.000E+00	0.000E+00
360	21.03	40.33	1.000E+01	1.000E+01	0.000E+00	0.000E+00	0.000E+00
361	19.70	59.83	1.000E+01	1.000E+01	0.000E+00	0.000E+00	0.000E+00
362	101.00	40.00	1.000E+01	1.000E+01	0.000E+00	0.000E+00	0.000E+00
363	87.33	40.00	1.000E+01	1.000E+01	0.000E+00	0.000E+00	0.000E+00
364	78.33	40.00	7.500E+01	7.500E+01	0.000E+00	0.000E+00	0.000E+00
365	77.33	40.00	7.500E+01	7.500E+01	0.000E+00	0.000E+00	0.000E+00
366	66.67	42.17	7.500E+01	7.500E+01	0.000E+00	0.000E+00	0.000E+00
367	55.67	42.00	7.500E+01	7.500E+01	0.000E+00	0.000E+00	0.000E+00
368	54.67	42.00	7.500E+01	7.500E+01	0.000E+00	0.000E+00	0.000E+00
369	48.33	39.67	7.500E+01	7.500E+01	0.000E+00	0.000E+00	0.000E+00
370	48.10	39.83	5.000E+00	5.000E+00	0.000E+00	0.000E+00	0.000E+00
371	29.10	47.73	5.000E+00	5.000E+00	0.000E+00	0.000E+00	0.000E+00
372	28.10	47.90	5.000E+00	5.000E+00	0.000E+00	0.000E+00	0.000E+00
373	15.00	51.90	5.000E+00	5.000E+00	0.000E+00	0.000E+00	0.000E+00
374	101.33	53.33	1.000E+01	1.000E+01	0.000E+00	0.000E+00	0.000E+00
375	93.00	53.33	5.000E+00	5.000E+00	0.000E+00	0.000E+00	0.000E+00
376	78.00	40.00	7.500E+01	7.500E+01	0.000E+00	0.000E+00	0.000E+00
377	66.67	39.83	7.500E+01	7.500E+01	0.000E+00	0.000E+00	0.000E+00
378	73.33	53.17	5.000E+00	5.000E+00	0.000E+00	0.000E+00	0.000E+00
379	61.00	39.67	1.000E+01	1.000E+01	0.000E+00	0.000E+00	0.000E+00
380	56.00	39.67	7.500E+01	7.500E+01	0.000E+00	0.000E+00	0.000E+00
381	46.00	39.67	7.500E+01	7.500E+01	0.000E+00	0.000E+00	0.000E+00
382	38.67	39.67	7.500E+01	7.500E+01	0.000E+00	0.000E+00	0.000E+00
383	22.00	47.57	5.000E+00	5.000E+00	0.000E+00	0.000E+00	0.000E+00
384	9.33	57.57	5.000E+00	5.000E+00	0.000E+00	0.000E+00	0.000E+00
385	3.33	61.73	5.000E+00	5.000E+00	0.000E+00	0.000E+00	0.000E+00
386	-5.00	65.83	7.500E+01	7.500E+01	0.000E+00	0.000E+00	0.000E+00
387	1.33	61.67	1.000E+01	1.000E+01	0.000E+00	0.000E+00	0.000E+00
388	11.33	52.33	1.000E+01	1.000E+01	0.000E+00	0.000E+00	0.000E+00
389	23.03	40.33	7.500E+01	7.500E+01	0.000E+00	0.000E+00	0.000E+00
390	28.37	38.77	1.000E+01	1.000E+01	0.000E+00	0.000E+00	0.000E+00
391	25.70	58.93	1.000E+01	1.000E+01	0.000E+00	0.000E+00	0.000E+00
392	27.33	78.93	1.000E+01	1.000E+01	0.000E+00	0.000E+00	0.000E+00
393	35.33	100.00	5.020E+00	5.020E+00	0.000E+00	0.000E+00	0.000E+00
394	70.00	66.50	5.000E+00	5.000E+00	0.000E+00	0.000E+00	0.000E+00
395	57.67	53.17	5.000E+00	5.000E+00	0.000E+00	0.000E+00	0.000E+00
396	56.00	39.83	7.500E+01	7.500E+01	0.000E+00	0.000E+00	0.000E+00
397	49.67	40.00	7.500E+01	7.500E+01	0.000E+00	0.000E+00	0.000E+00
398	42.33	39.83	7.500E+01	7.500E+01	0.000E+00	0.000E+00	0.000E+00
399	28.67	39.67	7.500E+01	7.500E+01	0.000E+00	0.000E+00	0.000E+00
400	12.33	49.50	7.500E+01	7.500E+01	0.000E+00	0.000E+00	0.000E+00
401	11.33	52.33	7.500E+01	7.500E+01	0.000E+00	0.000E+00	0.000E+00
402	12.00	51.83	7.500E+01	7.500E+01	0.000E+00	0.000E+00	0.000E+00
403	13.33	49.00	7.500E+01	7.500E+01	0.000E+00	0.000E+00	0.000E+00
404	28.67	38.10	7.500E+01	7.500E+01	0.000E+00	0.000E+00	0.000E+00

405	60.00	66.67	5.000E+00	5.000E+00	0.000E+00	0.000E+00	0.000E+00
406	53.00	53.33	5.000E+00	5.000E+00	0.000E+00	0.000E+00	0.000E+00
407	44.33	40.00	7.500E+01	7.500E+01	0.000E+00	0.000E+00	0.000E+00
408	38.67	39.83	7.500E+01	7.500E+01	0.000E+00	0.000E+00	0.000E+00
409	30.33	39.67	7.500E+01	7.500E+01	0.000E+00	0.000E+00	0.000E+00
410	26.83	39.67	7.500E+01	7.500E+01	0.000E+00	0.000E+00	0.000E+00
411	24.17	42.50	7.500E+01	7.500E+01	0.000E+00	0.000E+00	0.000E+00
412	25.17	42.50	7.500E+01	7.500E+01	0.000E+00	0.000E+00	0.000E+00
413	24.33	41.83	1.000E+01	1.000E+01	0.000E+00	0.000E+00	0.000E+00
414	32.67	39.17	1.000E+01	1.000E+01	0.000E+00	0.000E+00	0.000E+00
415	35.67	38.27	1.000E+01	1.000E+01	0.000E+00	0.000E+00	0.000E+00
416	39.67	38.77	1.000E+01	1.000E+01	0.000E+00	0.000E+00	0.000E+00
417	34.67	58.77	1.000E+01	1.000E+01	0.000E+00	0.000E+00	0.000E+00
418	52.00	53.33	5.000E+00	5.000E+00	0.000E+00	0.000E+00	0.000E+00
419	41.00	39.83	1.000E+01	1.000E+01	0.000E+00	0.000E+00	0.000E+00
420	36.33	39.67	1.000E+01	1.000E+01	0.000E+00	0.000E+00	0.000E+00
421	31.00	39.67	1.000E+01	1.000E+01	0.000E+00	0.000E+00	0.000E+00
422	29.83	39.83	7.500E+01	7.500E+01	0.000E+00	0.000E+00	0.000E+00
423	29.50	39.83	7.500E+01	7.500E+01	0.000E+00	0.000E+00	0.000E+00
424	38.33	48.17	1.000E+01	1.000E+01	0.000E+00	0.000E+00	0.000E+00
425	38.33	48.00	1.000E+01	1.000E+01	0.000E+00	0.000E+00	0.000E+00
426	35.00	39.67	1.000E+01	1.000E+01	0.000E+00	0.000E+00	0.000E+00
427	39.00	39.83	1.000E+01	1.000E+01	0.000E+00	0.000E+00	0.000E+00
428	42.67	39.83	1.000E+01	1.000E+01	0.000E+00	0.000E+00	0.000E+00
429	40.67	39.67	1.000E+01	1.000E+01	0.000E+00	0.000E+00	0.000E+00
430	35.67	59.67	1.000E+01	1.000E+01	0.000E+00	0.000E+00	0.000E+00
431	46.33	59.83	1.000E+01	1.000E+01	0.000E+00	0.000E+00	0.000E+00
432	49.00	53.33	1.000E+01	1.000E+01	0.000E+00	0.000E+00	0.000E+00
433	43.00	40.00	7.500E+01	7.500E+01	0.000E+00	0.000E+00	0.000E+00
434	47.33	40.00	7.500E+01	7.500E+01	0.000E+00	0.000E+00	0.000E+00
435	43.00	39.83	7.500E+01	7.500E+01	0.000E+00	0.000E+00	0.000E+00
436	38.00	39.67	7.500E+01	7.500E+01	0.000E+00	0.000E+00	0.000E+00
437	38.00	39.67	7.500E+01	7.500E+01	0.000E+00	0.000E+00	0.000E+00
438	41.33	39.83	7.500E+01	7.500E+01	0.000E+00	0.000E+00	0.000E+00
439	46.33	48.33	7.500E+01	7.500E+01	0.000E+00	0.000E+00	0.000E+00
440	55.00	48.33	1.000E+01	1.000E+01	0.000E+00	0.000E+00	0.000E+00
441	52.00	48.17	1.000E+01	1.000E+01	0.000E+00	0.000E+00	0.000E+00
442	45.33	39.67	1.000E+01	1.000E+01	0.000E+00	0.000E+00	0.000E+00
443	35.33	39.67	1.000E+01	1.000E+01	0.000E+00	0.000E+00	0.000E+00
444	38.67	39.83	1.000E+01	1.000E+01	0.000E+00	0.000E+00	0.000E+00
445	40.67	39.83	1.000E+01	1.000E+01	0.000E+00	0.000E+00	0.000E+00
446	42.33	39.83	1.000E+01	1.000E+01	0.000E+00	0.000E+00	0.000E+00
447	43.00	39.67	1.000E+01	1.000E+01	0.000E+00	0.000E+00	0.000E+00
448	49.67	39.67	1.000E+01	1.000E+01	0.000E+00	0.000E+00	0.000E+00
449	51.67	39.67	1.000E+01	1.000E+01	0.000E+00	0.000E+00	0.000E+00
450	74.33	39.83	1.000E+01	1.000E+01	0.000E+00	0.000E+00	0.000E+00
451	53.33	40.00	7.500E+01	7.500E+01	0.000E+00	0.000E+00	0.000E+00
452	48.90	39.83	7.500E+01	7.500E+01	0.000E+00	0.000E+00	0.000E+00
453	46.10	39.83	7.500E+01	7.500E+01	0.000E+00	0.000E+00	0.000E+00
454	42.77	39.67	7.500E+01	7.500E+01	0.000E+00	0.000E+00	0.000E+00
455	41.10	42.33	7.500E+01	7.500E+01	0.000E+00	0.000E+00	0.000E+00
456	41.33	42.50	7.500E+01	7.500E+01	0.000E+00	0.000E+00	0.000E+00
457	50.67	42.67	1.000E+01	1.000E+01	0.000E+00	0.000E+00	0.000E+00
458	47.77	40.00	7.500E+01	7.500E+01	0.000E+00	0.000E+00	0.000E+00
459	46.67	39.83	7.500E+01	7.500E+01	0.000E+00	0.000E+00	0.000E+00
460	45.10	40.00	7.500E+01	7.500E+01	0.000E+00	0.000E+00	0.000E+00
461	44.00	39.83	7.500E+01	7.500E+01	0.000E+00	0.000E+00	0.000E+00
462	50.90	39.83	7.500E+01	7.500E+01	0.000E+00	0.000E+00	0.000E+00

463	49.00	39.67	7.500E+01	7.500E+01	0.000E+00	0.000E+00	0.000E+00
464	60.10	39.83	1.000E+01	1.000E+01	0.000E+00	0.000E+00	0.000E+00
465	52.77	42.50	1.000E+01	1.000E+01	0.000E+00	0.000E+00	0.000E+00
466	67.33	42.67	1.000E+01	1.000E+01	0.000E+00	0.000E+00	0.000E+00
467	65.00	42.67	1.000E+01	1.000E+01	0.000E+00	0.000E+00	0.000E+00
468	62.67	39.83	1.000E+01	1.000E+01	0.000E+00	0.000E+00	0.000E+00
469	55.00	39.83	1.000E+01	1.000E+01	0.000E+00	0.000E+00	0.000E+00
470	39.33	39.67	1.000E+01	1.000E+01	0.000E+00	0.000E+00	0.000E+00
471	37.00	39.67	1.000E+01	1.000E+01	0.000E+00	0.000E+00	0.000E+00
472	42.00	39.83	1.000E+01	1.000E+01	0.000E+00	0.000E+00	0.000E+00
473	42.67	39.67	1.000E+01	1.000E+01	0.000E+00	0.000E+00	0.000E+00
474	44.33	39.67	1.000E+01	1.000E+01	0.000E+00	0.000E+00	0.000E+00
475	47.67	39.83	1.000E+01	1.000E+01	0.000E+00	0.000E+00	0.000E+00
476	51.00	39.83	1.000E+01	1.000E+01	0.000E+00	0.000E+00	0.000E+00
477	46.67	39.67	1.000E+01	1.000E+01	0.000E+00	0.000E+00	0.000E+00
478	55.00	39.83	1.000E+01	1.000E+01	0.000E+00	0.000E+00	0.000E+00
479	52.67	39.67	1.000E+01	1.000E+01	0.000E+00	0.000E+00	0.000E+00
480	67.00	39.67	1.000E+01	1.000E+01	0.000E+00	0.000E+00	0.000E+00
481	83.67	39.83	1.000E+01	1.000E+01	0.000E+00	0.000E+00	0.000E+00
482	64.00	39.67	1.000E+01	1.000E+01	0.000E+00	0.000E+00	0.000E+00
483	54.00	39.67	1.000E+01	1.000E+01	0.000E+00	0.000E+00	0.000E+00
484	66.33	39.83	1.000E+01	1.000E+01	0.000E+00	0.000E+00	0.000E+00
485	73.00	39.83	1.000E+01	1.000E+01	0.000E+00	0.000E+00	0.000E+00
486	76.33	39.83	1.000E+01	1.000E+01	0.000E+00	0.000E+00	0.000E+00
487	-58.00	105.33	7.500E+01	7.500E+01	0.000E+00	0.000E+00	0.000E+00
488	-48.00	88.00	7.500E+01	7.500E+01	0.000E+00	0.000E+00	0.000E+00
489	-112.77	136.33	5.000E+01	5.000E+01	0.000E+00	0.000E+00	0.000E+00
490	-90.00	120.00	7.500E+01	7.500E+01	0.000E+00	0.000E+00	0.000E+00
491	-88.33	116.77	7.500E+01	7.500E+01	0.000E+00	0.000E+00	0.000E+00
492	-42.33	83.67	7.500E+01	7.500E+01	0.000E+00	0.000E+00	0.000E+00
493	94.00	66.67	5.000E+00	5.000E+00	0.000E+00	0.000E+00	0.000E+00
494	43.33	48.33	7.500E+01	7.500E+01	0.000E+00	0.000E+00	0.000E+00
495	35.67	39.83	7.500E+01	7.500E+01	0.000E+00	0.000E+00	0.000E+00
496	-28.00	89.17	1.000E+00	1.000E+00	0.000E+00	0.000E+00	0.000E+00
497	-22.00	63.00	7.500E+01	7.500E+01	0.000E+00	0.000E+00	0.000E+00
498	44.33	39.67	7.500E+01	7.500E+01	0.000E+00	0.000E+00	0.000E+00
499	-86.67	123.30	1.000E+01	1.000E+01	0.000E+00	0.000E+00	0.000E+00

PRESCRIBED HEAD BOUNDARY DATA - SPECIFIED PIEZOMETRIC HEADS AND ASSOCIATED NODE NUMBERS
==========================

TIMES......

0.000

NODE NO	HEADS UP TO AND INCLUDING THE ABOVE TIMES......
5	8.500
6	9.200
7	10.000
12	10.700
14	11.400
18	12.200
19	12.900
21	13.600
24	14.400
27	14.500
29	15.800
33	16.600
37	17.300
41	18.000
42	18.800
44	19.500
45	19.800
49	21.300
52	22.800
53	23.900
54	25.100
58	26.200
64	27.300
66	28.000
70	29.500
72	30.500
80	31.000
82	32.500
88	33.500
93	34.000
102	35.500
107	36.500
110	37.500
115	38.500
122	39.500
124	40.200
127	40.800
136	41.500
141	42.200
144	42.800
147	43.500
152	44.200
161	45.500
168	46.200
169	46.800
173	47.500
175	48.200
186	48.800

187	49.500
198	50.000
205	52.500
207	50.000
215	55.000
217	51.000
225	56.500
226	58.500
230	60.500
232	60.000
234	63.000
236	72.800
237	75.000
245	76.000
253	65.000
256	79.500
264	65.500
273	77.500
276	84.300
279	87.500
282	88.500
241	64.500
249	73.000
250	68.000
261	76.800
265	77.200
211	80.500
212	73.500
222	86.000
210	118.000
201	119.000
193	120.000
195	94.000
224	62.500
89	44.000
95	49.000
103	51.500
104	70.000
118	71.000
131	75.000
57	24.200
62	32.000

GROUND LEVEL DATA - FOR NODES WHICH MAY BE AFFECTED BY A RISING WATER TABLE
================

TIMES......

0.000

NODE NO	GROUND LEVELS UP TO AND INCLUDING THE ABOVE TIMES......
78	43.000
91	47.000
101	47.500
1	75.000

2	50.000
3	70.000
4	140.000
8	75.000
9	180.000
10	160.000
11	50.000
13	55.000
15	45.000
16	230.000
17	55.000
20	55.000
22	40.000
23	22.000
25	48.000
26	230.000
28	45.000
30	30.000
31	45.000
32	53.000
34	37.000
35	210.000
36	45.000
38	30.000
39	40.000
40	60.000
43	100.000
46	43.000
47	152.000
48	40.000
50	150.000
51	40.000
55	39.000
56	150.000
59	28.000
60	80.000
61	160.000
63	52.000
65	30.000
67	32.000
68	116.000
69	52.000
71	33.000
73	50.000
74	100.000
75	162.000
76	163.000
77	68.000
79	47.000
81	52.000
83	169.000
84	105.000
85	168.000
86	145.000
87	180.000
90	175.000
92	65.000
94	60.000

96	70.000
97	78.000
98	45.000
99	50.000
100	50.000
105	190.000
106	70.000
108	48.000
109	100.000
111	172.000
112	45.000
113	45.000
114	49.000
116	48.000
117	130.000
119	150.000
120	82.500
121	40.000
123	52.000
125	42.000
126	49.000
128	43.000
129	68.000
130	135.000
132	170.000
133	147.000
134	105.000
135	50.000
137	45.000
138	72.000
139	140.000
140	45.000
142	48.000
143	44.200
145	43.600
146	44.300
148	44.500
149	49.000
150	45.000
151	60.000
153	45.000
155	49.000
156	44.000
157	46.000
158	72.000
159	95.000
160	51.000
162	48.000
163	140.000
164	105.000
165	62.000
166	63.000
167	50.000
170	85.000
171	62.000
172	53.600
174	50.000
176	57.500

177	101.000
178	140.000
179	150.000
180	124.000
181	130.000
182	124.000
183	104.000
184	91.000
185	[illegible]0.000
188	54.000
189	61.000
190	122.000
191	114.000
192	160.000
194	122.000
196	95.000
197	80.000
199	120.000
200	145.000
202	115.000
203	112.000
204	84.300
206	70.000
208	155.000
209	200.000
213	78.700
214	65.000
216	66.000
218	65.100
219	116.000
220	160.000
221	162.000
223	105.000
227	150.000
228	78.000
229	79.000
231	68.000
233	68.500
235	6[illegible].000
238	130.[illegible]
239	145.000
240	[illegible]9.000
242	73.000
243	120.000
244	85.000
246	110.000
247	84.000
248	89.000
251	82.000
252	82.000
254	78.000
255	90.000
257	95.000
258	87.000
259	95.000
260	90.000
262	90.000
263	108.000

266	85.000
267	83.300
268	87.000
269	104.000
270	115.000
271	125.000
272	85.000
274	100.000
275	95.000
278	148.000
280	105.000
281	135.000
283	125.000
284	125.000

PRESCRIBED FLUXES DISTRIBUTED OVER ELEMENTS (L/T) - VOLUME PER UNIT TIME PER UNIT ELEMENT AREA

all elements 0.0365

INITIAL HEAD VECTOR

NODE	HEAD	NODE	HEAD	NODE	HEAD	NODE	HEAD	NODE	HEAD	NODE	HEAD	NODE	HEAD	NODE	HEAD	NODE	HEAD	NODE	HEAD
1	55.00	2	30.00	3	30.00	4	120.00	5	-55.50	6	-55.15	7	-54.50	8	52.50	9	160.00	10	140.00
11	-25.00	12	-53.80	13	-20.00	14	-53.10	15	-10.00	16	210.00	17	-15.00	18	-53.65	19	-53.30	20	-20.00
21	-52.95	22	-10.00	23	-49.00	24	-52.55	25	0.00	26	210.00	27	-39.40	28	-30.00	29	-51.85	30	-22.00
31	5.00	32	-7.00	33	-51.45	34	-38.00	35	190.00	36	-30.00	37	-36.10	38	-45.00	39	-35.00	40	20.00
41	-40.75	42	-50.35	43	60.00	44	-50.00	45	-49.45	46	-23.50	47	132.00	48	15.00	49	-48.90	50	130.00
51	-15.00	52	-35.85	53	-47.80	54	-47.20	55	17.00	56	130.00	57	-12.50	58	-46.65	59	-13.50	60	25.00
61	140.00	62	-2.50	63	-16.50	64	-31.10	65	-45.00	66	-25.55	67	-31.50	68	73.00	69	-31.50	70	-17.50
71	-13.00	72	-9.50	73	-6.00	74	27.50	75	142.00	76	136.50	77	48.00	78	-11.50	79	-19.00	80	-9.00
81	-14.00	82	4.00	83	149.00	84	57.00	85	134.00	86	122.50	87	147.50	88	-1.00	89	19.00	90	140.00
91	-16.00	92	-10.00	93	10.00	94	35.00	95	22.50	96	35.00	97	55.50	98	25.00	99	27.50	100	27.50
101	14.50	102	13.00	103	32.00	104	50.00	105	170.00	106	10.00	107	-11.50	108	14.00	109	57.50	110	-3.50
111	138.50	112	19.00	113	22.50	114	9.50	115	4.50	116	14.00	117	85.00	118	59.00	119	130.00	120	43.75
121	5.00	122	5.00	123	11.00	124	5.35	125	5.00	126	9.50	127	10.65	128	13.00	129	48.00	130	107.50
131	70.00	132	150.00	133	123.50	134	67.50	135	25.00	136	8.50	137	15.00	138	51.00	139	118.00	140	2.50
141	-1.15	142	19.00	143	2.10	144	-10.85	145	1.80	146	2.15	147	-5.50	148	-12.75	149	22.00	150	-17.50
151	40.00	152	-15.15	153	7.50	155	14.50	156	-13.00	157	-22.00	158	26.00	159	65.00	160	13.50	161	-14.00
162	-13.50	163	120.00	164	85.00	165	42.00	166	31.50	167	7.50	168	-11.65	169	-16.35	170	55.00	171	36.00
172	6.80	173	-8.50	174	10.00	175	1.85	176	16.25	177	66.00	178	110.00	179	130.00	180	72.50	181	95.00
182	104.00	183	84.00	184	55.00	185	45.00	186	9.40	187	10.00	188	26.70	159	38.00	190	102.00	191	84.00
192	140.00	193	98.00	194	98.00	195	70.50	196	75.00	197	60.00	198	21.25	199	81.00	200	125.00	201	99.00
202	95.00	203	92.00	204	64.30	205	35.00	206	45.00	207	38.00	208	135.00	209	180.00	210	100.00	211	65.00
212	48.00	213	46.85	214	45.00	215	31.25	216	28.00	217	41.00	218	45.10	219	95.50	220	140.00	221	142.00
222	78.00	223	85.00	224	43.00	225	25.00	226	44.00	227	130.00	228	65.00	229	59.00	230	44.00	231	44.00
232	46.00	233	48.50	234	47.00	235	65.00	236	56.00	237	58.00	238	110.00	239	125.00	240	69.00	241	48.00
242	53.00	243	97.50	244	65.00	245	59.00	246	90.00	247	60.00	248	62.00	249	60.00	250	52.00	251	62.00
252	62.00	253	53.00	254	58.00	255	70.00	256	60.00	257	75.00	258	67.00	259	75.00	260	70.00	261	61.30
262	62.00	263	88.00	264	55.00	265	61.70	266	65.00	267	63.30	268	67.00	269	84.00	270	95.00	271	105.00
272	65.00	273	58.00	274	80.00	275	75.00	276	65.00	278	128.00	279	68.00	280	85.00	281	115.00	282	68.00
283	105.00	284	105.00																

****

TIME STEP = 0 TIME = 0.00000 ERROR = 0.46024 NUMBER OF ITERATIONS = 14 LINEAR =.F.

****

NODE NO	PIEZOMETRIC HEAD		INTERNAL FLUXES (INSIDE THE AQUIFER)		EXTERNAL FLUXES (THROUGH THE BOUNDARIES)				LOCATION OF NODE	
	HEAD	DELTA H	QX	QY	SOURCE/SINK INFLOWS	LEAKAGE INFLOWS	INFLOWS AT BOUNDARIES	ID	X	Y
	(L)	(L)	(L2/T)	(L2/T)	(L3/T)	(L3/T)	(L3/T)		(L)	(L)
1	51.689 PHR	0.00	-4.231	4.316	3649.585	0.000	0.000	0	20893.93[illegible]	625.100
2	11.437 PHR	0.00	-7.560	6.395	3237.913	0.000	0.000	0	19667.720	2429.150
3	14.072 PHR	0.00	-5.176	3.082	8454.991	0.000	0.000	0	20782.970	2978.360
4	58.415 PHR	0.01	-3.286	0.994	5484.409	0.000	0.000	0	22240.590	1930.640
5	8.500	0.00	-5.585	-2.486	949.255	0.000	-10292.766	1	18842.000	3118.590
6	9.200	0.00	-6.081	-2.713	1868.086	0.000	-17941.288	1	19405.950	3479.910
7	10.000	0.00	-8.515	0.738	3559.149	0.000	-16819.636	1	19998.580	3724.760
8	13.056 PHR	0.00	-7.783	0.182	4170.407	0.000	0.000	0	21143.550	4232.360
9	96.072 PHR	0.03	-2.220	0.685	10331.503	0.000	0.000	0	22496.100	4291.140
10	103.558 PHR	0.04	-0.907	-0.132	2515.359	0.000	0.000	0	23224.990	3224.240
11	11.108 PHR	0.00	-0.010	-7.828	2999.374	0.000	0.000	0	18708.330	4581.420
12	10.700	0.00	-4.522	-5.616	2008.660	0.000	-12993.491	1	20074.130	4463.050
13	11.827 PHR	0.00	0.395	-4.975	1903.781	0.000	0.000	0	18168.240	5405.610
14	11.400	0.00	-3.208	-5.071	4115.126	0.000	-9502.552	1	20071.320	5070.230
15	13.540 PHR	0.00	-7.122	-1.228	4340.806	0.000	0.000	0	21154.580	5248.350
16	89.119 PHR	0.04	-5.442	1.676	7115.425	0.000	0.000	0	23909.860	5160.060
17	12.389 PHR	0.00	-1.090	-5.959	1887.768	0.000	0.000	0	19441.300	6096.690
18	12.200	0.00	-5.298	-5.754	1900.127	0.000	-3607.439	1	20212.600	5618.290
19	12.900	0.00	-9.702	-3.784	2279.852	0.000	-8202.819	1	20591.360	6084.910
20	13.568 PHR	0.00	-1.971	-6.510	1785.621	0.000	0.000	0	19946.510	6912.250
21	13.600	0.00	-9.655	-2.212	3199.539	0.000	-21511.879	1	20886.420	6755.970
22	16.621 PHR	0.00	-7.203	1.380	10635.141	0.000	0.000	0	21757.920	6525.680
23	14.428 PHR	0.00	0.801	-6.485	1293.812	0.000	0.000	0	20280.650	7679.560
24	14.400	0.00	-10.241	-6.989	2439.522	0.000	-20172.056	1	20999.800	7756.900
25	17.690 PHR	0.00	-7.634	-1.990	6646.912	0.000	0.000	0	22315.270	7661.090
26	97.192 PHR	0.04	-5.451	0.889	9616.210	0.000	0.000	0	24532.760	7438.810
27	14.500	0.00	-0.782	-10.097	1146.741	0.000	-9565.224	1	20747.200	7937.120
28	15.967 PHR	0.00	4.710	-8.739	962.434	0.000	0.000	0	19966.000	8562.980
29	15.800	0.00	-3.158	-10.046	1173.322	0.000	-8334.076	1	20369.170	8671.650
30	16.999 PHR	0.00	-9.213	-8.496	3095.138	0.000	0.000	0	21068.420	8907.030
31	19.444 PHR	0.00	-4.518	-0.868	8978.772	0.000	0.000	0	22401.090	8871.660
32	17.332 PHR	0.00	4.179	-6.792	1085.772	0.000	0.000	0	19565.490	9250.320
33	16.600	0.00	0.348	-8.102	1316.752	0.000	-6786.863	1	20349.160	9222.370
34	17.685 PHR	0.00	-8.298	-5.210	2289.411	0.000	0.000	0	21079.970	9423.220
35	108.491 PHR	0.03	-3.157	0.804	6549.803	0.000	0.000	0	25059.230	9293.500
36	17.484 PHR	0.00	3.200	-5.866	2396.109	0.000	0.000	0	20048.600	9664.720
37	17.300	0.00	0.371	-6.470	1984.761	0.000	-10335.672	1	20523.340	9829.380
38	18.697 PHR	0.00	-7.820	-1.157	3007.075	0.000	0.000	0	21555.760	9970.420
39	20.279 PHR	0.00	-5.844	0.677	7471.143	0.000	0.000	0	22834.680	9946.220
40	19.599 PHR	0.00	2.474	-5.137	1449.228	0.000	0.000	0	18774.340	10474.200

41	18.000		0.00	-0.938	-7.023	4657.376	0.000	-12373.198	1	20910.570	10287.710
42	18.800		0.00	-0.186	-8.089	2828.063	0.000	-9989.853	1	21582.290	10673.630
43	20.822	PHR	0.00	1.292	-5.273	6196.130	0.000	0.000	0	19161.400	11376.570
44	19.500		0.00	-11.567	-1.675	2536.703	0.000	-15970.224	1	22406.970	10842.720
45	19.800	PHR	0.00	-3.258	-10.129	2841.590	0.000	-26678.108	1	22353.190	11423.200
46	22.831	PHR	0.00	-10.267	-3.838	6125.770	0.000	0.000	0	23584.620	11438.650
47	84.652	PHR	0.01	-3.172	1.572	5952.643	0.000	0.000	0	24897.280	10862.870
48	22.865	PHR	0.00	1.177	-6.981	7586.702	0.000	0.000	0	20986.480	12369.830
49	21.300		0.00	-8.100	-12.644	1913.175	0.000	-8262.572	1	22447.970	12010.450
50	49.074	PHR	0.00	1.528	-3.110	6782.228	0.000	0.000	0	19958.980	13353.310
51	22.271	PHR	0.00	1.024	-5.539	2940.592	0.000	0.000	0	22269.610	12406.500
52	22.800		0.00	-13.087	-13.127	1349.414	0.000	-2980.714	1	22788.450	12532.630
53	23.900		0.00	-14.179	-10.268	1116.868	0.000	-3866.601	1	23293.130	12545.920
54	25.100		0.00	-15.552	-9.512	1790.828	0.000	-5574.729	1	23777.060	12717.130
55	26.877	PHR	0.00	-6.088	-0.877	5254.295	0.000	0.000	0	24622.590	12393.450
56	120.827	PHR	0.01	-2.816	0.833	4840.434	0.000	0.000	0	26147.440	11752.740
57	24.200	PHR	0.00	-0.997	-6.054	7766.780	0.000	-21276.258	1	22988.670	13184.530
58	26.200		0.00	-15.335	-21.615	1641.017	0.000	-8219.745	1	24039.560	13112.480
59	27.681	PHR	0.00	-7.908	-2.607	784.194	0.000	0.000	0	24784.380	13199.360
60	64.887		0.00	-4.038	1.183	3746.041	0.000	0.000	0	25328.270	13273.780
61	61.723	PHR	0.01	2.376	-1.578	7627.792	0.000	0.000	0	20784.710	14810.830
62	32.000	PH	0.00	2.437	-1.221	4789.901	0.000	-7124.372	1	22863.910	14456.220
63	28.772	PHR	0.00	-4.946	-23.347	2577.646	0.000	0.000	0	23545.010	13993.660
64	27.300		0.00	-6.292	-20.032	1305.446	0.000	-11323.897	1	24375.110	13499.080
65	27.800	PHR	0.00	-14.958	-9.968	129.516	0.000	0.000	0	24568.660	13638.550
66	28.000	PHR	0.00	1.170	-18.969	260.463	0.000	-2346.274	1	24603.010	13754.740
67	28.085	PHR	0.00	-7.437	-2.220	448.249	0.000	0.000	0	24681.380	13735.100
68	110.726	PHR	0.00	-2.619	0.920	3454.515	0.000	0.000	0	26275.590	13433.210
69	29.775	PHR	0.00	-0.273	-31.597	2000.795	0.000	0.000	0	24272.250	14166.240
70	29.500		0.00	-4.300	-20.644	687.246	0.000	-11151.275	1	24885.500	14000.490
71	29.779		0.00	-4.817	1.947	658.757	0.000	0.000	0	24997.320	13968.360
72	30.500		0.00	-0.124	-9.770	764.217	0.000	-4914.511	1	25201.030	14290.530
73	50.000	PHR	0.00	-4.453	2.819	1159.308	0.000	-3233.358	1	25667.160	14175.690
74	96.930		0.00	-3.221	2.109	3745.409	0.000	0.000	0	26291.800	14129.430
75	145.206	PHR	0.00	-0.675	1.392	7318.531	0.000	0.000	0	27742.520	13684.340
76	87.601	PHR	0.17	2.543	-0.442	4610.271	0.000	0.000	0	20642.410	16296.630
77	37.306	PHR	0.00	3.447	-2.131	8221.137	0.000	0.000	0	22483.970	15826.560
78	33.473	PHR	0.00	5.136	-14.456	2884.981	0.000	0.000	0	23437.690	15115.340
79	32.053	PHR	0.00	1.901	-24.097	1667.126	0.000	0.000	0	24750.210	14874.500
80	31.000		0.00	-1.148	-2.508	944.008	0.000	-2711.004	1	25638.960	14747.550
81	33.128	PHR	0.00	4.307	-18.496	4262.370	0.000	0.000	0	23705.210	15079.690
82	32.500		0.00	-0.484	-3.567	3325.486	0.000	-8912.470	1	25882.990	15237.650
83	112.041	PHR	0.00	-1.969	2.170	6508.017	0.000	0.000	0	30484.620	13759.820
84	97.813		0.00	-1.303	2.455	5346.281	0.000	0.000	0	27122.680	15090.040
85	91.320	PHR	0.00	-3.788	5.081	12070.103	0.000	0.000	0	28934.810	15240.250
86	104.688	PHR	0.00	-4.425	5.442	9037.958	0.000	0.000	0	30874.360	15450.470
87	119.455	PHR	0.00	-5.854	3.764	9903.940	0.000	0.000	0	32877.460	15609.720
88	33.500		0.00	2.507	-12.698	3605.962	0.000	-5400.888	1	25845.910	15817.500
89	44.000		0.00	-1.407	1.553	1584.746	0.000	-4958.162	1	26871.490	15685.080
90	83.472	PHR	0.16	3.052	-0.051	2211.818	0.000	0.000	0	20657.700	17304.290
91	36.148	PHR	0.00	7.369	-9.915	3547.822	0.000	0.000	0	23685.700	16546.480
92	36.156	PHR	0.00	5.301	-13.915	5408.753	0.000	0.000	0	24055.830	16661.210
93	34.000	PHR	0.00	1.679	-8.227	1957.921	0.000	-12640.448	1	25840.370	16242.850
94	37.840	PHR	0.00	-2.290	-0.785	3098.138	0.000	0.000	0	26600.250	16218.670
95	49.000		0.00	-1.426	1.567	1075.760	0.000	-10674.179	1	27477.980	15978.850
96	62.357	PHR	0.00	-3.941	7.370	2379.864	0.000	0.000	0	27772.010	16089.630
97	58.184	PHR	0.00	0.005	-0.769	2308.852	0.000	0.000	0	27408.360	16473.740
98	45.000	PHR	0.00	3.326	-0.361	6426.634	0.000	-7490.831	1	22362.640	17592.820

99	39.533	PHR	0.00	3.030	-2.100	1691.116	0.000	0.000	0	22814.730	17346.290
100	39.695	PHR	0.00	6.886	-6.938	2021.960	0.000	0.000	0	22992.680	17668.700
101	38.178	PHR	0.00	7.029	-9.797	3213.672	0.000	0.000	0	23867.150	17637.360
102	35.500		0.00	1.275	-7.208	4435.034	0.000	-10254.248	1	25890.210	17074.720
103	51.500	PHR	0.00	-4.464	4.281	6226.030	0.000	-34621.667	1	28495.850	17079.210
104	70.000	PHR	0.00	-6.126	4.126	16761.207	0.000	-25907.228	1	29610.800	17446.190
105	123.105	PHR	0.00	-6.914	1.720	16066.939	0.000	0.000	0	33847.350	17745.220
106	37.339	PHR	0.00	6.501	-10.260	3187.581	0.000	0.000	0	24729.490	17746.210
107	36.500		0.00	-3.053	-11.793	1216.715	0.000	-16434.716	1	25506.460	17760.090
108	38.411	PHR	0.00	-9.403	-10.109	2080.375	0.000	0.000	0	26320.410	17847.620
109	71.137	PHR	0.00	-0.789	-0.249	5400.362	0.000	0.000	0	27210.480	17646.860
110	37.500		0.00	-8.657	-18.345	1606.679	0.000	-22190.995	1	25416.370	18301.700
111	92.417	PHR	0.19	3.238	0.928	8668.054	0.000	0.000	0	20443.880	18395.580
112	42.644	PHR	0.00	4.859	-0.349	5684.071	0.000	0.000	0	22666.090	18669.270
113	41.140	PHR	0.00	6.951	-4.991	4061.496	0.000	0.000	0	23215.530	18547.810
114	38.939	PHR	0.00	6.815	-6.969	2597.926	0.000	0.000	0	24690.640	18721.940
115	38.500		0.00	-8.518	-27.835	1537.570	0.000	-28424.645	1	25099.130	18717.550
116	42.030	PHR	0.00	-7.926	-13.719	3118.655	0.000	0.000	0	26282.220	18756.330
117	69.794	PHR	0.00	-1.591	0.524	9367.234	0.000	0.000	0	27636.550	18847.050
118	71.000	PHR	0.00	-4.219	0.837	12279.532	0.000	-26917.419	1	29978.040	18341.050
119	99.010	PHR	0.37	3.077	1.857	3341.136	0.000	0.000	0	19496.060	19144.570
120	42.685	PHR	0.00	7.728	-1.353	2582.601	0.000	0.000	0	22881.890	19655.130
121	40.000	PHR	0.00	-25.241	-34.957	649.611	0.000	-1118.662	1	25101.030	18954.240
122	39.500		0.00	-8.244	-18.675	415.789	0.000	-22040.556	1	24644.020	19207.430
123	45.690	PHR	0.00	-18.812	-20.146	4911.397	0.000	0.000	0	25935.550	19302.260
124	40.200		0.00	4.006	-5.529	1766.200	0.000	-14387.538	1	24326.810	19514.340
125	41.315		0.00	-25.608	-33.142	1505.071	0.000	0.000	0	24647.330	19511.190
126	41.291	PHR	0.00	6.721	-2.302	1673.364	0.000	0.000	0	23740.040	19973.610
127	40.800		0.00	-7.203	-13.837	364.590	0.000	-23019.232	1	24111.150	19937.420
128	41.849		0.00	-18.703	-23.672	1869.741	0.000	0.000	0	24461.080	19794.290
129	49.841	PHR	0.00	-26.018	-29.552	4065.408	0.000	0.000	0	25729.960	20183.660
130	65.607	PHR	0.00	-7.562	-7.877	27296.356	0.000	0.000	0	27830.300	20455.530
131	75.000	PHR	0.00	-4.481	-1.925	20462.013	0.000	-40443.348	1	30469.890	19841.080
132	111.451	PHR	0.00	-4.890	-2.082	9851.673	0.000	0.000	0	33489.360	20299.250
133	105.601	PHR	0.46	3.151	1.232	6033.956	0.000	0.000	0	18642.050	20158.400
134	53.047	PHR	-0.02	5.102	2.019	10934.475	0.000	0.000	0	20899.870	20819.320
135	44.602	PHR	0.00	6.736	1.407	6538.063	0.000	0.000	0	22103.420	20553.090
136	41.500		0.00	3.474	-4.939	978.322	0.000	-17430.644	1	23544.060	20308.930
137	42.126	PHR	0.00	-16.041	-20.490	1325.042	0.000	0.000	0	23913.810	20283.270
138	52.925	PHR	0.00	-18.146	-19.427	8052.747	0.000	0.000	0	25193.720	21043.480
139	109.271	PHR	0.00	-2.877	-5.396	15571.862	0.000	0.000	0	30283.400	22567.800
140	42.647	PHR	0.00	10.849	1.064	1402.700	0.000	0.000	0	22927.920	20556.350
141	42.200		0.00	-3.134	-11.540	555.675	0.000	-17257.787	1	23159.200	20680.110
142	43.016	PHR	0.00	-13.479	-15.485	2269.725	0.000	0.000	0	23598.890	20701.140
143	43.623	PHR	0.00	14.132	3.271	701.187	0.000	0.000	0	22366.400	21109.470
144	42.800		0.00	3.410	-8.056	574.885	0.000	-23305.815	1	22717.180	21181.180
145	43.600	PHR	0.00	-14.715	-20.330	905.985	0.000	-2285.213	1	23048.470	21237.240
146	44.300	PHR	0.00	23.591	5.192	1253.330	0.000	-3866.991	1	22053.150	21366.000
147	43.500		0.00	11.476	-4.387	588.349	0.000	-14739.748	1	22352.000	21442.860
148	43.781	PHR	0.00	-8.443	-13.991	417.127	0.000	0.000	0	22614.930	21543.580
149	47.053	PHR	0.00	8.858	3.979	1248.336	0.000	0.000	0	21509.780	21424.340
150	44.079	PHR	0.00	-23.494	-18.773	402.874	0.000	0.000	0	22770.770	21592.940
151	47.699	PHR	0.00	-17.880	-15.844	4880.119	0.000	0.000	0	23459.460	21828.660
152	44.200		0.00	-20.806	-8.914	652.018	0.000	-11331.876	1	22675.960	21895.670
153	45.000	PHR	0.00	22.442	-4.257	585.051	0.000	-2690.951	1	21861.880	21823.020
155	46.941	PHR	0.00	16.703	-2.496	1510.597	0.000	0.000	0	21475.790	21901.560
156	44.000	PHR	0.00	5.326	-16.945	857.624	0.000	-36351.108	1	22290.190	22118.560
157	44.923	PHR	0.00	-15.255	-26.220	266.339	0.000	0.000	0	22637.170	22165.300

158	46.342	PHR	0.00	-7.237	-5.329	2246.906	0.000	0.000	0	23243.690	22325.200
159	61.505	PHR	0.00	-11.607	-13.935	14544.440	0.000	0.000	0	25311.400	22453.330
160	45.748	PHR	0.00	20.341	-10.624	839.883	0.000	0.000	0	21850.410	22146.090
161	45.500		0.00	-11.141	-30.559	392.726	0.000	4528.993	1	22625.250	22343.850
162	46.068	PHR	0.00	-6.009	-14.414	1667.390	0.000	0.000	0	22674.010	22533.280
163	102.572	PHR	0.21	1.091	1.022	3228.846	0.000	0.000	0	17520.970	21921.570
164	92.111	PHR	0.08	3.959	1.633	13977.932	0.000	0.000	0	18728.900	22221.090
165	51.720	PHR	0.00	7.704	0.490	4807.434	0.000	0.000	0	20570.300	22177.590
166	49.910	PHR	0.00	17.696	-1.546	1315.435	0.000	0.000	0	20938.830	23079.070
167	48.127	PHR	0.00	18.081	-4.814	1642.948	0.000	0.000	0	21421.630	23074.390
168	46.200		0.00	9.053	-17.226	940.870	0.000	-2091.399	1	22069.450	22667.710
169	46.800		0.00	4.099	-10.505	1267.487	0.000	-13510.946	1	21983.260	23127.670
170	57.843	PHR	0.00	-9.143	-10.015	5401.394	0.000	0.000	0	24213.910	22928.280
171	51.160	PHR	0.00	12.421	-0.589	4891.516	0.000	0.000	0	20673.750	23596.660
172	48.260	PHR	0.00	19.852	-4.242	1380.068	0.000	0.000	0	21431.470	23638.690
173	47.500		0.00	2.033	-10.354	581.449	0.000	-14054.337	1	21775.140	23632.550
174	48.398	PHR	0.00	-5.356	-13.072	1705.459	0.000	0.000	0	22321.650	23899.210
175	48.200		0.00	11.073	-7.117	1369.865	0.000	-18367.035	1	21504.950	24061.410
176	48.730	PHR	0.00	-5.132	-6.610	4454.824	0.000	0.000	0	22919.910	23741.650
177	88.223	PHR	0.00	-5.642	-13.671	6495.261	0.000	0.000	0	25216.100	23748.900
178	121.638	PHR	0.00	-5.163	-8.347	22254.865	0.000	0.000	0	28271.310	24325.800
179	121.536	PHR	0.00	-0.297	-5.109	3045.786	0.000	0.000	0	29285.110	24251.830
180	124.000	PHR	0.00	5.543	2.085	5722.285	0.000	-1185.485	1	9946.930	22497.870
181	119.089		0.00	9.372	2.032	7339.050	0.000	0.000	0	12408.510	23280.830
182	101.288	PHR	0.00	15.515	5.443	7521.347	0.000	0.000	0	15437.070	23716.740
183	91.651	PHR	0.01	10.481	2.945	13428.016	0.000	0.000	0	16944.450	24131.500
184	62.569	PHR	0.00	15.347	1.517	9658.367	0.000	0.000	0	19689.590	24219.260
185	53.152	PHR	0.00	23.540	-0.449	3711.319	0.000	0.000	0	20601.890	24627.050
186	48.800		0.00	12.996	-7.200	935.249	0.000	-20057.968	1	21552.100	24712.260
187	49.500		0.00	1.479	-1.367	3976.758	0.000	-9683.351	1	21542.060	25082.490
188	49.158	PHR	0.00	-5.550	-8.529	1587.041	0.000	0.000	0	22100.120	24422.720
189	50.552	PHR	0.00	-6.025	-1.672	6795.971	0.000	0.000	0	22536.730	24991.130
190	89.182	PHR	0.00	-3.679	-4.702	7761.293	0.000	0.000	0	23808.780	24562.680
191	108.204		0.00	-3.980	-4.060	21876.988	0.000	0.000	0	26208.760	24439.480
192	125.554	PHR	0.00	3.515	0.356	5144.715	0.000	0.000	0	8713.120	23541.700
193	120.000		0.00	4.940	0.739	13243.470	0.000	-11057.411	1	11250.420	24951.320
194	115.802	PHR	0.00	15.200	2.467	12328.199	0.000	0.000	0	12885.500	24823.000
195	94.000		0.00	17.617	9.341	12597.777	0.000	-39091.423	1	15589.970	25637.310
196	75.856	PHR	0.00	14.594	0.824	8394.433	0.000	0.000	0	18563.500	25641.020
197	57.830	PHR	0.00	14.936	1.989	5848.955	0.000	0.000	0	19884.630	25564.600
198	50.000	PHR	0.00	12.346	1.191	3500.652	0.000	-32130.990	1	20968.300	25612.220
199	101.975		0.00	-5.593	-1.364	20534.311	0.000	0.000	0	24003.500	26112.270
200	132.064	PHR	-0.01	2.002	-1.366	5670.982	0.000	0.000	0	9961.840	25839.250
201	119.000		0.00	6.817	-2.393	9257.858	0.000	4126.089	1	12027.620	26634.700
202	110.674	PHR	0.00	27.979	2.209	9628.745	0.000	0.000	0	13620.370	26104.560
203	87.388	PHR	0.00	6.470	7.246	10380.928	0.000	0.000	0	16727.330	26484.330
204	80.853	PHR	0.00	1.479	0.671	7367.553	0.000	0.000	0	18635.690	26845.070
205	52.500	PHR	0.00	6.551	-2.028	5690.832	0.000	-14831.082	1	20319.650	27061.610
206	50.994	PHR	0.00	2.903	-3.625	4267.064	0.000	0.000	0	21416.810	26803.140
207	50.000	PHR	0.00	-7.643	-0.958	7814.360	0.000	-30670.209	1	22151.760	27398.910
208	143.137	PHR	0.00	-3.468	-3.888	12235.096	0.000	0.000	0	29068.250	27595.080
209	131.739	PHR	-0.01	1.390	-0.855	4669.141	0.000	0.000	0	1166.920	27461.940
210	118.000	PHR	0.00	14.214	-2.664	9948.928	0.000	49219.736	1	13400.790	27783.570
211	80.500	PHR	0.00	19.449	7.680	12311.818	0.000	-83882.372	1	15498.390	27904.870
212	73.500		0.00	7.022	6.455	7580.485	0.000	-21125.807	1	17354.160	27910.680
213	69.810	PHR	0.00	1.750	1.587	4212.943	0.000	0.000	0	18823.940	27857.870
214	56.936	PHR	0.00	5.741	0.384	1733.060	0.000	0.000	0	19558.460	27571.970
215	55.000	PHR	0.00	4.597	-4.697	2288.909	0.000	-6185.562	1	20009.080	28018.620

216	54.800	PHR	0.00	1.380	-4.619	4446.688	0.000	0.000	0	20967.160	28143.300
217	51.000	PHR	0.00	-3.586	-5.088	2426.367	0.000	-29529.415	1	22063.410	28066.200
218	59.446	PHR	0.00	-11.354	-3.556	3618.652	0.000	0.000	0	22442.290	28414.490
219	89.565	PHR	0.00	-7.747	1.463	19010.002	0.000	0.000	0	23479.820	28231.040
220	142.949	PHR	0.00	-4.411	-0.776	24185.456	0.000	0.000	0	27310.450	29119.330
221	119.964	PHR	0.00	2.384	0.051	4801.906	0.000	0.000	0	13140.010	29159.260
222	86.000	PHR	0.00	5.999	0.878	3280.118	0.000	1761.596	1	14759.090	29166.910
223	77.198	PHR	0.00	11.884	1.709	8566.279	0.000	0.000	0	16364.050	29115.760
224	62.500		0.00	11.799	-1.291	7220.657	0.000	-37197.084	1	18234.420	28916.400
225	56.500	PHR	0.00	2.579	-5.150	6895.339	0.000	-28129.018	1	19854.130	28828.560
226	58.500	PHR	0.00	-5.729	-7.192	4962.116	0.000	-16489.937	1	21650.540	29161.320
227	93.769	PHR	0.00	2.458	-0.312	3819.523	0.000	0.000	0	14479.840	30714.130
228	78.000	PHR	0.00	5.468	0.511	8945.668	0.000	-9999.981	1	15541.930	30705.320
229	69.682	PHR	0.00	11.405	-3.214	8631.582	0.000	0.000	0	17679.560	30204.980
230	60.500	PHR	0.00	11.036	-7.879	4277.967	0.000	-26569.293	1	19335.860	30208.640
231	60.925	PHR	0.00	-0.167	-8.673	3243.509	0.000	0.000	0	19772.080	30225.590
232	60.000	PHR	0.00	-3.836	-7.340	5035.501	0.000	-1925.567	1	21207.240	29919.830
233	63.741	PHR	0.00	0.943	-11.663	2475.113	0.000	0.000	0	19526.210	30881.060
234	63.000	PHR	0.00	-0.439	-3.171	7168.317	0.000	-12826.622	1	21071.440	30940.650
235	69.665	PHR	0.00	-1.699	-1.026	3396.414	0.000	0.000	0	21807.860	30818.070
236	72.800		0.00	-7.541	-0.431	11040.207	0.000	-12485.075	1	22839.510	30398.680
237	75.000	PHR	0.00	-3.780	1.403	5713.454	0.000	-8655.171	1	23208.480	31523.160
238	108.089	PHR	0.00	-6.612	2.771	16209.693	0.000	0.000	0	25876.360	31164.150
239	86.698	PHR	0.00	1.188	-0.037	4459.769	0.000	0.000	0	15418.350	32712.420
240	75.005	PHR	0.00	4.216	-1.372	8636.856	0.000	0.000	0	16854.200	31655.090
241	64.500	PHR	0.00	6.022	-3.507	5170.337	0.000	-6448.776	1	19016.890	31069.450
242	68.637	PHR	0.00	-0.087	-6.384	4429.553	0.000	0.000	0	19586.530	32032.150
243	70.358	PHR	0.00	0.425	-2.710	6126.668	0.000	0.000	0	20654.490	32434.160
244	76.331	PHR	0.00	-1.712	-0.044	6551.126	0.000	0.000	0	22509.330	32111.110
245	76.000	PHR	0.00	-3.454	1.702	12932.345	0.000	-29459.859	1	24046.350	32365.100
246	109.242	PHR	0.00	-4.573	2.777	11956.906	0.000	0.000	0	27018.580	33030.320
247	79.988	PHR	0.00	4.857	1.688	1452.724	0.000	0.000	0	15600.870	33133.880
248	76.647	PHR	0.00	4.610	-0.956	4538.388	0.000	0.000	0	16828.980	33002.240
249	73.000	PHR	0.00	3.547	-7.263	4550.829	0.000	-17687.259	1	17833.510	33369.000
250	68.000	PHR	0.00	2.131	-3.371	5132.604	0.000	-22843.972	1	18364.910	32759.760
251	70.852	PHR	0.00	-1.297	-8.761	2518.698	0.000	0.000	0	18864.650	32770.640
252	72.842	PHR	0.00	-0.910	-4.156	4679.573	0.000	0.000	0	18840.830	33297.050
253	65.000	PHR	0.00	-0.314	-0.377	6976.304	0.000	-19166.241	1	21461.500	33040.810
254	76.334	PHR	0.00	-2.007	0.571	6940.105	0.000	0.000	0	22833.330	33871.700
255	80.522	PHR	0.00	-0.428	-0.199	4463.580	0.000	0.000	0	24006.260	34300.130
256	79.500		0.00	-2.535	0.933	10098.948	0.000	-20394.578	1	25149.720	34533.480
257	79.433	PHR	0.00	3.909	1.421	1162.220	0.000	0.000	0	15481.890	34018.880
258	77.310	PHR	0.00	6.589	-0.683	2672.056	0.000	0.000	0	16648.180	33714.150
259	78.865	PHR	0.00	2.558	-0.488	1646.562	0.000	0.000	0	15639.740	35000.720
260	77.703	PHR	0.00	3.033	0.333	1323.444	0.000	0.000	0	16504.620	34586.310
261	76.800	PHR	0.00	0.782	-3.627	4405.717	0.000	-3676.975	1	17186.660	34548.730
262	77.347	PHR	0.00	-1.270	-3.908	6148.838	0.000	0.000	0	18756.390	34378.060
263	87.841	PHR	0.00	0.822	-1.791	8473.992	0.000	0.000	0	20527.150	34295.010
264	65.500	PHR	0.00	0.785	-1.275	6899.707	0.000	-23358.870	1	22249.970	34509.760
265	77.200	PHR	0.00	0.604	-2.708	2176.953	0.000	-8656.625	1	16784.020	34938.750
266	78.788	PHR	0.00	0.229	-0.782	765.253	0.000	0.000	0	15874.130	36079.680
267	78.582	PHR	0.00	1.332	-2.359	1617.214	0.000	0.000	0	16373.310	35588.190
268	79.031	PHR	0.00	-0.721	-2.974	1271.900	0.000	0.000	0	17131.150	36052.320
269	79.425	PHR	0.00	-1.583	-1.670	1765.658	0.000	0.000	0	17756.350	35742.230
270	83.948	PHR	0.00	-0.829	-1.167	2643.195	0.000	0.000	0	18699.400	35267.700
271	97.841	PHR	0.00	0.826	-1.877	5117.538	0.000	0.000	0	20429.770	35670.210
272	77.951	PHR	0.00	0.804	-2.805	3570.450	0.000	0.000	0	22284.160	35604.790
273	77.500		0.00	-1.248	-1.077	7868.416	0.000	-13181.925	1	23793.710	35460.520

274	85.669 PHR	0.00	-0.755	-2.026	2942.232	0.000	0.000	0	23316.070	36949.280
275	86.896 PHR	0.00	-0.896	-1.975	5010.755	0.000	0.000	0	25452.920	35853.980
276	84.500	0.00	-2.494	1.396	10791.620	0.000	-20438.666	1	26534.330	35370.360
278	121.864 PHR	0.00	-2.806	2.254	8609.420	0.000	0.000	0	29115.200	34281.560
279	87.500	0.00	-1.665	1.428	7627.160	0.000	-14845.134	1	27408.620	36556.180
280	94.069 PHR	0.00	1.225	-3.168	5664.143	0.000	0.000	0	26851.110	37015.650
281	105.088 PHR	0.00	-2.410	1.807	6058.474	0.000	0.000	0	29665.360	36260.140
282	88.500	0.00	-0.918	-2.834	11801.748	0.000	-32562.261	1	28694.440	37218.220
283	122.913 PHR	0.00	-0.116	-4.551	7974.714	0.000	0.000	0	27352.310	39976.220
284	116.771 PHR	0.00	-2.104	-3.382	6819.270	0.000	0.000	0	30769.910	38730.140
				TOTALS	1433977.090	0.000	-1433977.084			

NET FLOW INTO AQUIFER (L3/T) 0.006

EXECUTION ENDED NORMALLY -- 2 WARNING(S)

Appendix 6. Errors calculated for two-dimensional modeling

ERROR ESTIMATE FOR FULL DATA SET.
NUMBER KNOWN VALUES: 187
MAXIMUM ERROR: -33.87
RMS ERROR: 6.07
BIAS: -0.38

Location X [ft]	Location Y [ft]	Error [ft]	Measured Head [ft]	Predicted Head [ft]	Well	Element
18864.65	32779.64	-2.15	73.00	70.85	1	437
22839.51	30398.68	0.70	72.10	72.80	2	390
17679.56	30204.98	4.28	65.40	69.68	3	397
21552.10	24712.26	0.30	48.50	48.80	4	320
22100.12	24422.72	2.76	46.40	49.16	5	317
22919.91	23741.65	-6.17	54.90	48.73	6	245
25216.10	23748.90	-1.68	89.90	88.22	7	286
22718.76	21892.69	1.50	43.00	44.50	8	231
22666.09	18669.27	1.54	41.10	42.64	9	171
22881.89	19655.13	0.58	42.10	42.68	10	192
23601.44	20054.76	-0.89	42.40	41.51	11	252
29978.04	18341.05	0.80	70.20	71.00	13	186
27477.98	15978.85	9.90	39.10	49.00	14	159
25840.37	16242.85	2.30	31.70	34.00	15	153
25638.96	14747.55	0.60	30.40	31.00	16	110
22447.97	12010.45	-2.70	24.00	21.30	18	75
19558.46	27571.97	5.04	51.90	56.94	19	354
24055.83	16661.21	-15.74	51.90	36.16	20	148
23697.70	23133.07	-4.82	57.10	52.28	21	283
17186.66	34548.73	-0.20	77.00	76.80	23	453
16648.18	33714.15	-1.09	78.40	77.31	24	433
17833.51	33369.00	1.10	71.90	73.00	25	435
19517.74	30963.16	1.04	63.10	64.14	26	422
19526.21	30881.06	-1.36	65.10	63.74	27	410
19507.97	29976.17	2.89	57.30	60.19	28	401
19438.23	29938.96	3.64	56.50	60.14	29	401
22536.73	24991.13	-2.95	53.50	50.55	34	319
22637.17	22165.30	1.22	43.70	44.92	39	232
22770.77	21592.94	0.18	43.90	44.08	40	223
23459.46	21828.66	2.70	45.00	47.70	41	230
25311.40	22453.33	-18.50	80.00	61.50	44	271
23913.81	20283.27	-0.87	43.00	42.13	45	210
22103.42	20553.09	-0.40	45.00	44.60	46	190
21846.33	20440.11	0.18	50.00	50.18	47	190
24054.56	16782.46	0.48	36.00	36.48	50	149
25192.34	15882.79	-8.70	42.80	34.10	53	152
73808.78	24562.68	-7.02	96.20	89.18	60	306
30469.89	19841.08	0.30	74.70	75.00	62	263
17431.62	34149.68	-5.48	81.30	75.82	63	455
17168.78	33807.86	-5.15	81.10	75.95	64	454
16954.66	34900.88	0.71	76.60	77.31	65	463
16726.17	33350.25	-2.31	79.70	77.39	66	433
17241.27	33548.97	-2.15	77.70	75.55	67	454
17418.73	33137.31	0.59	72.90	73.49	68	436
17659.12	33719.48	-2.82	77.50	74.68	70	455
15600.87	33133.88	9.99	70.00	79.99	72	432
16828.98	33002.24	-0.75	77.40	76.65	73	418
22249.97	34509.76	-4.50	70.00	65.50	79	442
21461.50	33040.81	3.00	62.00	65.00	81	425
19016.89	31069.45	0.00	64.50	64.50	85	408
19277.18	30922.59	-0.79	64.30	63.51	86	410
19199.40	30673.99	-0.57	63.60	63.03	87	410
19696.51	30402.22	1.50	59.90	61.40	88	411
19335.86	30208.64	1.60	58.90	60.50	89	399
19772.08	30225.59	1.93	59.00	60.93	90	401
19771.11	29864.58	-0.98	61.00	60.02	91	401
19739.55	29344.59	0.76	58.00	58.76	92	401
19854.13	28828.56	5.50	51.00	56.50	93	384
22480.73	30323.70	8.95	61.00	69.95	94	415
22718.75	24500.90	5.61	53.00	58.61	104	326
22866.73	27575.41	12.95	61.00	73.95	105	341
22151.76	27398.91	-4.00	54.00	50.00	106	338
22471.36	26907.36	3.83	57.00	60.83	107	340
21158.03	26947.45	3.91	48.00	51.91	108	357
20982.70	26536.29	5.16	46.00	51.16	113	336

26675.96	25124.02	13.95	105.00	118.95	124	330
25721.73	24284.49	3.55	95.00	98.55	125	308
29816.65	17211.92	-8.17	86.00	77.83	130	168
24285.82	16102.27	11.80	23.00	34.80	141	152
24417.56	16142.51	-5.21	40.00	34.79	142	152
27138.18	15990.15	9.59	40.00	49.59	144	159
27122.68	15090.04	22.81	75.00	97.81	146	127
26275.59	13433.21	7.73	103.00	110.73	150	96
23777.06	12717.13	-1.90	27.00	25.10	152	81
22269.61	12406.50	-2.73	25.00	22.27	153	74
21365.37	12479.11	8.44	18.00	26.44	154	74
20986.48	12369.83	0.86	22.00	22.86	155	60
22353.19	11423.20	-0.20	20.00	19.80	157	70
21582.29	10603.63	0.80	18.00	18.80	158	63
21555.76	9970.42	0.70	18.00	18.70	159	53
20048.60	9664.72	-12.52	30.00	17.48	160	47
21079.97	9423.22	0.69	17.00	17.69	161	49
21068.42	8907.03	-1.00	18.00	17.00	162	39
20747.20	7937.12	4.50	10.00	14.50	163	36
20999.80	7756.90	0.40	14.00	14.40	164	32
20280.65	7679.56	-6.57	21.00	14.43	165	31
28271.31	24325.80	4.64	117.00	121.64	170	272
27018.58	33030.32	3.24	106.00	109.24	172	431
15418.35	32712.42	18.70	68.00	86.70	173	405
23801.96	24716.40	-8.92	95.50	86.58	174	327
23799.94	24853.36	-14.69	99.80	85.11	175	327
13620.37	26104.56	-2.33	113.00	110.67	177	365
13361.68	27750.18	-0.19	118.00	117.81	178	376
15318.15	24344.89	6.41	95.00	101.41	179	347
9946.93	22497.87	4.00	120.00	124.00	180	343
11227.97	23420.59	-2.17	123.00	120.83	181	344
15437.07	23716.74	6.29	95.00	101.29	182	346
27352.31	39976.22	-3.09	126.00	122.91	183	484
15531.93	30705.32	0.00	78.00	78.00	187	395
16653.32	30065.04	2.79	72.00	74.79	188	397
18563.50	25641.02	-10.14	86.00	75.86	189	331
18458.51	31280.87	4.51	63.00	67.51	190	420
20134.85	5707.12	-4.67	17.00	12.33	195	26
20847.45	6632.63	-8.20	22.00	13.80	196	29
20074.13	4463.05	0.70	10.00	10.70	197	13
19678.13	3806.99	0.84	9.00	9.84	198	9
19405.95	3479.91	0.20	9.00	9.20	199	3
27577.82	14236.77	-33.87	155.00	121.13	200	138
21861.88	21823.02	1.00	44.00	45.00	201	224
22321.65	23899.21	0.20	48.20	48.40	202	241
21757.22	23809.84	1.15	46.70	47.85	203	316
22053.15	21366.00	1.00	43.30	44.30	204	197
22625.25	22343.85	0.60	44.90	45.50	205	237
22675.96	21895.67	0.20	44.00	44.20	206	228
22352.00	21442.86	0.20	43.30	43.50	207	219
22366.40	21109.47	0.42	43.20	43.62	208	215
22902.75	22409.28	0.75	45.20	45.95	209	240
22290.19	22118.56	-0.20	44.20	44.00	210	226
23341.19	23108.96	-7.23	57.90	50.67	211	283
24213.91	22928.28	-11.26	69.10	57.84	212	283
23095.64	23825.72	-1.34	56.80	55.46	213	306
23394.57	23690.84	-0.23	61.40	61.17	214	306
22356.60	22718.86	1.29	45.00	46.29	215	248
22630.78	22473.42	1.69	44.20	45.89	216	246
23048.47	21237.24	0.00	43.60	43.60	217	217
22614.93	21543.58	0.28	43.50	43.78	218	221
22717.18	21181.18	-0.30	43.10	42.80	219	215
22924.45	23349.04	-4.42	52.00	47.58	220	282
24126.01	23488.71	2.07	71.30	73.37	221	307
24531.87	23470.01	-10.82	86.20	75.38	222	307
24757.35	23940.68	-9.78	91.20	81.42	223	307
19972.87	28067.25	6.38	49.40	55.78	224	385
19499.20	28251.41	7.96	51.70	59.66	227	385
19162.62	31813.67	1.08	66.20	67.28	228	421
19125.62	32146.99	2.53	66.60	69.13	230	495
19586.53	32032.15	2.24	66.40	68.64	233	421
18842.30	30398.94	3.74	60.00	63.74	238	409
18509.51	31776.94	-2.15	70.20	68.05	241	420
18305.59	32275.70	-3.90	72.50	68.60	242	436
18359.31	32717.35	-2.80	73.00	70.20	243	437
19001.25	29627.59	-5.96	66.00	60.04	244	400
19156.91	29121.76	-6.26	65.80	59.54	245	400
18635.69	26845.07	0.05	80.80	80.85	246	351
17843.86	27322.06	3.27	76.00	79.27	247	370
18315.99	27313.51	-1.39	76.90	75.51	248	371

18169.08	27833.73	2.60	71.20	73.80	249	371
18416.03	27070.45	0.01	77.30	77.31	250	371
18623.45	27553.94	-1.65	75.20	73.55	251	371
18051.93	27209.86	2.86	77.00	79.86	252	370
18213.24	27533.65	0.50	74.00	74.50	253	371
18823.94	27857.87	-3.59	73.40	69.81	254	371
18484.24	27662.20	-0.62	74.00	73.38	255	371
21270.76	23724.54	1.00	48.40	49.40	256	313
21350.98	23676.40	-0.03	48.90	48.87	257	313
21431.47	23638.69	1.06	47.20	48.26	258	300
22442.29	28414.49	2.05	57.40	59.45	259	360
22458.42	28547.83	2.73	57.40	60.13	260	390
22471.20	28323.84	3.75	57.30	61.05	261	361
27772.01	16089.63	-2.14	64.50	62.36	262	161
21687.39	22642.59	-0.65	47.30	46.65	275	244
22694.34	20886.56	0.40	42.60	43.00	276	215
22985.27	21919.32	1.69	44.10	45.79	280	231
22536.57	22163.74	0.88	44.00	44.88	285	238
22771.45	22182.33	0.46	44.50	44.96	286	232
22903.35	21661.96	0.96	43.70	44.66	290	230
22035.02	21375.47	-0.07	44.50	44.43	294	224
21989.28	20511.11	5.51	41.80	47.31	295	190
22278.83	20855.05	0.90	42.90	43.80	296	250
22060.59	20888.63	3.12	42.60	45.72	297	198
22171.47	21095.40	0.52	43.50	44.02	298	249
22069.84	21523.75	0.54	43.70	44.24	299	225
22113.78	21210.45	0.52	43.60	44.12	300	249
22184.61	21305.74	0.29	43.60	43.89	301	219
23642.24	23193.08	-7.37	59.30	51.93	302	283
24482.95	23496.06	-9.94	85.20	75.26	305	307
24840.11	23517.07	-6.92	86.70	79.78	306	307
24890.47	23674.78	-8.75	90.70	81.95	307	307
24602.61	23672.46	-13.08	91.60	78.52	308	307
24306.09	23418.46	-3.04	75.60	72.56	309	307
24111.25	23608.79	0.73	74.60	75.33	310	307
24364.83	23591.17	-2.83	78.60	75.77	311	307
24430.84	23599.45	-6.31	82.60	76.29	312	307
24097.55	23724.68	1.69	75.30	76.99	313	307
24139.20	23564.17	0.24	74.40	74.64	314	307
24663.31	23760.13	-12.30	92.10	79.80	316	307
24591.83	23754.19	-16.06	95.20	79.14	317	307
24256.22	23569.32	2.35	72.60	74.95	318	307